January 2018

Constraining The Small Binary Asteroid Population Of The Main Belt Using Doublet Craters On Ceres

Paul F. Wren

CONSTRAINING THE SMALL BINARY ASTEROID POPULATION OF THE MAIN BELT USING DOUBLET CRATERS ON CERES

by

Paul Fredrick Wren
Bachelor of Science, Arizona State University, 1985

A Thesis

Submitted to the Graduate Faculty

Of the

University of North Dakota

In partial fulfillment of the requirements

For the degree of

Master of Science

Grand Forks, North Dakota

May 2018

This thesis, submitted by Paul Fredrick Wren in partial fulfillment of the requirements for the Degree of Master of Science from the University of North Dakota, has been read by the Faculty Advisory Committee under whom the work has been done and is hereby approved.

Ronald Fevig
Dr. Ronald Fevig

Gerri Dunnigan
Dr. Gerri Dunnigan

Dr. Michael Gaffey

This thesis is being submitted by the appointed advisory committee as having met all the requirements of the School of Graduate Studies at the University of North Dakota and is hereby approved.

Grant McGimpsey
Dean of the School of Graduate Studies

May 1, 2018
Date

PERMISSION

Title	Constraining the Small Binary Asteroid Population of the Main Belt Using Doublet Craters on Ceres
Department	Space Studies
Degree	Master of Science

In presenting this thesis in partial fulfillment of the requirements for a graduate degree from the University of North Dakota, I agree that the library of this University shall make it freely available for inspection. I further agree that permission for extensive copying for scholarly purposes may be granted by the professor who supervised my thesis work or, in his absence, by the Chairperson of the department or the dean of the School of Graduate Studies. It is understood that any copying or publication or other use of this thesis or part thereof for financial gain shall not be allowed without my written permission. It is also understood that due recognition shall be given to me and to the University of North Dakota in any scholarly use which may be made of any material in my thesis.

Paul Fredrick Wren
May 12, 2018

TABLE OF CONTENTS

APPENDICES

LIST OF FIGURES

LIST OF TABLES

ACKNOWLEDGEMENTS

This achievement would not have been possible without the tireless encouragement, advice, and support provided by my M.S. advisor, Dr. Ron Fevig. I am also grateful to my committee, for their thoughtful questions and feedback, and to Bev Fetter for always being so helpful with the nuts and bolts of being a Space Studies graduate student.

I want to thank my employer, Dr. Phil Christensen, for being supportive of my continuing education, and all of the staff and students of the Mars Space Flight Facility at Arizona State University. In particular, I owe a large debt to the MSFF software team for their development of JMARS, the tool that made my research possible.

Finally, I want to express my appreciation for my family. I feel tremendous gratitude toward my wife Teri for always supporting and encouraging me in this endeavor, even though I repeatedly disappeared into my office on far too many evenings and weekends. I also am very grateful to my daughters Emily and Hannah, and my stepson Bradley, for their great enthusiasm and support.

ABSTRACT

Binary asteroids have been observed among the Near Earth Asteroids, among the Main Belt Asteroids, and even in the Trans-Neptunian Object population. Many were discovered by light curve analysis, some by direct or radar imaging, and a few by stellar occultation. Some were discovered using ground-based telescopes, and others by space-based assets such as the Hubble Space Telescope. As good as these instruments may be, no confirmed binary asteroids in the Main Belt have a primary body less than one kilometer in diameter.

The primary goal of this research was to confirm the existence of Main Belt binary asteroid systems with components smaller than one kilometer in diameter. Another goal of this research was to estimate a lower bound for the percentage of all Main Belt asteroids less than one kilometer in diameter that are binary systems. Doublet craters are believed to be caused by binary asteroid impacts, and their numbers can serve as a proxy for the number of binary asteroids among all impactors. Doublet craters were studied on the surface of Ceres using the latest detailed imagery returned by NASA's Dawn spacecraft. A large sample area on the surface of Ceres was systematically surveyed to identify and locate all impact craters greater than a minimum diameter. All possible pairings were examined and evaluated for their potential as doublets, and the likely doublets allowed the percentage of impact events in the sample area that are created by binary asteroids to be determined. This percentage is proportional to the percentage of Main Belt asteroids that are themselves binary systems.

The sizes of impactors that created the observed impact craters were determined using a crater scaling law, providing conformation of small binary asteroid systems in the Main Belt.

1 INTRODUCTION

1.1 Motivation

Doublet craters, i.e., pairs of impact craters in proximity to one another that are created by the same primary impact event, appear on all planetary bodies in the inner Solar System (Miljković et al., 2013; Oberbeck, 1973; Oberbeck et al., 1977; Trego, 1989; Trask et al., 1975; Cook et al., 2003; Melosh et al., 1996). Early research attributed their formation to a single impactor broken up by either atmospheric disruption (Passey and Melosh, 1980) or tidal forces (Sekiguchi, 1970; Oberbeck and Aoyagi, 1972), but further analysis revealed that these processes could not result in sufficient separation of the components to create observed doublets (Melosh and Stansberry, 1991; Bottke and Melosh, 1996). It is now believed that well-separated binary asteroids are the true source of doublet craters (Bottke and Melosh, 1996), making doublets an excellent source of evidence for the prevalence of binary asteroid systems.

The percentage of asteroids in the near-earth population that are binary is fairly well established at 15%, and doublet craters on Mars, Earth, Venus, and the Moon have been used to confirm this value (Miljković et al., 2013; Pravec et al., 2006). A total of 144 binary asteroids have been identified in the main belt using ground-based and spacecraft observations (Johnston 2016), but small binary systems have likely gone undetected. NASA's recent Dawn mission (Russell and Raymond, 2011; Nathues, 2016) has provided a large catalog of detailed images of the surface of Ceres, which was only a smudge of light in the best telescopes prior to Dawn

(Drummond et al., 2014). Doublet craters on Ceres provide evidence for the abundance of binary asteroid systems in the main belt, down to smaller diameters than previously detected.

1.2 State of Research

This section describes the history and current state of research into doublet craters, binary asteroids, and the morphology of impact craters.

1.2.1 Doublet Impact Craters

This section addresses doublet crater observations and formation theories.

1.2.1.1 Observations

As early as the 1950s, the concept of simultaneous impactors creating crater pairs was discussed. Twin meteorites were proposed as the likely origin of Clearwater Lakes in Quebec, two adjacent circular depressions of diameters 32 and 21 kilometers (Dence et al., 1965). As compelling as the evidence was, recent (U-Th)/He isotopic dating of the Clearwater Lakes impact structures reveal that the two craters were formed on the order of 200 million years apart (Biren et al., 2016). Two other likely crater pairs (doublet craters) have been identified on Earth (Melosh and Stansberry, 1991) along with two more possible doublets (Miljković et al., 2013), out of 190 total impact sites on Earth identified as of August 2016 (Spray, 2016). When we consider the two to four known doublets, approximately 1.0-2.1% of impacts on Earth are identifiable as doublet craters.

Following the arrival of images from Mariner 6 and 7 showing Mars and its surprisingly cratered surface, Verne Oberbeck and Michio Aoyagi (1972) examined craters present in photographs of Meridiani Sinus, Deucaleonus Regio, and Hellespontus. They identified 461 potential doublet crater pairs in five photographs, a large percentage of the 906 total craters counted in the images. Suspecting that this number was higher than would be expected from randomly distributed single impacts, the authors created a Monte Carlo simulation of Martian cratering that drew at random from the crater size frequency distribution derived from the 906 craters recorded in the Mariner images. The results of the simulation showed a 0.3% probability that the number of randomly-produced doublets could exceed 163.

Doublet craters have been observed on the Moon (Oberbeck, 1973; Oberbeck et al., 1977; Trego, 1989), on Mercury (Trask and Guest, 1975; Oberbeck et al., 1977), and on the surface of Venus (Cook et al., 2003). Cheryl Cook and colleagues find that 2.2% of the total impacts on Venus are doublets. While the high number of doublets reported by Oberbeck and Aoyagi (1972) suggest a large percentage of impact sites on Mars may represent doublets, a later examination of more lightly-cratered terrain in Vasitas Borealis yields a proportion of doublets of about 2.3% (Melosh et al., 1996). These percentages are consistent with more recent estimates of 2-3% for impacts in the inner Solar system (Miljković et al., 2013). This percentage is much lower than the percentage mentioned above for asteroids believed to be binary (15%). It is lower because a majority of binary impacts not resulting in visible doublet impact structures.

1.2.1.2 Doublet Crater Formation

In this section, the proposed formation processes for doublet craters are summarized.

1.2.1.2.1 Tidal fissioning of an incoming impactor

Oberbeck and Aoyagi (1972) propose that doublets, on Mars and elsewhere, are caused by impactors broken apart by the tidal force of the target body, as predicted by (Sekiguchi, 1970).

Multiple authors took issue with Oberbeck and Aoyagi's findings. Clark Chapman (1974) is not persuaded that all Martian doublets are caused by tidally-fissioned impactors, instead believing that true doublets are caused by 'relatively rare' already-fractured asteroids. Alex Woronow (1978) challenges their conclusions that the abundances of doublet craters are the result of non-random processes. Claiming their models are too elementary, Woronow proposes an alternative probabilistic model that shows no excess in doublets on Mars, i.e., the proximity of pairs of craters could be entirely the result of randomly-placed impacts.

1.2.1.2.2 Tidal Disruption of Contact Binaries Prior to Impact

In the late 1980s, radar imaging of Earth-crossing asteroids revealed that bi-lobed bodies might be two components making contact with each other (Ostro et al., 1990). Jay Melosh and John Stansberry (1991) built an orbital mechanics-based model to test whether such contact binary asteroids, when disrupted by tidal forces, could be the source of doublet craters. Running 1000 random cases through their model, their results seemed to undermine this possibility: 1. the median crater separation resulting from the experiments was nearly equal to the initial separation of the binary components, as measured between their centers of mass; 2. as a result of their rotation around each other, the resulting crater separation is just as likely to be less than the initial separation of the binary components; 3. orbital separations between the centers of the two components rarely become greater than twice the original separations. They conclude that "tidal forces are incapable of disrupting contact binary asteroids," and could not separate the two components sufficiently to create doublet craters. They also point out that the relative velocity of an Earth-crossing asteroid is around 10km/sec. The impactor would reach the surface before tidal effects could result in significant disruption. They suggest that the observed doublet craters are formed by the impact of well-separated binary asteroids, although at the time of their publication, no evidence had yet been presented that such systems might exist. Extrapolating from the (now outdated) estimate that 3 out of 28 impact sites on Earth are doublets, Melosh and Stansberry predict that as much as 20% of all Earth-crossing asteroids are well-separated binaries (Melosh and Stansberry, 1991 p.178).

1.2.1.2.3 Tidal Disruption of Rubble Pile and Contact Binary Asteroids

Paola Farinella (1992) believed that binary asteroids are likely the side effects of catastrophic collisions in the Main Asteroid Belt. Farinella proposed that binary asteroids whose separations were only a few times the sum of their radii could have their orbital energy changed during a close encounter with Earth. This encounter would result in the two components becoming gravitationally unbound, cause them to collide, or increase their orbital separation. Further modeling work (Chauvineau, Farinella, and Harris, 1995) demonstrated that slightly separated binaries repeatedly encountering Earth become well separated, become contact binaries, or entirely disrupt the system.

William Bottke and Jay Melosh (1996) were very interested in this hypothesis. They proposed that rubble piles and also contact binaries, after experiencing a close approach with a planet, could be tidally pulled into two or more fragments whose separation is sufficient to create the doublet craters seen in the inner solar system. Using a revised model for asteroid interaction with tidal forces based upon previous work by Farinella and Chauvineau, they produced percentage estimates for tidally-created widely-separated binaries that are consistent with the rates of doublet craters on the Earth, the Moon, and Mars. Modeling impacts of such widely-separated binaries, they found that as the impactors approach, planetary tidal forces tend to align the two bodies along their velocity vector, resulting in them impacting closely. This accounts for why 15% of the impacts on Earth may be binaries, but do not always produce a recognizable doublet crater. As noted earlier, the latest estimate for Earth doublets is 1.0-2.1% (Miljković et al., 2013; Spray, 2016).

1.2.2 Binary Asteroids

This section provides a review of research in the area of binary asteroids.

1.2.2.1 Do Binary Asteroids Exist?

The existence of binary asteroids was discussed in the early 1970s by Allan F. Cook (1971) following the publication of light curves for 624 Hektor, a Trojan Asteroid. The unusual asymmetry of the light curves prompted Cook to propose two different possibilities: The light curves may represent an eclipsing binary asteroid system, or Hektor may be a contact binary.

The first evidence for binary asteroids began to trickle in a few years later, in the form of anomalous data collected as part of stellar occultation observations. The first was during the occultation of γ Ceti A by 6 Hebe on March 7, 1977. One of multiple observers, Paul Maley, detected a short period occultation that could not have been the limb of Hebe, as he was positioned too far north. His data indicated a satellite with a possible diameter of 20 km (Dunham and Maley, 1977). June 7 of the following year, three independent observers measured the occultation of star SAO 120774 by 532 Herculina. All three detected 532 Herculina, and two of the three also saw an additional extinction, indicating a satellite of 532 Herculina with an estimated diameter of 45.6 +/- 3.6 km (McMahon, 1978).

Following these reports of possible asteroid satellites, anomalous sightings from earlier observations now became the focus of renewed interest. Re-examination of previous data for secondary extinctions resulted in the identification of seven new probable satellites, bringing the list of suspected asteroids with satellites to eight: 2 Pallas, 3 Juno, 6 Hebe, 9 Metis, 12 Victoria, 129 Antigone, 433 Eros, and 532 Herculina (Binzel and Van Flandern, 1979).

The idea of satellites orbiting minor planets was intriguing, and there were multiple attempts to observe them using ground-based telescopes. Gehrels, et al., (1987) set out in 1984 to confirm the existence of such satellites with CCD imaging of several main belt asteroids, including two previously identified as having probable satellites. They were unable to identify any satellites within the limits of resolution and sensitivity. They suggested that the only binary asteroids likely to exist are contact binaries. During roughly the same time period, 57 asteroids were observed using speckle interferometry on the 4-meter Mayall Telescope at Kitt Peak. No satellites were found (Roberts et al., 1995).

1.2.2.2 Discovery

The conflicting results from occultation and light curve observations versus optical observations in the 1980s may have left the question of asteroid satellites somewhat unanswered, but the Galileo mission to Jupiter put the question to rest. Planned photographs of main belt asteroid 243 Ida taken on August 28, 1993 included a surprise guest: a satellite orbiting the asteroid (see Figure 1-1). This first confirmed moon of an asteroid, named Dactyl, measured 1.6 km across in its largest axis, compare to 31.4 km for 243 Ida (Chapman et al., 1995).

Observations of near-Earth asteroids (NEAs) beginning in the late 1980s provided more evidence for the existence of binary asteroids, some separated, and some in the form of contact binaries. Shortly after its discovery, delay-Doppler images using radio telescopes at both Arecibo and Goldstone showed that 1989 PB (now named 4769 Castalia) was extremely bifurcated, appearing to be two distinct lobes. They saw no evidence of separation, so it is likely a contact binary (Ostro et al., 1990). By the time Asteroids III (Bottke et al., 2002) was published, five additional NEAs were confirmed to be separated binary systems using the delay-Doppler technique (Ostro et al., 2002).

The first ground-based, direct observation of a moon orbiting an asteroid was made on the first night of a planned survey of 200 asteroids for possible companions in 1998. A team using the 3.6-meter Canada-France-Hawaii Telescope atop Mauna Kea equipped with adaptive optics was able to observe a satellite of 45 Eugenia multiple times, and determine the characteristics of its orbit (Merline et al., 1999).

1.2.2.3 Observations

1.2.2.3.1 Photometric Observations

A photometric light curve is a time series of measurements of the brightness of the observed object. Binary asteroids can be identified by periodic patterns in the light curve caused by differential rotational rates, or by the bodies eclipsing each other (Margot et al., 2015).

Figure 1-1. Galileo false-color image of 243 Ida and satellite (NASA image P-44131).

Most observed binary NEAs are asynchronous, meaning that at least one of the bodies rotates at a rate that differs from the period of their revolution. Asynchronous binaries are easy to detect via photometry, since their differing rotational periods scatter sunlight at their own rate. Even though the light curves of the two components are received as a single light curve, individual periods for the two bodies can still be identified by fitting a two-period Fourier series (Pravec et al., 2006).

Photometry can also detect partial or complete eclipse events, if the plane of the binary system's orbit is close to edge-on when observed. These events have characteristic features, and once identified indicate the period of orbit (Pravec et al., 2006).

Photometric observations have discovered 175 binary systems (Johnston, 2018) representing all broad types of asteroids: NEAs, Mars crossing, MBAs, Jupiter Trojans, and TNOs (Margot et al., 2015).

1.2.2.3.2 Ground-based Direct Imaging

To directly observe an asteroid and its much smaller satellite, an instrument must possess sufficient resolution and contrast sensitivity. For example: a 50-100km asteroid in the Main Belt with a satellite only a few km in diameter, the angular separation between them is typically less than an arc second, and the contrast between the two bodies will be 5 to 10 magnitudes. Large aperture (at least 10-meter) ground-based telescopes equipped with adaptive optics (AO) are capable of such observations (Margot et al., 2015).

Since the AO-assisted discovery of a satellite orbiting 45 Eugenia in 1998 (Merline et al., 1999), ground-based telescopes using adaptive optics have discovered 16 binaries in the main belt, two among the Jupiter Trojans, and 14 Trans-Neptunian Objects (TNOs) that are binary systems (Johnston 2016).

1.2.2.3.3 Space-based Direct Imaging

The Hubble Space Telescope (HST) has the capability to resolve binary separations in the Main Belt (Margot et al., 2015), and successfully imaged a companion to 107 Camilla (Merline et al., 2002). HST has also been used to identify satellites of TNOs, including some around dwarf planets (considered TNOs) such as Pluto and Haumea (Johnston, 2016).

Deep space probes making close approaches to asteroids should be able to detect satellites, but none were discovered during visits to several, including Ceres (McFadden et al., 2018): 4 Vesta (McFadden et al., 2015), 21 Lutetia (Barucci et al., 2015), 253 Mathilde (Veverka et al., 1997), 433 Eros (Veverka et al., 2000), 951 Gaspra (Belton et al., 1992), 2867 Šteins (Barucci et al., 2015), 4179 Toutatis (Barucci et al., 2015), 5535 Annefrank (Duxbury et al., 2004), 25143 Itokawa (Fuse et al., 2008), and 132524 APL (Young et al., 2008). Only the Galileo spacecraft successfully identified a satellite around a minor planet, i.e., Dactyl orbiting 243 Ida (Chapman et al., 1995).

A total of 70 binary minor planet systems have been discovered to date via space-based imaging, with the vast majority being TNOs (Johnston, 2016).

1.2.2.3.4 Radar Imaging

Radar observations of asteroids, which usually involve a bi-static configuration where one radio telescope is used to transmit a radar signal, and another radio telescope is used to receive the signal that bounces off the asteroid and returns to Earth. The Arecibo radio telescope is the most sensitive in the U.S., and is the preferred receiver (Benner et al., 2015). The attenuation of the transmitted signal of existing systems is such that the discovery of binary asteroid systems is only possible for near-Earth objects (Ostro et al., 2002).

As of July of 2016, 41 binary asteroids have been identified in the NEA population using radar imaging (Johnston, 2016). In addition, over 30 NEAs are deeply bifurcated, making them strong candidates for contact binaries (Benner et al., 2015).

1.2.2.3.5 Stellar Occultation

Stellar occultation is an effective and simple method for determining the size and profile of asteroids. The approach requires multiple observers located at some distance (many miles) from one another roughly positioned along a line normal to the path of the asteroid's shadow along the Earth as it passes in front of a star. Each observer records the start and end time of the occultation from their vantage point. Data are later combined, taking into account the latitude/longitude of each observer, allowing both the shape and the angular size to be determined (Millis and Dunham, 1989).

Individual components of binary asteroids could be detected if a sufficient number of observers are regularly spaced across the viewing zone. The earliest discoveries of satellites of asteroids used the stellar occultation technique (Van Flandern et al., 1979), but despite concerted efforts, most of these early observations remain unconfirmed. As recently as 2012, a team of five observers recorded the stellar occultation of HIP 41337 by the Trojan asteroid 911 Agamemnon, and a likely satellite was detected (Timerson et al., 2013). This observation has yet to be confirmed (Margot et al., 2015).

With 290 binary asteroids now identified (Johnston 2016), it is unfortunate that not a single asteroid satellite detected by those early stellar occultation observations (Binzel and Van Flandern, 1979) has been confirmed, despite extensive follow-up searches (Margot et al., 2015).

1.2.2.4 Formation Processes – Main Belt Binaries

Models for the formation of binary asteroids among the Main Belt and Trojan asteroids have not changed drastically over time. All of the candidate mechanisms for forming binary systems start with a collision. Such formation mechanisms that have been proposed and discussed since the 1980s, are described here. The first two are supported by observational data (Walsh and Jacobson, 2015).

1.2.2.4.1 Rotational Fission

For bodies larger than a few tens of kilometers in diameter (considered large in size), a sufficiently large impactor would result in a "catastrophic" collision. Such a collision would shatter the body, but most of the mass would remain gravitationally bound, creating what is commonly referred to as a "rubble pile" (Davis et al., 1979). Models of catastrophic collisions revealed cases where off-center impacts impart angular momentum that is too great for all of the mass to remain in a single body, resulting in some mass fissioning off the primary and forming a satellite (Weidenschilling 1980, Zappala et al., 1980, Farinella et al., 1982).

Numeric modeling of 161 catastrophic collisions involving large asteroids (100 km in diameter) was done by Daniel Durda and his colleagues (2004). They produced large rubble pile asteroids with small satellites (they call them SMATS, short for "SMAshed Target Satellites"). These SMATS formed from some of the highly fractured debris of the collision, and enter into orbit around the rubble pile formed from the majority of the remaining debris. In a single simulation of a large asteroid collision, 92 SMATS entered stable orbits around the single large rubble pile. The authors expect that these small bodies in highly eccentric orbits will eventually accrete into a single satellite.

1.2.2.4.2 Orbiting Ejecta

In the case where a large asteroid is struck obliquely by an impactor too small to cause the main body to fracture, some material from the crater may be ejected with sufficient velocity to enter orbit (Weidenschilling et al., 1989). This is only possible if the primary component is remarkably aspherical; otherwise the ejected material would collide again (Doressoundiram, 1997). Even if orbit is achieved, it is unlikely to remain stable (Weidenschilling et al., 1989).

1.2.2.4.3 Mutual Capture of Escaping Fragments

William Hartmann's (1979) study of collisions between two comparably-sized bodies identified a number of possible outcome categories. He introduced the idea that conditions could exist where a high-energy impact could completely disrupt both bodies, and that most of the fragments would escape. Even so, some of the fragments moving along the same vector and having a low relative velocity could become gravitationally bound, forming small binaries. Weidenschilling et al. (1989) concluded after some simple modeling that very few of the fragments could become gravitationally bound.

More recent modeling efforts (Durda et al., 2004) report on the plentiful creation of both SMATS (see above) and the mutual captures we are discussing which they have named Escaping Ejecta Binaries (EEBs). They employed smooth-particle hydrodynamics (SPH) algorithms to model pressure, temperature, and kinetic energy during collisions, and fed the output into N-body simulations to track hundreds of thousands of fragments over time from the moment of the impact. Simulating 161 impacts onto asteroids 100 kilometers in diameter, varying the impact velocity, impact angle, and ratio of the object masses. A typical outcome for a single simulated collision produced over 1000 EEBs.

The SMATS (SMAshed Target Satellites) created in the modeled collisions and their resulting orbits around large primaries match up well with known satellites around large Main Belt asteroids. EEBs seem as though they should be plentiful, but are rare in the known catalog. Most small binaries have a primary with a rapid rotation rate, which better matches binaries formed via YORP effect, described later (Walsh and Jacobson, 2015).

1.2.2.4.4 Low Velocity Collision

Another mechanism for creating a binary could involve an encounter by two asteroids with a relative velocity sufficiently low that they could become gravitationally bound, and become a contact binary. The statistical rarity of such an event caused Doressoundiram et al. (1997) to dismiss this mechanism as a realistic possibility.

1.2.2.5 Formation Processes – Planet-crossing Binaries

We discussed in section 1.2.1.2 that planet-crossing, well-separated binary asteroids are considered to be the impactors responsible for doublet craters on Mercury, Venus, Earth, and Mars (e.g. Bottke and Melosh, 1996). But how do these planet-crossing binaries form?

1.2.2.5.1 Tidal Distortion of Planet-crossing Satellites

Paola Farinella alone (1992), and later joining Chauvineau and Harris (Chauvineau et al., 1995), proposed that slightly-separated Earth-crossing binaries (originating from collisions in the Main Belt) that repeatedly experience close encounters with Earth will experience orbital energy changes from the tidal forces. These changes will result in one of three outcomes: the reduction of their separation or even collision (creating a contact binary), becoming gravitationally unbound, or they become a well-separated binary.

William Bottke and Jay Melosh (1996) were inspired by the work begun by Farinella, and conceived of their own mechanism to produce sufficiently separated binary asteroids that could explain the observed doublet craters on the inner planets. They propose Earth-crossing rubble-pile asteroids (including contact binaries) are the source of doublet craters, and that a single close planetary approach will tidally pull the rubble into two or more fragments. They created a model to evaluate contact binaries involved in close encounters with Earth, and ran the model against thousands of contact binaries with varying characteristics.

When a test binary was run through the simulation, its initial position was 60 Earth radii away from the planet. Encounter velocity and closest approach distance were varied for each case. For some pairs, the components were no longer gravitationally bound and would escape. Others remained bound to one another. For these pairs, further computation of their semi-major axis, eccentricity, and perihelion allowed Bottke and Melosh to determine whether objects 1) remained in contact, 2) separated but collided again, or 3) separated and entered orbit around each other.

Bottke and Melosh (1996) also created a Monte Carlo model that determined 15% of the time, close planetary encounters for rubble piles or contact binaries should produce a satellite. They note some implications revealed by their models:

1. Close approaches are much more likely than collisions with a planet.
2. Asteroid satellites are almost always stripped from the primary during close approaches.

Even though satellite stripping occurs, rubble piles can keep on giving—there is a lot of rubble to provide more satellites.

Richardson et al., (1998) carried forward the work of Bottke and Melosh (1996), enhancing the model to represent true multi-particle rubble piles, and to include more realistic shapes, trajectories, spin rates and orientations. In the end, the improved model also predicts that 15% of Earth-crossing asteroids experiencing a close encounter with Earth should become binaries. Walsh and Richardson (2006) took advantage of improved computer capabilities to run N-body simulations of rubble piles being tidally disrupted by close planetary encounters. These simulations produced binary systems similar to observed NEA binaries, although 110,500 runs resulted in only 5747 binaries (~5%).

Building on their N-body simulations of rubble piles after collisions, Walsh and Richardson (2008) fed those results into a Monte Carlo routine. This routine simulated the transport of bodies from the Main Belt, close encounters with Earth for those bodies, the formation of binary systems, and the subsequent evolution of their orbits and spins over a period of one billion years. Their results show that tidally disrupted binaries do not survive very long due to large semi-major axes and high eccentricities. They estimate that such binaries should only account for 1-2% of all NEAs, and conclude that tidal disruption may not be the primary mechanism for binary asteroid formation in the planet-crossing population.

1.2.2.5.2 Thermal Torque Rotational Fission

If only 1-2% of NEAs were binary systems, it would not be sufficient to explain the doublet cratering record, which is estimated to require around 15% of all NEAs be binary (Miljković et al., 2013). Among observed NEAs and MBAs under 10km, 15% are binary (Walsh et al., 2008). Recent observations indicated the abundance of small satellites among small MBAs is the same as that among NEAs (Ćuk, 2007). Upon noting this, Matija Ćuk observed that with no planetary tidal encounters in the main belt to create such binaries, another process must exist to strip material from small MBAs, giving them satellites. This also raises the question of whether NEA binaries are created by tidal disruption, or by the process at work in the main belt? Ćuk suspected a common origin for both: Spinning up of the asteroid's rotation by the YORP effect.

The Yarkovsky-O'Keefe-Radzievskii-Paddack effect, or YORP effect (Rubincam, 2000), can impart rotational torque to irregularly-shaped small bodies (< 10 km in diameter). This causes them to spin faster or slow down depending on the nature of the body and its direction of spin. Solar infrared radiation striking the day side of an asteroid is absorbed and then re-emitted as thermal radiation. A perfect sphere would emit the photons radially and symmetrically, having no effect. On the other hand, a highly irregular body would emit photons both radially and tangentially, typically creating asymmetric force that can affect its spin rate.

Kevin Walsh, Derek Richardson and Patrick Michel (2008) presented a model showing that binary asteroids <10 km in both the near-Earth and Main Belt populations are formed by the same mechanism: the slow spin up of rubble pile asteroids by the YORP effect, ultimately reaching a critical rotational rate that sheds mass from the pile. The binaries produced by their model are consistent with known small binaries in both populations.

The big shift in the first decade of the 21st century was to move away from thinking planet-crossing asteroids and Main Belt asteroids were fundamentally different.

112 confirmed asteroids with satellites had been observed in these two populations (Johnston 2016), and Pravec and Harris (2007) created a classification system for them:

- Group L: Large asteroids with relatively very small satellites
- Group A: Small asteroids with relatively *small* satellites in *tight* orbits
- Group B: Small asteroids with relatively *large* satellites in *tight* orbits
- Group W: Small asteroids with relatively *small* satellites in *wide* orbits

Where the boundary between “Large” and “Small” asteroids falls at a diameter of 20 km for the primary (D_P), the boundary between relatively *large* and *small* satellites is a ratio of the secondary to primary diameters (D_S/D_P) around 0.7, and the boundary between *tight* and *wide* orbits is defined as a semi-major axis at 9 times the radius of the primary. New observational data and the application of YORP theory to binary formation resulted in some movement of the categorical boundaries (the updated values are presented here) since the creation of the classification system in 2007 (Walsh and Jacobson, 2015).

Group L was addressed in section 1.2.2.4: collisional processes dominate the creation of these binaries with large primaries. At sizes exceeding 20 km, YORP does not play a role since spin-up timescales increase with surface area (Walsh and Jacobson, 2015). This group is represented exclusively by Main Belt asteroids.

Groups A, B, and W are composed of binary asteroids from both the Main Belt and the planet-crossing populations, and the systems in these groups can all be accounted for by YORP-based formation processes.

Seth Jacobson and Daniel Scheeres (2011) presented a model for small asteroid binary system creation through rotational fission that depends only on the YORP effect, the existence of rubble pile asteroids, and their gravitational interactions. They note that previous YORP-based models (such as presented in Walsh et al., 2008) do not adequately predict all observed binary system characteristics. Their model differs from others in that it covers longer timescales, thus it more realistically represents the time it would take to develop YORP torque (on the order of 10^6 orbits).

Their model is comprised of two parts: a YORP-based rotational fission model to create the initial binary, followed by a purely gravitational model for post-fission evolution of the system (gravitational timescales are much shorter than those required to perceive YORP effects). They ran 526 varying rubble piles through their simulation, letting the post-fission dynamical model proceed for 1000 years. At the end of that time, 41 of these became stable binary systems, representing synchronous binaries (secondary spin matches orbital period), doubly synchronous binaries, and contact binaries. The authors believe their rotational fission model creates all types of observed binaries that begin with a rubble pile in the size range of 100 meters to 10 kilometers (Jacobson and Scheeres, 2011).

While the Jacobson and Scheeres (2011) simulation modeled bodies as monolithic entities until they fissioned into multiple components, Walsh, Richardson, and Michel (2012) continued and expanded the YORP spin up numerical experiments described in Walsh et al. (2008) which model the rubble pile and any fissioned satellites as thousands of constituent particles. Walsh et al. (2012) demonstrate through their model that an equatorial ridge (observed on some near-Earth asteroids) is formed as spin approaches the critical speed necessary to fission, and that mass is then stripped from the equatorial ridge to form satellite(s). Jacobson and Scheeres (2011) attribute the equatorial ridge to mass that is further fissioned from satellites, and falls back onto the primary.

Though taking different approaches, both of these YORP effect-based models are very good at explaining the population of small asteroid binaries in the Main Belt and planet-crossing populations.

1.2.3 Impact Crater Morphology

The morphology of impact craters is of particular interest for this study, as it allows for analysis both during the determination of whether two craters could have been formed in the same impact event, and during the computation of the mass of the impactor that created a crater. This section begins with a brief overview of basic crater forms seen on planetary bodies, summarized from Jay Melosh's book, *Impact Cratering* (1989).

1.2.3.1 Overview

As the sizes of impact craters increase on a particular body, transitions occur in their overall form. The smallest craters are called "simple" craters. Simple craters possess a circular raised rim, and present a generally featureless, bowl-shaped interior that is close in profile to a parabola. At some threshold diameter (it varies by target body), there is a transition to a more complex morphology for the crater's interior, thus the name "complex" craters. These larger craters maintain a circular rim, and the inner walls are steep near the rim, just as in a simple crater. The difference comes at the crater floor, which is flat and covered by material that has the appearance of landslide debris. Complex craters are more shallow, in comparison to their diameter, than simple craters. As larger complex craters are examined, they also exhibit terracing in the crater walls, and raised structures at the center of the crater floor referred to as central peaks.

The candidate doublets identified in the study (with the exception of one pair) each have a diameter that falls below 7 km, the observed transition from simple to complex craters on Ceres (Hiesinger et al., 2016), so the primary morphological concern of this study is that of simple impact craters.

1.2.3.2 Oblique Impacts

The chance that an impacting body strikes a planetary surface vertically is quite small indeed, given that random objects meeting in space can come at one another at any angle. Virtually every impactor strikes a target surface at some angle above horizontal that is less than 90°, with 45° being both the average angle and the one with the highest probability of occurring (Melosh, 1989, p. 49). The probability of an impact at an angle falling between θ and $\theta + d\theta$ (θ is measured from target surface horizontal), is defined as

$$dP = 2\sin\theta\cos\theta\, d\theta \qquad (1)$$

and based on this equation (Pierazzo & Melosh 2000), the angle with the highest frequency is 45°. Equation 1 also indicates the probability of a vertical ($\theta = 90°$) or a grazing ($\theta = 0°$) is essentially zero. Equation 1 predicts that 50% of impacts will occur for angles between 30° and 60°. The conclusion to be drawn from this is that all impacts should be considered oblique impacts.

If it is the case that essentially all impact craters have been created by bodies striking the surface at varying degrees of obliquity, surely one should be able to detect that in the shape of the crater itself. It turns out to not be so easy, since hypervelocity impacts, i.e., where the velocity is higher than the speed of resulting compression waves in the target material (Burchell and Grey, 2001), produce circular crater rims for all but the most oblique angles. Elliptical crater shapes do not appear until the angle of impact is within 10-15° of horizontal (Melosh 1989), and such oblique impact events are likely to occur less than 7% of the time (Pierazzo and Melosh 2000).

Elliptical crater rims may not occur in most cases, but there are other morphological indicators associated with oblique impacts. In an oblique strike, much of the vertical velocity component is absorbed by the shock, but the horizontal velocity component is less affected by the initial impact. Both the remains of the projectile and the excavated target material are carried along the horizontal velocity vector, depositing more material downrange. The downrange rim is pushed away as this lateral energy is spent, resulting in the deepest excavation of the crater bowl occurring up-range of the center of the new crater. This effect is more pronounced as obliquity increases (Melosh, 1989, pp. 49-51). These same processes result in radially asymmetrical ejecta blankets (Wallis et al., 2005; Poelchau and Kenkmann, 2008), however all but the freshest craters tend to lose their well-defined ejecta blankets to erosion. Herrick and Forsberg-Taylor (2003) examined craters on the Moon and on Venus, looking for evidence of oblique impacts. They observed that craters possessing a single depression along a portion of the crater rim showed ejecta concentrated on the opposite side of the crater. This is consistent with experimental results that found up-range rim depressions and downrange ejecta concentrations for impact angles less than 30° (Gault and Wedekind, 1978). It should be noted that not all impact experiments support this oblique morphology. Burchell and Grey (2001) fired aluminum projectiles into thick glass, and found that regardless of the angle of impact, the deepest point of the resulting craters remained at the center. Numeric modeling has been supportive of an oblique morphology. Three-dimensional simulation of high-velocity oblique impacts produced crater profiles that were asymmetric: the crater floors showed a steeper slope in the up-range direction, with a shallower (and elongated) slope in the downrange direction (Elbeshausen et al., 2009).

1.2.3.3 Impact Crater Scaling Laws

There have been numerous attempts to determine a reliable impact crater scaling law, dating back to at least the late 1960s (Öpik, 1969; Gault, 1974; Melosh, 1980; Holsapple and Schmidt, 1982; Schmidt and Housen, 1987, and others). It is generally agreed that the size and form a crater will take is dependent on a number of variables: impactor velocity, impactor size, impactor density, target density, target strength, and the gravity of the target body. Some models also consider separately the porosity, cohesion, and friction of the target, and these values can be considered for impactors as well (Elbeshausen et al., 2009; Wünnemann et al., 2011).

Donald Gault (1974) stated that the final size and shape of impact craters is primarily dependent on the material strength and gravity of the target body. The strength of the target is most important for determining the shape of very small craters, whereas gravity dominates for larger craters (i.e., kilometers in size). Unable to create a scaling law that covers all impact crater sizes, Gault developed three equations for Lunar impacts that differed in a coefficient value and in the power to which the kinetic energy was raised. One equation was valid for craters up to 10 meters in diameter, the second was applicable in craters between 10 and 100 meters, and the third equation was useful for larger craters. They are all three of the form shown in Equation 2, but different values are used for the coefficients A and E:

$$D = A\, \rho_p^{1/6}\, \rho_t^{-1/2}\, E^X\, (\sin\theta)^{2/3} \qquad (2)$$

Where:

D	=	Crater diameter
ρ_p	=	Projectile density
ρ_t	=	Target density
E	=	Kinetic energy of the projectile
θ	=	Impact angle away from vertical (different from Eq. 1)

Horedt and Neukum (1984) took a look at six crater-scaling laws that had been published in the previous decade or so. They found Gault's (1974) crater-scaling equation for large craters to be straightforward and useful, even though they note that Holsapple and Schmidt (1982) were critical of it. They conclude that current crater scaling laws lack a firm theoretical base, and much more theoretical work and experimentation is needed. This assessment agrees with the view held by Jay Melosh (1980).

Extending the work of Elbenhausen et al., (2009), Kai Wünnemann and colleagues (2011) developed a scaling formula based on the results of over 150 numerical models of impact crater creation in targets that varied in their physical properties. Initially creating separate laws for the strength- and gravity-dominated regimes, they were able to combine them into a single scaling law that applied to both. The equation is quite complex. It combines the variables seen in many previous scaling laws with additional properties of the target material: cohesion, porosity, and friction.

Kevin Zahnle and colleagues developed a more manageable scaling formula for relating transient simple crater diameter to impactor diameter (2003). Their study primarily looked at impact cratering rates on the icy moons of the outer solar system. They desired a simpler scaling rule than most of those mentioned above. Equation 3 shows their formula for determining the diameter of the transient crater. They state that the final crater diameter (D) is equal to the transient crater diameter (D_S) for craters whose D_S is smaller than the diameter marking the transition to complex craters (D_C) on the target body.

$$D_S = 11.9(v^2/g)^{0.217}(\rho_{p/}\,\rho_t)^{0.333}d^{0.783} \text{ km} \qquad (3)$$

The new variables appearing in Equation 3 are projectile velocity (v) in km/s, gravity (g) in cm/s^2, and projectile diameter (d) in km (D_S is also expressed in kilometers).

1.3 Goals and Outline

The primary objective of this work is to demonstrate that the impact cratering record of Ceres provides conclusive evidence for the existence of binary asteroid systems with components smaller than one kilometer in diameter within the Main Belt. To do this, the percentage of small impact events on Ceres that are doublets will be estimated by a sampling of its surface. This percentage, when interpreted in the context of prior studies, will lead to an overall percentage of small asteroids that are binaries within the Main Belt.

Chapter 2 details the methodology employed in this research. It describes the methods used to estimate impactor diameter from crater diameter, covers the approach to impact crater sampling, and the source data upon which the sampling depends. A method for evaluating crater pairs is described, and finally a Monte Carlo simulation for determining an expected random distribution of impact craters in the study area is presented. Limitations for all these methods are addressed. Chapter 3 describes the application of the methods presented in Chapter 2, including detailed examination of likely doublet craters. Chapter 4 begins with interpretations of the analyzed data from Chapter 3, and presents the conclusions of the work along with opportunities for additional research.

2 METHODS

This chapter begins with a brief review of methods used in previous doublet crater studies that have influenced this research, then goes on to describe the source data for this study, and provides details about the methods and tools used to identify doublet craters on Ceres.

Multiple attempts have been made to quantify the number of impact events on planetary surfaces that may be doublets. Oberbeck and Aoyagi (1972) performed the first systematic survey of impact craters on Mars, using Mariner 6 and 7 images. They counted all craters larger than 4 km in diameter within their total study area (3,818,095 km^2). Likely choosing the area based on the most useful photographs, they examined the heavily cratered terrain to the west of Hellas Planitia. They defined possible doublets as any two craters whose rims either overlap by no more than 12.5 km, or whose rims are separated by no more than 12.5 km. Using these criteria, they identified 461 doublets among 906 craters.

Melosh et al. (1996) noted that Oberbeck and Aoyagi had sought out doublets on heavily-cratered terrain, where saturation could have occurred. They instead chose to search for doublet craters on the lightly-cratered northern plains, examining approximately 2 million square kilometers in Vasitas Borealis. Using Viking image mosaics, they counted all craters greater than 5 km in diameter. They considered any pairing of craters whose separation was less than 100 km as potential pairs, and further evaluated the pairs based on visible geologic information. They categorized pairs as "unlikely" if evidence against being a doublet was present (e.g. different degradation), "likely" if positive evidence was observed, and "possible" if no particular evidence for or against simultaneous impact was seen. They identified only 133 craters in their study area with diameters greater than 5 km, and found only three pairs that they considered "likely."

Similar studies have been performed on the satellites of Saturn (Wagner et al., 2012), on the Moon (Oberbeck et al., 1977), and on Venus (Cook et al., 2003).

2.1 Source Data

Existing data sets from NASA's Dawn mission form the basis of this research. This section describes those data.

2.1.1 Imagery

The Dawn spacecraft has been orbiting the dwarf planet Ceres and making observations since March 6, 2015 (Ciarniello et al., 2017). It is equipped with two Framing Cameras (FC), each of whose 1024x1024 CCD can acquire visible light images through a clear filter, or through one of seven distinct band pass filters (Sierks et al., 2011).

To get the highest resolution images of Ceres in the most convenient form, a global mosaic of Dawn Framing Camera images captured during the Low Altitude Mapping Orbit (LAMO) is used for the crater survey. This global map depicts the surface of Ceres at a resolution of 35 meters per pixel (Roatsch, et al., 2017). When more detailed examination of specific craters is desired, individual Framing Camera images taken during LAMO (Nathues et al., 2016) can provide varied lighting and improved contrast when compared to the global mosaic product.

2.1.2 Elevation Data

To effectively study the morphology of impact craters, elevation data of the Ceres surface, presented with sufficient resolution to perceive the shape of craters on the order of 5 km in diameter, are essential. The Dawn team has produced a global Digital Terrain Model (DTM) of Ceres, derived using stereo photogrammetry based on Framing Camera images from the High Altitude Mapping Orbit. This terrain model has a lateral spacing of approximately 136.7 meters per pixel, and a vertical accuracy of approximately10 meters (Preusker et al., 2016).

Examination of crater morphology will be done using the Ceres Relative Elevation for Oblate Spheroid (HAMO), a global numeric map derived from the above-described DTM.

2.2 Determining Impactor Size from Craters on Ceres

It is essential to determine the size of asteroids that created the impact craters examined in our study, since the intention it to characterize the binary systems within the population of small asteroids (≤ 1 km) in the Main Belt. A scaling law is needed to determine impactor sizes from the craters they create, and the inputs to such a scaling law must be determined.

2.2.1 Impact Crater Scaling Laws

We are interested in craters whose diameters fall below the transition from simple to complex craters, which Hiesinger et al., (2016) estimate to be between 7.5 and 12 kilometers in diameter. Since we will be focusing on simple craters, the diameter of the transient crater rim is a sufficient approximation of the final rim diameter for simple craters (Ivanov, 2001; Turtle et al., 2006).

This study is concerned with ranges of impactor sizes, and does not require exacting size determinations for impactors. As discussed in section 1.2.3.3, Kevin Zahnle and colleagues (2003) developed a scaling formula for relating simple crater diameter to impactor diameter that is suitable for this study.

Modifying their equation to solve for the diameter of the projectile, we get

$$d = [D/(11.9(v^2/g)^{0.217}(\rho_p/\rho_t)^{0.333})]^{1.277} \quad (4)$$

where v is impactor velocity in km/s, g = Ceres gravity in cm/s^2, ρ_p is the density of the projectile in g/cm^3, ρ_t is the density of the crust of the target Ceres, and D is the diameter of the impact crater in km.

Some of these values are well known. We have already measured the craters and know each diameter D, and the gravity of Ceres is 28 cm/s^2 (Mao et al., 2018). The following sections describe how the remaining values needed for this equation were determined.

2.2.2 Estimating the Velocity of an Impacting Main Belt Asteroid

The closing velocity is different for every impactor that collides with Ceres, and we cannot hope to know these velocities with any certainty. For the purposes of this study, a representative mean collisional velocity for main belt asteroids will be used as input to a crater scaling model.

Farinella and Davis (1992) computed collision probabilities for 682 known asteroids larger than 50 km from a set of 4100 numbered main belt asteroids whose orbits are known. They also computed their probable collision velocities.

This foundational work led to additional, similar computational studies. Bottke et al. (1994) computed a mean velocity for Main Belt asteroids of 5.3 kilometers per second, yet the most probable value was 4.4 km/s. John Vedder (1998) expanded his sample size to 4506 Main Belt asteroids, and propagated their known orbits for 48,000 days. He found an average closing velocity of 3.78 km/s for predicted collisions.

Taking a different approach, Hiesinger at al. (2016) used a global study of impact craters on Ceres (also taking advantage of the new detailed images from the Dawn space craft) and computed an average impact velocity of 4.57 km/s. As this value is close to the highest probability velocity predicted by Bottke et al. (1994), and it is a value more directly associated with the specific orbit of Ceres, it will be the value used for this study.

2.2.3 Estimating the Density of an Impacting Main Belt Asteroid

Benoit Carry (2012) published a review of the known densities of small bodies in the solar system. He compiled mass and density data for 287 bodies, which included Main Belt asteroids, comets, near-Earth asteroids (NEAs), and trans-Neptunian objects (TNOs), which are presented in his Table 1. He also assigned a quality grade to the data for each asteroid (A through F) based on the estimated accuracy.

For this study, we focused the Main Belt asteroids (175), eliminating those of grade E or F (indicating a relative density accuracy cruder than 100%), and restricted our final list to only stony MBAs. The average density for these remaining 138 stony Main Belt Asteroids (see Appendix B) is 2.788 g/cm^3.

2.2.4 The Density of Ceres' Crust

Ermakov et al. (2017) report that based on the shape model and gravity field of Ceres, as determined by Dawn, they compute a best-fit global averaged crustal density of 1.287 g/cm^3. This value will be used in our crater-scaling formula to determine the size of impactors.

2.2.5 Crater Scaling Equation for Ceres

Entering the values we have determined for Ceres and the Main Belt into Equation 4 results in the following:

$$d = [D/(11.9(4.57^2/27)^{0.217}(2.788/1.287)^{0.333})]^{1.277} \qquad (5)$$

which simplifies to:

$$d = [D/14.44475]^{1.277} \tag{6}$$

This work will use Equation 6 to determine approximate impactor crater diameters.

2.3 Impact Crater Survey

All impact craters at or above a chosen diameter, occurring within a predetermined area on Ceres, will be recorded. Much of the work is done using JMARS, the Java Mission-planning and Analysis for Remote Sensing software created at Arizona State University (Christensen et al., 2009).

2.3.1 Survey Area

An earlier pilot study (Wren and Fevig, 2017) searched terrain near large craters *Urvala* and *Yalode* for its low crater density, to minimize the number of randomly-adjacent impact craters (Heisinger et al., 2016). The full study region was extended to the west and somewhat north, bounded by 110°E to 270°E and 10°N to 30°S, roughly 430,000 km^2 (see Figure 2-1).

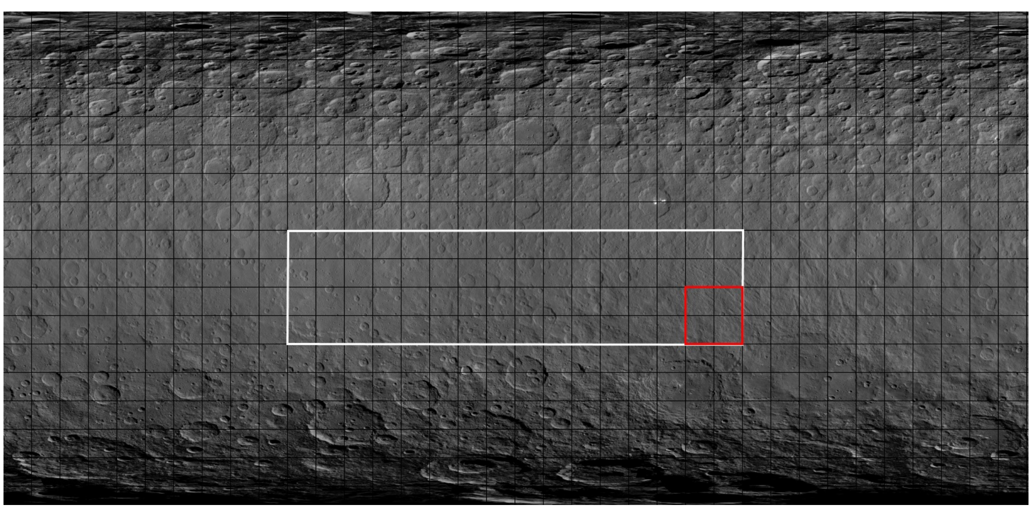

Figure 2-1. Study area on Ceres. Red line is the original pilot study, white line encompasses the total study area for this work: 110°E to 270°E and 10°N to 30°S.

2.3.2 Identifying and Recording Craters

To ensure sufficient resolution for crater identification in FC images and to provide sufficient resolution in the Digital Elevation Model, only craters with a minimum diameter of 3 kilometers will be considered.

The Crater Counting layer of JMARS (Described in Appendix D) is used to locate all craters within the study area. When the user selects a crater, the Crater Counting layer automatically records the location (latitude, longitude) and diameter of each impact crater in a table that can be exported. The Crater Counting layer was configured to record the diameter to the nearest 100 meters.

2.3.3 Upper Limit for Crater Diameters

Using Equation 3 in section 1.2.3.3, we enter the values determined in section 2.2 along with a value of 1 for projectile diameter in kilometers (d). The resulting simple crater diameter is 14.44 kilometers. Candidate pairs are limited to those whose craters are less than or equal to 15 kilometers in diameter.

2.3.4 Limitations

This approach to locating and identifying impact craters, as with all approaches, introduces some errors and biases into the collected data. Setting a 3 km lower limit on crater diameter may be necessary to ensure the craters included in the study can be accurately measured, but it also means smaller craters will not be included even though they may be part of a doublet, even one in which the other crater is above the 3 km limit.

The largest source of errors in the collected data is the human in the loop, who must judge the size of craters against the crater counting tool (the computer's cursor is a circle set to the 3 km-diameter minimum) and could miss some craters that are barely 3 km in diameter. The human could also misjudge the matching of the crater's actual diameter with the cursor tool, producing errors in the estimated diameter. This can be overcome later by performing more precise measurements of individual craters that are of interest later in the process.

2.4 Identifying and Evaluating Potential Doublet Craters

All potential crater pairs separated by an arbitrary upper limit will be identified automatically by custom software, and then individually examined for evidence for or against the pair being the result of a doublet impact event.

2.4.1 Identifying Crater Pairs

When looking for pairs of craters that could be considered doublets, a maximum distance of 20 kilometers was somewhat arbitrarily chosen as the upper limit for the separation between their centers. Twenty kilometers (vs. 100 km, as used in Melosh et al., 1996) was chosen to avoid nuisance pairings that were unlikely. Small craters whose separation is many times the craters' diameters would represent low-mass binary asteroids that would probably not be gravitationally stable. To identify candidate crater pairs, the following steps are performed:

1. Individual craters identified in the Crater Counting layer of JMARS are downloaded to a character-separated values (CSV) file.
2. Using the crater file as input, a Python program (Oliphant, 2007) assigns a unique number to each crater.
3. The program then examines all unique pairings of craters in the file, computing each pair's separation as a great circle arc between the latitude/longitude locations of the

craters' centers. The computation assumes Ceres is a sphere with a radius of 473 km, its mean radius (Ermakov et al., 2017).

4. Each crater pair whose separation is less than 20 km is output to a human-readable CSV file, and also output to a custom shape file that can be ingested by JMARS.
5. Lastly, the program creates a CSV file of information on all counted craters, including their assigned number. More details on this Python program can be found in Appendix D.

2.4.2 Evaluating Crater Pairs

Each candidate crater pair identified by the Python program is examined manually and graded using a scoring system.

To facilitate the evaluation of crater pairs, the custom shape file produced by the Python program is loaded into JMARS. This layer will draw a line between the centers of two craters, and label the line with the two craters' numbers. Each candidate crater pair identified in the previous section can be easily located and examined.

Each candidate doublet is assigned a score based on the observed presence of seven features/attributes: Heavy Erosion, Superposition, Differing Erosion, Differing Depth, Similar Erosion, Possible septum, and Possible Ejecta Lobes (see Table 2-1). Some examples are illustrated in Figure 2-2.

Scoring rationale: Differing erosion (when apparent to the human eye) and superposition are clear indications that a pair of craters do not represent a double impact, so a high magnitude negative score is assigned to these to ensure the pair will not ultimately receive a positive score. Differing Depth is a little trickier to interpret without detailed measurements of the craters, since the depth should be interpreted in relation to the diameter. Only fairly obvious differences will be detectable via visual inspection. Heavy Erosion subtracts one point because it makes much of the crater's original shape difficult to discern. Even though possible septa and ejecta lobes should indicate a doublet, it may take more analysis to be sure, so the positive evidence scores lower than negative evidence.

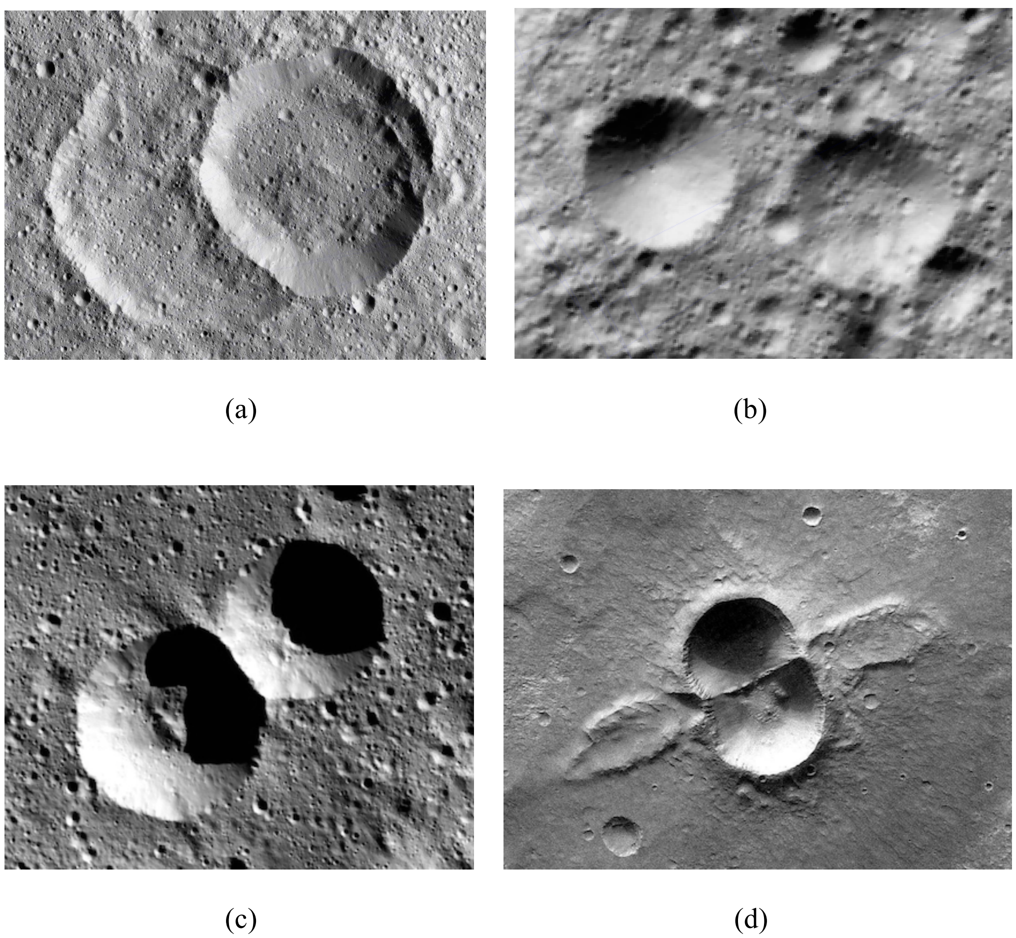

Figure 2-2. Examples of impact crater attributes used to identify doublets: a. Super-imposed craters; b. Differing erosion; c. Septum between craters; d. Radial ejecta lobes.

Table 2-1: Scoring System for evaluating potential doublet impact craters

Attribute	*Score*	*Description*
Superposition	-3	One crater clearly is superimposed over the other
Differing Erosion	-3	One crater is clearly more eroded than the other
Differing Depth	-2	One crater is obviously deeper (in relation to its diameter)
Heavy Erosion	-1	Both craters are highly eroded
Similar Erosion	1	Both craters exhibit what seems to be the same amount of erosion
Possible Septum	2	A common rim segment shared by the two craters that is typically straight rather than curved
Possible Ejecta Lobes	2	Radial ejecta lobes deposited by two jets moving away from the crater pair in opposite directions along the axis of the septum (Miljković et al., 2013).

Crater pairs with negative scores are not considered to be doublets. Pairs with scores of zero are inconclusive. Pairs with positive scores will be considered possible doublets, and will be examined more closely.

2.4.3 Limitations

Choosing an arbitrary 20-kilometer maximum separation between craters to examine as possible doublets is a waste of time for the smallest craters (the impactors would not likely be in a stable orbit at such a separation). The same 20 km limit may cause us to miss double impacts entirely in cases where one of the components of the binary is large in comparison to its companion (the separation could then be larger than 20 km).

2.5 Monte Carlo Simulation

A Monte Carlo simulation has been created in Python. The objective of this simulation is to create the expected distribution of crater pair separations resulting from randomly located, single-projectile impact events (the same number as the count of craters observed in the study area on Ceres). This simulation is modeled after one employed in a similar doublet crater study on Mars by Melosh, Ingram, and Bottke (1992).

When provided with the boundaries of the study area (in latitude and longitude coordinates) and the number of craters counted in the Identifying and Recording Craters phase (described in section 2.3.2), the Python program will perform the following steps:

1. Use a random number generator to simulate latitude/longitude pairs representing randomly-occurring craters. The simulation creates the same number of random crater locations as the number of real craters counted in the same study region on Ceres.
2. The simulation then identifies all possible pairings of the simulated craters whose separations are less than the threshold separation used in the Identifying Crater Pairs phase (section 2.4.1).
3. All pairings are tallied into logarithmic bins based on their separation distance.

This simulation is executed 1000 times, and the average value for each bin is computed. A different Python program reads in the observed crater pair data produced by the activities in section 2.4.1, and tallies the separations of all pairs into the same logarithmic bins. The observed separation counts will be compared against the expected distribution produced by the simulation.

3 DATA ANALYSIS

This chapter presents the data collected in this study, and describes the processing and analysis of those data using the methods presented in Chapter 2.

3.1 Impact Crater Identification

Using JMARS, 1084 craters at least 3 kilometers in diameter were counted in the study area (110°E to 270°E and 10°N to 30°S). Craters counted ranged from 3 to 63.8 kilometers in diameter (1021 of these are at most 15 km in diameter). The resulting rows of crater data, i.e., the latitude/longitude of the crater centers and their diameters, are written by JMARS to a file named `craters_all_phases.csv`.

3.2 Finding Doublet Craters

The goal of this study is to address Main Belt asteroids with diameters that are at most one kilometer. No upper limit was placed on crater diameter during the counting phase, but as we analyze potential pairs to identify doublet impacts, we will restrict the pairs examined to those whose craters are at or below the estimated crater diameter predicted for a 1 km impactor on Ceres (see section 2.3.3).

3.2.1 Potential Crater Pairs

A Python program named `separations_shapes.py` read in the crater data from the file `craters_all_phases.csv`. It examined all unique combinations of craters, and recorded all pairs whose separations were less than 20 kilometers. There were 2037 crater pairs separated by less than 20 kilometers identified and output to the file `crater_pairs_20km.csv`.

A manual process using the sort function in Excel was employed to edit the file `crater_pairs_20km.csv` by removing all craters pairs that contain craters whose diameters are greater than 15 kilometers, resulting in the file named `crater_pairs_lt_15km.csv`. This new file contains 1878 crater pairs.

3.2.2 Identifying Doublet Craters

A two-step process is used to determine a final list of pairs that may be doublet craters. Each pair of craters is examined and scored. The crater pairs with a positive score weren revisited to classify them as inconclusive, possible, likely, very likely, or definite.

3.2.2.1 Scoring Crater Pairs

Of all crater pairs evaluated, 66 received a positive score. Of these, one is considered to be a "definite" doublet crater, two are considered "very likely" to be real doublet craters, three are considered "likely," and three are "possible." The remaining 57 are considered "inconclusive," and may be evaluated further. The nine crater pairs rated "possible" or better are listed in **Table 3-1**. Appendix C contains the complete list of the 2037 crater pairs analyzed, sorted by their total score.

3.2.2.2 Results

This section addresses the nine crater pairs from the study that show varying degrees of promise as doublet craters, as listed in **Table 3-1**.

Pair 1 is the only one classified as a "definite" doublet crater. This relatively fresh impact structure bears the hallmark septum wall between the two craters (Figure 3-1), which is the best evidence for a simultaneous impact of two bodies (Johnston and Miljković, 2014). The two impactors were close in size to one another, and were separated by about two kilometers upon impact.

Table 3-1: Doublet Crater candidates in the study area

Crater Pair	***Longitude***	***Latitude***	***Diameter (km)***	***Separation (km)***	***Doublet?***
Pair 1	228.633	-9.703	3.2	2.16	Definite
	228.367	-9.695	3.5		
Pair 2	170.487	9.613	10.8	10.47	Very Likely
	171.366	10.540	13.8		
Pair 3	216.578	9.367	4.3	1.63	Very Likely
	216.570	9.176	3.7		
Pair 4	154.906	-29.375	3.2	2.65	Likely
	154.93	-29.695	3		
Pair 5	252.679	-13.583	3.0	2.92	Likely
	252.938	-13.831	3.2		
Pair 6	251.772	-21.941	3.0	3.26	Likely
	252.024	-22.236	5.3		
Pair 7	218.295	-21.601	3	3.55	Likely
	218.064	-21.974	3.5		
Pair 8	255.199	-17.097	3.6	8.01	Possible
	255.426	-16.152	3.0		
Pair 9	132.27	-26.360	5.2	7.47	Possible
	132.016	-27.234	5.2		

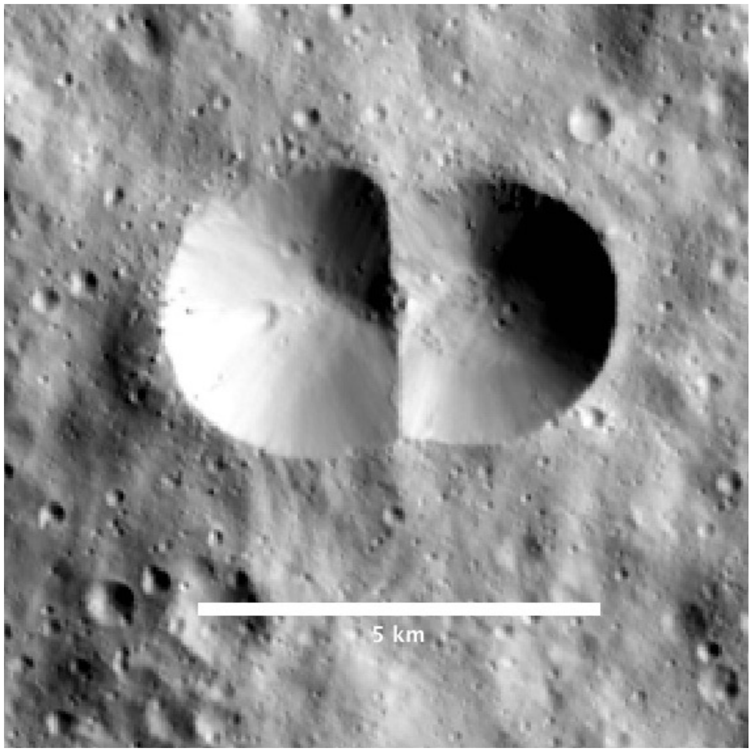

Figure 3-1. A "Definite" Doublet Crater on Ceres (NASA Dawn image FC0048556)

A larger pair of impact craters is depicted in Pair 2 (Figure 3-2). These two craters are not as young as those in Pair 1, showing a good number of small impact craters that occurred after the two large craters were formed. Even with the higher degree of erosion, the septum wall between the craters is nearly unmistakable. At diameters exceeding 10 km (the larger crater is nearly 14 km), this is the largest observed doublet in the study.

The impact structure shown in Figure 3-3 was initially mistaken for a single impact crater during the counting phase. It was not recognized as a potential double impact event until it came under closer scrutiny as a member of other potential pairs (see sections 2.3.1 and 2.3.2). The rim of this excavation fits well with two circular craters whose rims overlap far enough that there is only a single pit. These structures are often referred to as “peanut-shaped”. This pair is considered “highly likely” to be a true doublet crater. The impactors were separated by less

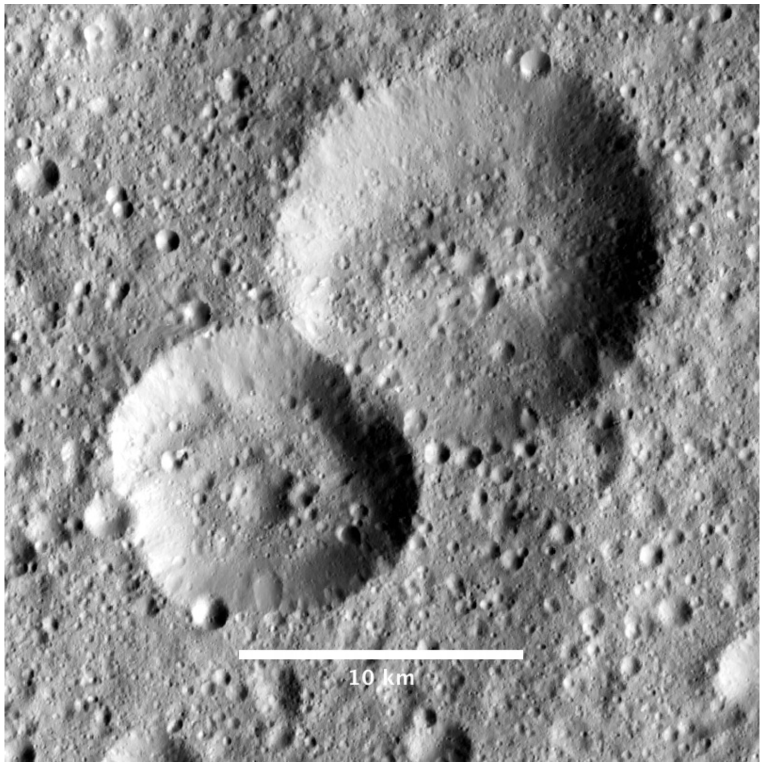

Figure 3-2. Large, "very likely" Doublet Crater on Ceres (NASA Dawn image FC0053565).

than 1.5 km when they struck the surface.

Pair 4 in the table is another example of a peanut-shaped doublet crater (Figure 3-4). It is categorized only as “likely” to be a doublet on the basis of its relatively heavy erosion, which could have erased evidence that it was not a doublet.

Pairs 5 (Figure 3-5) and 6 (Figure 3-6) are both highly eroded, but the remnants of possible radian ejecta lobes and a septum make these two pairs of craters “likely” doublets.

Pair 7 is less eroded than the two previous pairs, and may include a septum (Figure 3-7). Alternatively, these may be coincidental impacts that are fortuitously spaced such that the crater rims touch, but are not part of a single impact event.

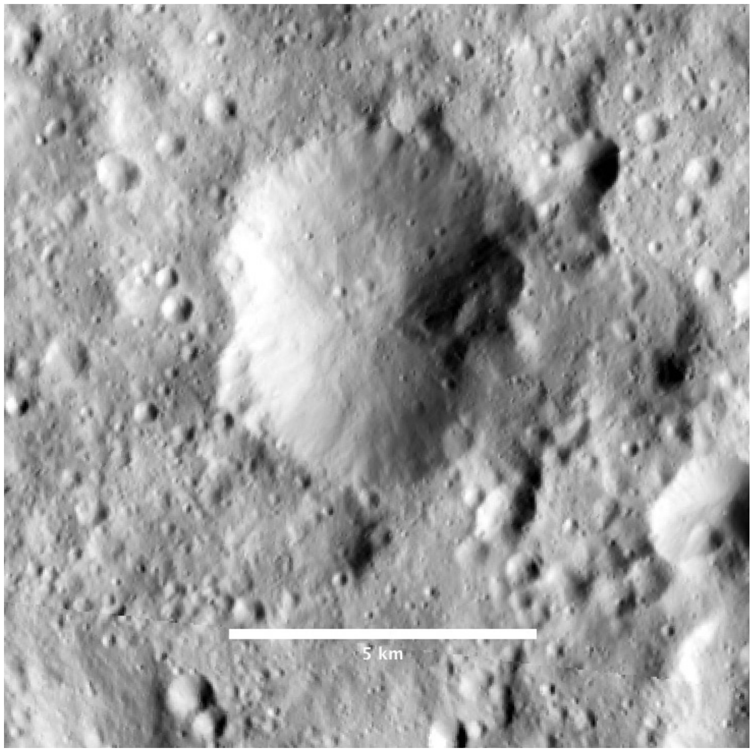

Figure 3-3. Peanut-shaped "very likely" Doublet on Ceres (NASA Dawn image FC0057993).

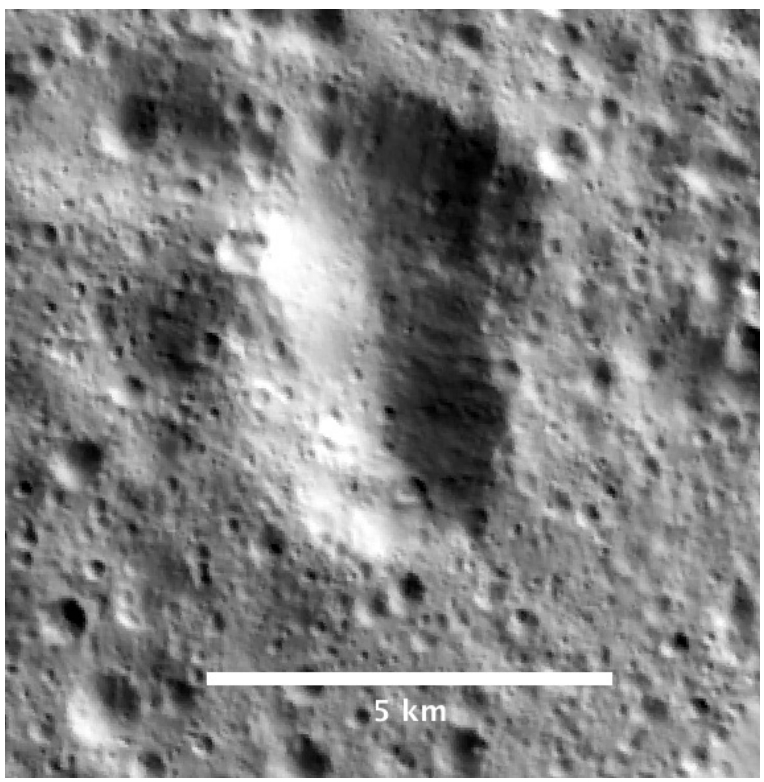

Figure 3-4. A "likely" Peanut Doublet Crater on Ceres (NASA Dawn image FC0064514).

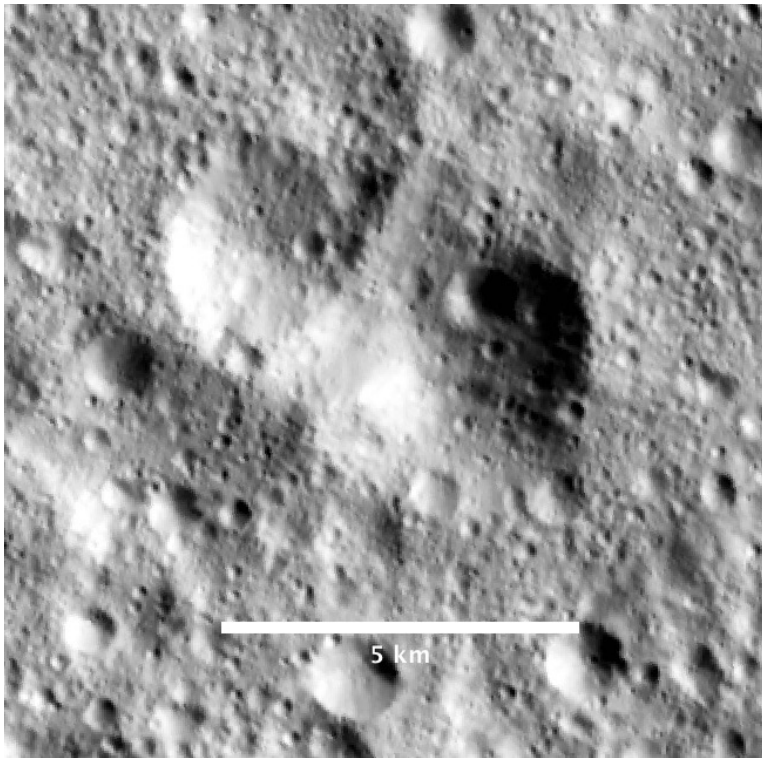

Figure 3-5. Highly-eroded "likely" Doublet with possible septum and ejecta lobes (NASA Dawn image FC0052195).

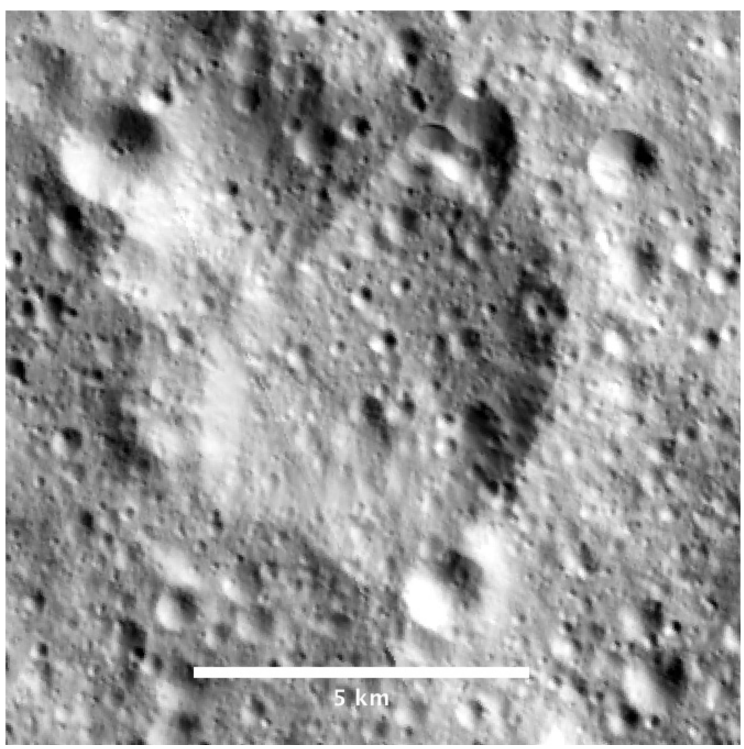

Figure 3-6. Highly-eroded Doublet with possible septum and lobes (Dawn image FC0051873).

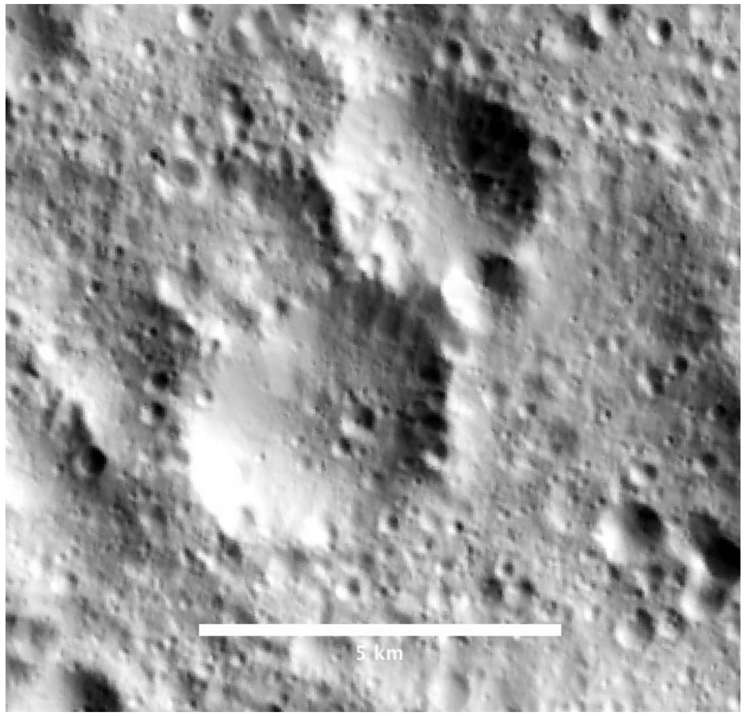

Figure 3-7. Eroded Doublet with possible septum (Dawn image FC 0056991).

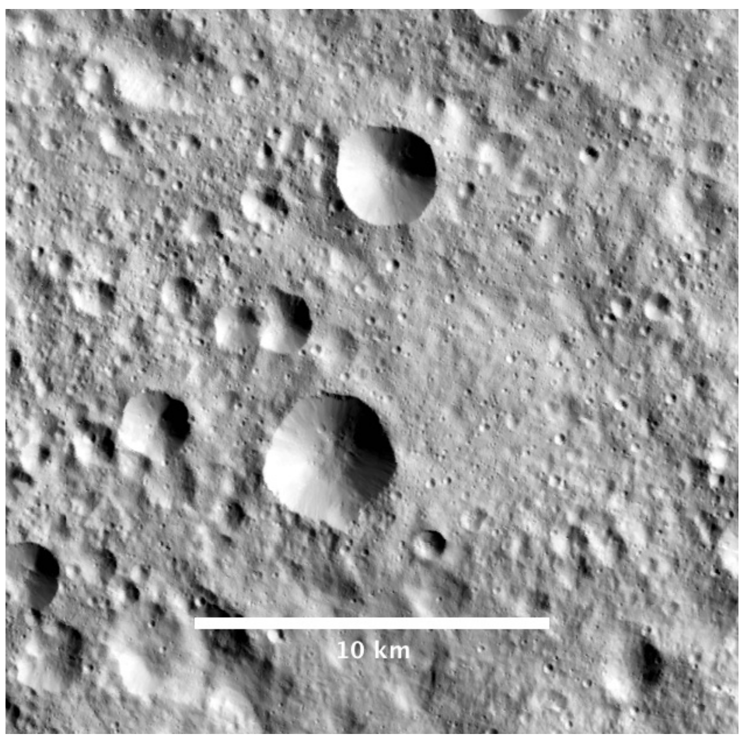

Figure 3-8. Fresh "possible" Doublet Crater (Dawn image FC0058469).

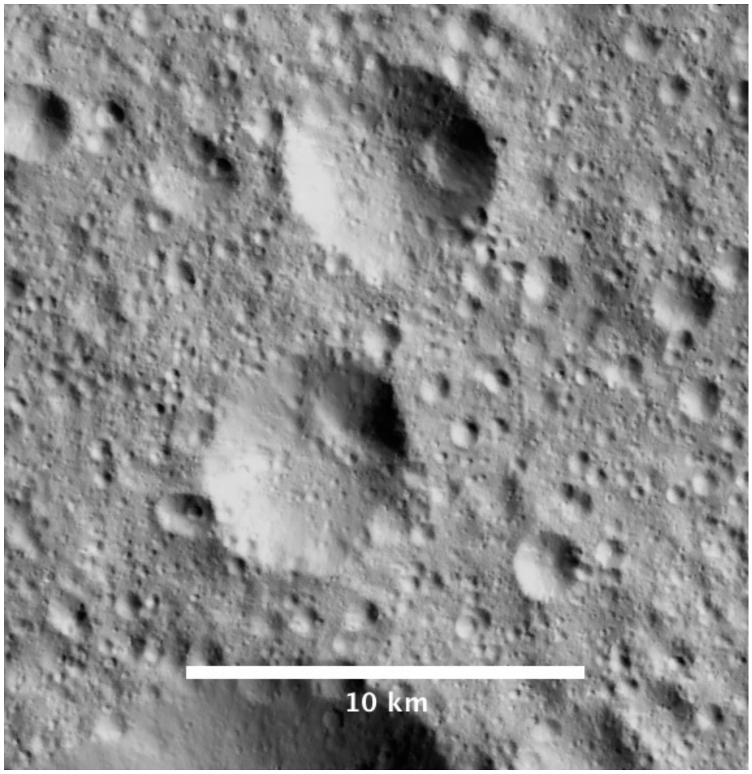

Figure 3-9. "Possible" Doublet Crater on Ceres (Dawn image FC0054371).

The last two crater pairs that are candidates to be true doublets lack any explicit evidence for being the results of binary asteroid impacts. Pair 8 is a fresh pair of similarly-sized craters that appear to be about the same age and have well-formed rims (Figure 3-8). They could be the result of a binary impact, so it is classified as "possible." The craters in Pair 9 are more eroded than Pair 8, but they are similarly eroded and close in size to each other (Figure 3-9). They are also considered to be a "possible" doublet.

3.3 Random Distribution of Craters

As described in section 3.1, 1084 impact craters with diameters equal to or greater than three kilometers were counted in the study area. The Monte Carlo simulation described in section 2.5

(`monetcarlo_phase123.py`) was executed to create 1084 random impact locations in the same area as the study (bounded by 110°E to 270°E and 10°N to 30°S). The software then identified all pairs of simulated craters whose separation was less than 20 km (the same process used in section 3.2.1 to identify candidate pairs of observed craters on Ceres). The Python code created algorithmic bins for tallying separations by distance, as shown in Table 3-2. For all bins except the final one, a separation s will be tallied in the bin if *lower bound* $\leq s <$ *upper bound*. For the final bin, the upper bound is inclusive, i.e., s is tallied if *lower bound* $\leq s \leq$ *upper bound*, but since we exclude the value of 20 kilometers from our selected crater separations, the final bin will never include any counts representing the upper bound value.

Table 3-2: Bins for tallying crater separations by distance in kilometers.

Bin #	***lower bound* (km)**	***upper bound* (km)**
1	1.0	1.349282848
2	1.349282848	1.820564203
3	1.820564203	2.456456052
4	2.456456052	3.314454017
5	3.314454017	4.472135955
6	4.472135955	6.034176337
7	6.034176337	8.141810631
8	8.141810631	10.98560543
9	10.98560543	14.82268898
10	14.82268898	20.0

The simulation was executed 1000 times. Each run produced a different set of 1084 craters, and the number of crater pairs whose separation was less than 20 kilometers varied, as expected. The averaged bin counts for the 1000 runs are shown in Table 3-3.

Table 3-3: Average simulated counts of crater pairs binned by separation.

Bin #	***Simulated crater pairs***
1	3.54
2	6.64
3	11.67
4	21.61
5	39.23
6	71.03
7	128.43
8	232.27
9	420.64
10	755.23

3.4 Estimating Impactor Diameters

Using the crater scaling law shown in Equation 4, estimates were produced for the diameters of the impactors that created all craters with diameters of at most 15 km counted in the study area. Impactor diameter ranged from 134 meters for the smallest crater measured at 3 km, to 1040 meters for the largest crater, which measured 14.9 km in diameter. A full list of these 1021 impact craters appears in Appendix A.

A size-frequency distribution for these 1021 impact craters (see section 3.1) is shown in **Figure 3-10**. The average impactor size is 248.2 meters in diameter. Note that we only counted craters that were at least 3 km in diameter, so we are excluding impactors that we would estimate to be below a diameter of 134 meters.

The 18 individual impact craters making up the nine candidate doublets are shown in Table 3-4 along with their estimated diameters. The mean diameter of impactors involved in candidate doublets is 246.8 meters.

Table 3-4: Candidate Doublet Craters with computed impactor diameters.

Crater Pair	***Longitude***	***Latitude***	***Diameter (km)***	***Separation (km)***	***Impactor Diameter (m)***
Pair 1	228.633	-9.703	3.2	2.16	145.9
	228.367	-9.695	3.5		163.6
Pair 2	170.487	9.613	10.8	10.47	686.2
	171.366	10.540	13.8		940.7
Pair 3	216.578	9.367	4.3	1.63	212.8
	216.570	9.176	3.7		175.6
Pair 4	154.906	-29.375	3.2	2.65	145.9
	154.93	-29.695	3		134.4
Pair 5	252.679	-13.583	3.0	2.92	134.4
	252.938	-13.831	3.2		145.9
Pair 6	251.772	-21.941	3.0	3.26	134.4
	252.024	-22.236	5.3		277.9
Pair 7	218.295	-21.601	3	3.55	134.4
	218.064	-21.974	3.5		163.6
Pair 8	255.199	-17.097	3.6	8.01	169.6
	255.426	-16.152	3.0		134.4
Pair 9	132.27	-26.360	5.2	7.47	271.3
	132.016	-27.234	5.2		271.3

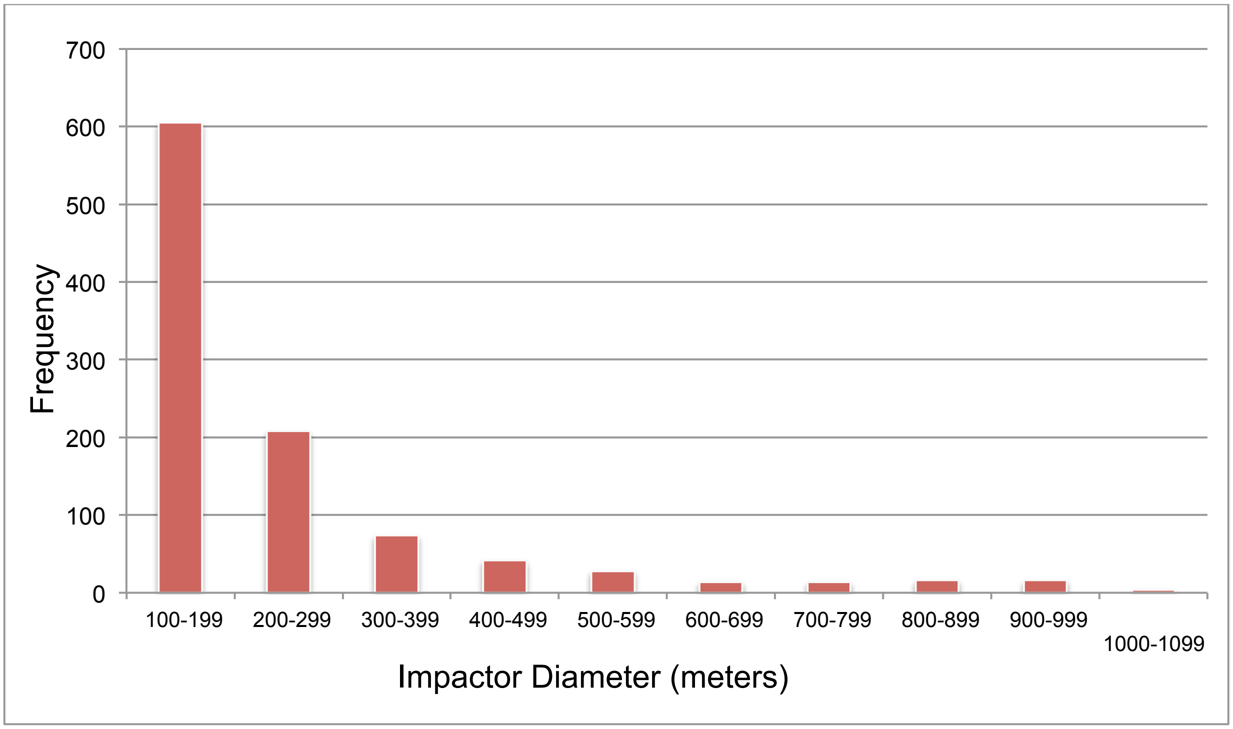

Figure 3-10. Size-frequency distribution of impactors that created craters ≤ 15 km in study area.

4 INTERPRETATION AND CONCLUSIONS

This chapter presents further analyses and interpretations of this study's results.

4.1 Comparing Random Crater Separations to Observed Separations

Comparing the results of the Monte Carlo simulation described in Section 3.3 with the distribution of actual separations between observed craters (the 2037 crater pairs identified in section 3.2.2) could reveal if there is a non-random pattern to the observed craters in the study area. The observed separations were tallied into the same logarithmic bins defined in Table 3-2, and the results are presented in Table 4-1.

Table 4-1: Observed counts of crater pairs binned by separation.

Bin #	***Observed crater pairs***
1	1
2	4
3	5
4	25
5	49
6	84
7	141
8	273
9	554
10	890

Figure 4-1 shows the graphing the bin values from Table 3-3 and Table 4-1. The blue line represents randomized crater separations, and the observed separations are the red line. While the same comparison showed some promising localized excesses that corresponded to the separations of observed doublets in the pilot study (as described in section 2.3.1), the graph in Figure 4-1 depicts no perceptible localized excesses. This is a result of the large sample size, which overpowers the handful of likely doublets discovered in the larger study area.

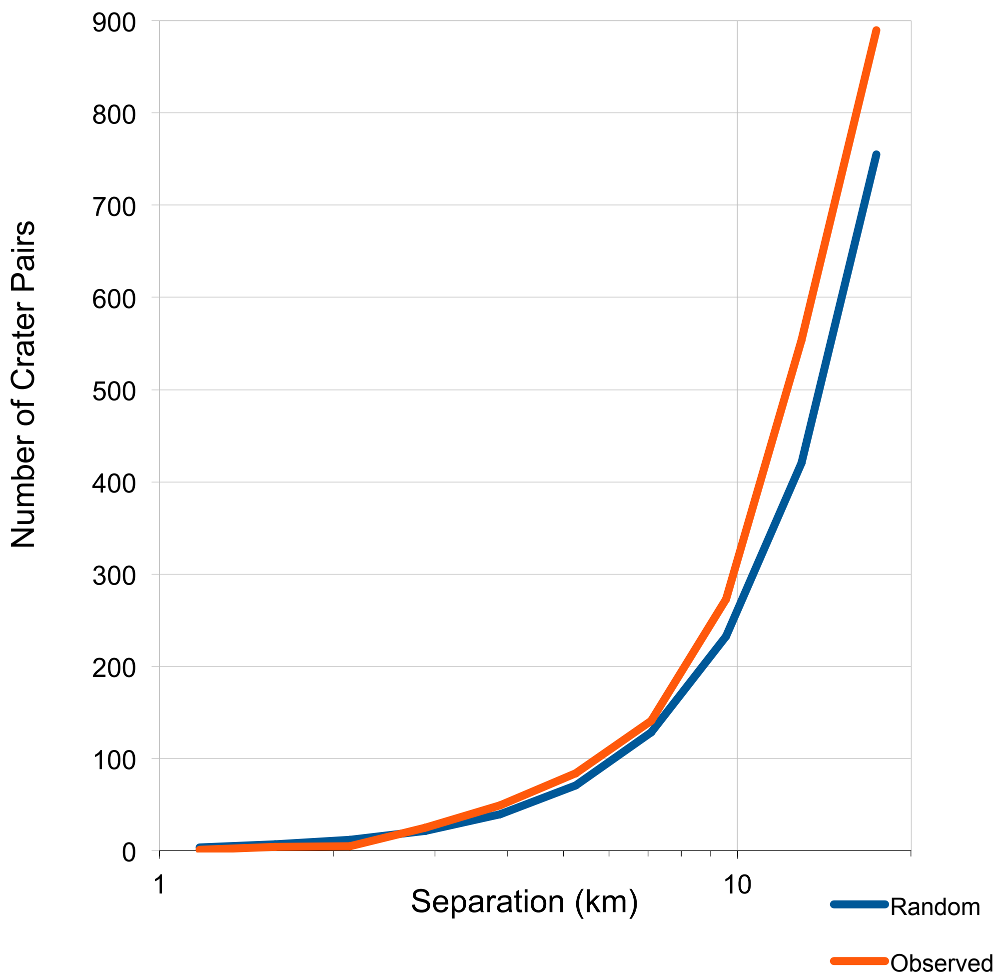

Figure 4-1. Observed counts of crater pairs by separation (Table 4-1), plotted against expected distribution of separations for random impacts (Table 3-3).

Plotting the same data without the 20-kilometer upper limit for crater separations revealed that the observed line (red) and the random line (blue) begin to converge at a separation of 150 km, and the observed line is ultimately overtaken by the random line at a separation of about 320 km. Why are the observed craters resulting in more pairs that are closer together than the Monte Carlo model showed? I suspect that secondary impact craters from some of the larger craters close to the study area are the cause. Secondary craters cluster in non-random patterns, since many of the impactors are ejected from the same primary impact source and strike nearly simultaneously. Since secondary ejecta are at the small end of the impactor size range and strike close together (sometimes in pairs or chains), they would inflate the number of crater pairs with small separations, lifting the observed graph line above the one produced solely from random impacts.

4.2 Doublet Craters on Ceres

If Pairs 1 through 7 (from Table 3-4) are true doublet craters, this sets 0.7% as a lower bound for the percentage of impact events (≤ 15 km in diameter) in the study area that resulted from binary asteroid impactors. This percentage is based on 1021 originally counted craters, reduced to 1014 unique impact events since the doublets are seven events each involving 2 craters. This bound of 0.7% is below the current estimate of 1-2% for Earth, and the estimate of 2-3% for Mars (Miljković et al., 2013).

4.3 Implications for Binary Asteroids in the Main Belt

Through the detection of even the one “definite” doublet crater (Figure 3.1), this research demonstrates that binary asteroids with components smaller than one kilometer in diameter exist in the Main Belt. The next question is: how many of the small asteroids in the Main Belt are binaries?

Two different situations can result in a pair of asteroids impacting a target surface with a separation smaller than their maximum orbital separation: The orbital plane of two co-orbiting asteroids relative to the planar surface on the target, and the positions of the two asteroids in their orbit (Melosh and Stansberry, 1991). Either of these can independently contribute to binaries impacting much closer to one another than their orbital distance, and a sizeable percentage of such impact events will result in one impactor landing on the other. In such a case, the result is a single crater with no visible evidence that two impactors were involved.

Bottke and Melosh (1996) applied Melosh and Stansberry's model (1991) to simulate 10,000 binary asteroid systems impacting various inner Solar System planets, and also concluded that to form a visible doublet crater, the following must be true: $\Delta/(r_1 + r_2) > 1.0$, where Δ is the separation at impact, and r_1 and r_2 are the radii of the respective impactors. They found that on average, only 23% of well-separated binary asteroids would produce a visible doublet crater. Miljković et al. (2013) estimate a more conservative range of 10-15% for impacting binaries that produce a visible doublet.

Assuming that 15% of impacting binaries create visible doublets, the observed percentage of 0.7% for impact events on Ceres that are doublets (Section 4.2) would allow the placement of a lower bound of 4.6% for the percentage of Main Belt asteroids of diameter less than 1 km that are binary. This is notably smaller than the radar and photometric studies that show approximately 15% of all NEAs and MBAs are binaries (Miljković et al., 2013; Pravec et al., 2006).

Why such a small percentage for these small binaries in the Main Belt, compared to planet-crossing and larger Main Belt asteroid populations? One contributing factor to a lower number of binary systems could be the lack of encounters with planetary masses in the Main Belt. Without such encounters, contact binaries are likely to stay contact binaries. Another possibility is that these small binary systems could be Escaping Ejecta Binaries (EEBs), produced by high-energy collisions (Durda et al., 2004). The binary asteroids that created the doublets identified in this study are small (most less than 0.5 km), and close in size to each other. They are consistent with the component sizes in EEBs predicted by Durda et al. (2004), and are not consistent with the YORP binaries described by Walsh and Jacobsen (2015), which feature large rubble pile primaries and much smaller satellites. Even though simulations showed large numbers of EEBs should result from catastrophic collisions (Durba et al., 2004), Walsh and Jacobsen (2015) suspect most EEBs would not be stable over long time scales (on the order of the age of the solar system), and since collisions are much rarer now, most EEBs created in the distant past may have become gravitationally unbound. This may not be inconsistent with the lower percentage of small binaries indicated by doublet craters on Ceres.

4.4 Future Work

Seldom is any line of inquiry exhausted, and this research is no exception. This section addresses some areas where the study could be improved or expanded.

For example, one could question whether all that could be done to eliminate crater pairs from the list of candidate doublets has been done. Craters resulting from secondary impacts of ejecta from much larger craters can be detected through morphological means, whether by determining the angles of oblique impacts don’t match, detecting their rims are irregular and not circular, or even if the depth to diameter ratio is not sufficiently large due to low impactor velocity.

Another improvement in crater pair filtering would be to estimate the upper limit for the separation between two craters if they were created by a binary asteroid impact. Computing the estimated masses of the two impactors from the crater diameters (using the crater scaling law in Section 2.2.5), force equations could be used to estimate the maximum stable orbital separation of the two asteroids, and that distance is used as the largest possible separation that could be supportive of a binary impact. This would be more effective in eliminating crater pairs that could not be doublets that were below the arbitrary 20-kilometer limit, and also open up the possible detection of doublets involving much larger craters with commensurate large separation distances.

During this work, multiple doublet impact structures were noted but not included, since their component craters were below the diameter threshold of the study. The Framing Camera images seem to have sufficient resolution to lower the diameter threshold.

Ceres is not the only crater-covered large body in the Main Belt that has been visited by the Dawn spacecraft. Similar data available for 4 Vesta would provide an opportunity to compare doublet craters on these two large asteroids, which show a different surface history and occupy a different region of the Main Belt. A separate study of doublet craters on 4 Vesta would likely be quite rewarding.

A Impact Craters Considered in Study

This appendix contains a list of the 1021 craters ≤ 15 km counted in the study area, including an estimated diameter for the impactor that created each crater.

Crater #	***Longitude***	***Latitude***	***Diameter (m)***	***Impactor Diameter (m)***
1	258.463	-17.341	3000	134.4
2	255.426	-16.152	3000	134.4
3	253.508	-16.685	3000	134.4
4	252.679	-13.583	3000	134.4
5	256.622	-11.029	3000	134.4
6	257.827	-16.434	3000	134.4
7	254.448	-19.573	3000	134.4
8	255.459	-20.777	3000	134.4
9	251.772	-21.941	3000	134.4
10	251.215	-24.928	3000	134.4
11	256.429	-21.995	3000	134.4
12	256.831	-24.793	3000	134.4
13	257.207	-29.123	3000	134.4
14	252.002	-28.994	3000	134.4
15	255.089	-23.205	3000	134.4
16	251.662	-21.559	3000	134.4
17	254.645	-21.797	3000	134.4
18	255.086	-20.572	3000	134.4
19	261.189	-23.371	3000	134.4
20	263.060	-23.443	3000	134.4
21	260.700	-24.108	3000	134.4
22	260.536	-21.280	3000	134.4
23	262.885	-27.650	3000	134.4
24	265.089	-24.617	3000	134.4
25	268.890	-25.130	3000	134.4
26	268.606	-24.971	3000	134.4
27	265.685	-20.394	3000	134.4
28	265.929	-15.805	3000	134.4
29	266.640	-11.073	3000	134.4
30	266.929	-17.207	3000	134.4
31	253.087	-10.138	3100	140.1
32	256.003	-15.443	3100	140.1
33	259.162	-15.154	3100	140.1
34	254.118	-13.202	3100	140.1
35	267.191	-24.860	3100	140.1
36	252.900	-11.827	3200	145.9
37	252.938	-13.831	3200	145.9
38	251.078	-11.975	3200	145.9
39	253.317	-14.742	3200	145.9
40	250.236	-17.949	3200	145.9

Crater #	*Longitude*	*Latitude*	*Diameter (m)*	*Impactor Diameter (m)*
41	253.515	-18.099	3200	145.9
42	257.898	-17.972	3200	145.9
43	250.785	-22.843	3200	145.9
44	250.413	-22.422	3200	145.9
45	256.439	-26.957	3200	145.9
46	258.755	-23.187	3200	145.9
47	264.955	-28.888	3200	145.9
48	267.537	-22.828	3200	145.9
49	269.228	-25.301	3200	145.9
50	259.953	-11.125	3200	145.9
51	258.482	-15.348	3300	151.8
52	256.699	-24.483	3300	151.8
53	269.500	-25.804	3400	157.7
54	250.016	-17.516	3500	163.6
55	259.771	-26.107	3500	163.6
56	262.257	-13.891	3500	163.6
57	255.199	-17.097	3600	169.6
58	252.719	-23.732	3600	169.6
59	261.951	-27.115	3600	169.6
60	261.398	-27.557	3600	169.6
61	253.952	-12.410	3800	181.7
62	256.281	-14.008	3800	181.7
63	252.014	-12.463	3800	181.7
64	259.332	-25.994	3800	181.7
65	252.699	-24.208	3900	187.9
66	254.925	-13.050	4000	194.0
67	250.910	-23.100	4000	194.0
68	265.570	-29.293	4000	194.0
69	258.159	-15.328	4100	200.3
70	259.445	-25.366	4100	200.3
71	260.451	-26.531	4200	206.5
72	257.001	-27.978	4300	212.8
73	252.965	-12.413	4400	219.1
74	256.002	-25.332	4700	238.4
75	259.747	-10.249	5000	258.0
76	269.025	-17.816	5100	264.6
77	252.054	-22.236	5300	277.9
78	251.144	-27.787	11600	755.7
79	263.038	-19.740	14900	1040.4
81	230.239	-11.093	3200	145.9
82	231.721	-10.781	3200	145.9
83	230.814	-13.637	3000	134.4
84	237.706	-13.735	3000	134.4
85	238.662	-14.034	3400	157.7
86	240.477	-10.296	4100	200.3
87	241.385	-14.924	3000	134.4
88	233.824	-11.505	11100	714.4
89	238.775	-12.878	6500	360.7
90	238.585	-11.916	8000	470.2
91	241.966	-12.340	3200	145.9
92	247.797	-13.377	3000	134.4
93	242.624	-16.832	3900	187.9
94	248.510	-14.173	3000	134.4
95	247.117	-14.079	3000	134.4
96	248.483	-17.506	3000	134.4

Crater #	***Longitude***	***Latitude***	***Diameter (m)***	***Impactor Diameter (m)***
97	249.554	-17.733	3000	134.4
98	248.822	-18.898	3000	134.4
99	247.457	-18.358	3700	175.6
100	248.185	-20.008	3300	151.8
101	243.393	-21.984	3500	163.6
102	242.273	-20.782	3000	134.4
103	241.301	-22.542	3300	151.8
104	238.001	-21.630	3000	134.4
105	237.993	-17.668	3000	134.4
106	240.153	-23.523	8900	538.8
107	240.957	-24.232	3400	157.7
108	238.070	-23.459	4100	200.3
109	238.802	-24.512	3600	169.6
110	239.974	-25.297	3600	169.6
111	241.919	-23.310	3400	157.7
112	242.103	-27.402	4600	231.9
113	242.049	-27.903	4600	231.9
114	243.246	-28.957	3700	175.6
115	235.400	-24.052	4200	206.5
116	234.072	-23.943	4000	194.0
117	233.802	-27.437	5100	264.6
118	233.159	-20.885	8100	477.7
119	232.140	-20.844	5700	305.0
120	234.287	-19.330	3300	151.8
121	235.840	-19.451	7600	440.4
122	235.278	-18.875	4700	238.4
123	237.139	-17.774	3000	134.4
124	240.777	-19.178	3000	134.4
125	235.344	-17.743	3000	134.4
126	237.617	-23.102	3000	134.4
127	241.561	-20.603	3000	134.4
128	241.412	-17.955	3000	134.4
129	213.444	-16.862	8500	508.1
131	217.438	-13.934	14100	969.6
132	213.044	-13.695	3000	134.4
133	214.115	-13.727	3000	134.4
134	218.853	-15.363	3000	134.4
135	220.623	-13.475	4900	251.4
136	215.762	-16.214	7900	462.7
137	213.398	-14.632	3000	134.4
138	220.692	-14.881	14900	1040.4
139	223.265	-15.868	3000	134.4
140	223.136	-16.737	3100	140.1
141	219.496	-16.390	14000	960.9
143	219.983	-19.203	4000	194.0
144	220.265	-19.539	5300	277.9
145	217.999	-19.809	7200	411.0
146	213.820	-17.915	5600	298.2
147	213.503	-18.639	5500	291.4
148	216.096	-18.832	3000	134.4
149	211.476	-16.581	3100	140.1
150	214.380	-19.974	9100	554.3
151	215.387	-21.355	3300	151.8
152	214.843	-21.840	4900	251.4
153	212.067	-21.302	3000	134.4

Crater #	***Longitude***	***Latitude***	***Diameter (m)***	***Impactor Diameter (m)***
154	217.354	-20.613	3000	134.4
155	218.295	-21.601	3000	134.4
156	218.063	-21.974	3500	163.6
157	220.971	-20.990	6000	325.6
158	216.527	-22.896	7100	403.7
159	212.314	-22.243	8400	500.4
160	220.923	-18.669	4100	200.3
161	222.599	-18.817	5900	318.7
162	214.642	-23.992	3000	134.4
163	217.390	-25.482	3400	157.7
164	221.111	-23.153	5000	258.0
165	222.845	-24.244	10000	625.2
166	222.052	-25.621	3400	157.7
167	218.176	-26.679	3200	145.9
168	221.197	-26.488	3000	134.4
169	223.789	-25.774	3000	134.4
170	213.499	-26.981	9000	546.5
171	220.819	-27.186	3800	181.7
172	220.123	-28.211	4100	200.3
173	219.631	-28.586	4100	200.3
174	225.538	-24.487	4000	194.0
175	225.036	-23.282	3000	134.4
176	226.505	-25.675	8300	492.8
177	228.357	-26.993	10500	665.4
178	228.433	-20.763	7200	411.0
179	225.129	-18.175	3000	134.4
180	225.483	-18.415	3000	134.4
181	225.635	-19.927	5000	258.0
182	229.505	-17.329	11300	730.9
183	227.646	-15.433	3000	134.4
184	227.420	-10.899	3000	134.4
185	211.491	-23.552	10000	625.2
186	210.724	-15.361	3300	151.8
187	210.641	6.938	7600	440.4
188	214.664	9.664	9300	569.9
189	216.578	9.367	4300	212.8
190	218.102	9.125	3000	134.4
191	213.406	7.719	6000	325.6
192	213.961	7.414	7200	411.0
193	217.344	6.883	14000	960.9
194	219.219	9.797	3700	175.6
197	217.086	4.320	10500	665.4
198	214.914	4.500	6200	339.6
199	212.484	5.328	5800	311.9
200	212.922	4.719	5900	318.7
201	220.211	3.617	3400	157.7
202	219.539	3.539	5000	258.0
203	220.227	3.078	6500	360.7
204	215.359	3.898	7600	440.4
205	213.617	2.547	11800	772.4
206	220.023	1.461	3600	169.6
207	212.172	1.766	4000	194.0
208	211.727	1.422	4500	225.5
209	216.461	2.047	14200	978.4
211	222.039	1.867	4000	194.0

Crater #	***Longitude***	***Latitude***	***Diameter (m)***	***Impactor Diameter (m)***
212	222.352	8.133	3500	163.6
213	223.000	5.953	3000	134.4
214	226.234	6.164	3000	134.4
215	226.609	6.102	4200	206.5
216	227.805	6.578	10000	625.2
217	229.516	6.016	3000	134.4
218	228.141	8.555	4200	206.5
219	223.195	4.086	5800	311.9
220	226.242	3.492	6800	382.1
221	228.344	3.906	8800	531.1
222	229.164	3.148	5500	291.4
223	227.766	4.242	3000	134.4
224	223.609	1.281	4300	212.8
225	229.211	2.406	7000	396.5
226	221.867	3.234	11800	772.4
228	228.633	-9.703	3200	145.9
229	228.367	-9.695	3500	163.6
230	218.141	-9.531	3000	134.4
231	215.219	-7.430	7200	411.0
232	213.695	-3.711	6500	360.7
234	211.406	-3.734	4100	200.3
235	210.953	-6.586	3300	151.8
236	210.469	-1.969	5100	264.6
237	232.109	9.227	3800	181.7
238	232.289	8.563	3400	157.7
239	232.516	8.289	3500	163.6
240	233.992	6.250	3700	175.6
241	231.094	6.211	3400	157.7
242	233.000	5.258	3000	134.4
243	235.180	7.086	3700	175.6
244	230.172	4.445	3200	145.9
245	237.680	5.406	3000	134.4
246	238.094	4.711	6100	332.6
247	237.406	3.109	3600	169.6
248	232.531	3.555	3200	145.9
249	236.398	3.320	3000	134.4
250	240.102	4.750	4300	212.8
251	240.078	5.141	3700	175.6
252	241.023	5.289	8900	538.8
253	246.516	5.961	4300	212.8
254	243.891	3.188	3000	134.4
255	246.867	6.531	3000	134.4
256	249.320	7.430	4500	225.5
257	248.656	6.688	4100	200.3
258	247.500	6.227	3600	169.6
259	246.609	8.383	3000	134.4
260	245.633	4.766	3400	157.7
261	248.375	3.656	3800	181.7
262	244.852	3.063	3000	134.4
263	249.969	3.742	4000	194.0
264	249.555	1.570	3000	134.4
265	247.539	1.445	4200	206.5
266	245.109	2.359	4100	200.3
267	242.281	0.469	4800	244.9
268	241.516	0.141	3000	134.4

Crater #	***Longitude***	***Latitude***	***Diameter (m)***	***Impactor Diameter (m)***
269	241.602	1.766	4900	251.4
270	241.141	0.477	4400	219.1
271	248.813	-1.383	3000	134.4
272	248.492	-1.656	3800	181.7
273	246.375	-1.875	4800	244.9
274	245.672	-2.422	4900	251.4
275	242.297	-1.578	4500	225.5
276	240.523	-1.117	4000	194.0
277	240.305	-1.969	5000	258.0
278	241.102	-2.375	6000	325.6
279	241.516	-2.703	5300	277.9
280	248.844	-0.250	8200	485.3
281	237.969	-2.125	4000	194.0
282	238.516	-3.000	5000	258.0
283	231.875	1.625	3600	169.6
284	233.156	1.984	8000	470.2
285	231.313	0.531	4000	194.0
286	232.102	0.430	4500	225.5
287	237.156	0.328	3000	134.4
288	233.258	0.703	3500	163.6
289	232.227	-0.617	11000	706.2
290	234.023	-0.672	7300	418.3
291	233.914	-1.023	5300	277.9
292	236.695	-0.250	5800	311.9
293	236.898	-2.320	3600	169.6
294	236.273	-3.000	3800	181.7
295	231.273	-2.984	3300	151.8
296	239.563	-2.078	3000	134.4
297	230.906	1.820	4900	251.4
298	233.039	-3.680	10600	673.5
299	238.398	-5.672	3000	134.4
300	238.805	-6.859	6700	374.9
301	236.180	-8.641	3000	134.4
302	238.203	-8.664	4000	194.0
303	243.938	-6.789	4000	194.0
304	242.555	-6.078	5800	311.9
305	239.750	-4.758	3000	134.4
306	239.703	-5.047	3000	134.4
307	248.273	-6.695	3000	134.4
308	248.430	-6.031	3500	163.6
309	245.383	-7.609	3000	134.4
310	247.086	-8.734	7500	433.0
311	244.461	-6.297	3000	134.4
312	245.617	-6.422	5000	258.0
313	245.078	-6.148	4300	212.8
314	242.633	-5.391	4500	225.5
315	249.008	-4.063	8400	500.4
316	246.219	-9.719	3000	134.4
317	255.680	9.758	3000	134.4
318	256.820	9.273	3000	134.4
319	251.219	6.781	4600	231.9
320	257.508	2.961	8200	485.3
321	255.461	1.930	3100	140.1
322	254.078	2.320	3800	181.7
323	250.172	2.563	5100	264.6

Crater #	***Longitude***	***Latitude***	***Diameter (m)***	***Impactor Diameter (m)***
324	251.297	1.742	4700	238.4
325	252.195	-0.031	5400	284.7
326	254.016	5.367	4000	194.0
327	258.156	-0.164	3000	134.4
328	257.625	-0.320	3300	151.8
329	256.258	-0.281	3000	134.4
330	256.648	-0.852	3300	151.8
331	256.211	-1.180	3200	145.9
332	259.047	-1.391	5400	284.7
333	255.141	-0.336	3400	157.7
334	258.570	-2.602	4600	231.9
335	251.938	-2.359	3000	134.4
336	253.836	-5.078	3000	134.4
337	261.172	-3.398	5700	305.0
338	260.625	-3.875	3300	151.8
339	257.242	-3.898	3000	134.4
340	258.453	-9.063	3000	134.4
341	257.930	-9.125	6200	339.6
342	256.836	-6.406	8200	485.3
343	258.055	-7.695	3000	134.4
344	262.680	-4.281	4300	212.8
345	265.328	-4.945	5600	298.2
346	268.906	-6.477	5100	264.6
347	269.305	-2.867	3000	134.4
348	269.266	-1.727	4000	194.0
349	262.898	4.547	3000	134.4
350	267.273	4.563	13000	874.1
351	259.352	3.555	3000	134.4
352	268.898	7.086	4100	200.3
353	267.320	8.789	3000	134.4
354	266.156	8.172	4200	206.5
355	263.789	7.125	3000	134.4
356	262.375	9.430	5100	264.6
358	216.570	9.176	3700	175.6
359	191.761	-10.611	8000	470.2
360	193.133	-12.721	11700	764.1
361	194.255	-10.245	12700	848.4
362	195.861	-10.215	13700	934.6
365	190.163	-13.945	4700	238.4
366	190.518	-15.976	3000	134.4
367	196.794	-12.509	6000	325.6
368	194.372	-11.844	4000	194.0
369	195.070	-13.867	13200	891.3
370	197.439	-13.895	3200	145.9
371	196.537	-15.293	3000	134.4
372	193.398	-14.037	3000	134.4
373	197.997	-13.449	8100	477.7
374	192.841	-15.947	12500	831.4
375	191.595	-15.101	9000	546.5
376	200.808	-10.607	4000	194.0
377	200.168	-14.031	3000	134.4
378	201.049	-15.286	5000	258.0
379	195.616	-18.571	7000	396.5
381	201.102	-15.942	3000	134.4
383	202.763	-21.088	12200	806.0

Crater #	***Longitude***	***Latitude***	***Diameter (m)***	***Impactor Diameter (m)***
385	208.141	-14.668	3000	134.4
386	191.537	-25.791	11200	722.6
387	200.618	-24.890	3800	181.7
388	193.119	-27.475	6000	325.6
389	190.442	-28.868	7000	396.5
390	194.939	-29.667	4300	212.8
391	197.192	-29.565	6700	374.9
392	199.026	-29.568	8000	470.2
393	200.834	-28.248	3000	134.4
394	202.908	-27.962	3000	134.4
395	203.902	-28.436	3000	134.4
396	205.136	-22.724	3800	181.7
397	205.805	-22.735	3600	169.6
398	204.003	-27.957	3000	134.4
400	204.891	-17.127	3000	134.4
401	208.883	-18.066	12700	848.4
402	204.804	-13.425	10000	625.2
403	205.587	-10.446	8000	470.2
404	205.760	-11.347	3000	134.4
405	170.250	-11.328	3700	175.6
406	172.961	-12.070	3000	134.4
407	170.664	-14.102	6300	346.6
408	170.320	-15.336	3000	134.4
409	173.188	-15.391	3000	134.4
410	172.375	-15.859	4000	194.0
411	170.914	-16.641	4000	194.0
412	170.984	-16.297	3000	134.4
413	172.641	-16.492	3400	157.7
414	175.844	-11.313	3300	151.8
415	176.656	-11.602	3000	134.4
416	178.188	-16.148	3300	151.8
417	180.141	-13.750	6700	374.9
418	181.305	-12.273	3800	181.7
419	179.430	-11.953	7100	403.7
420	179.469	-11.273	8200	485.3
421	179.375	-16.727	3700	175.6
422	179.906	-16.484	6100	332.6
423	172.781	-17.320	3000	134.4
424	173.203	-17.344	3000	134.4
425	174.547	-17.703	6100	332.6
427	178.867	-17.680	6900	389.3
428	174.586	-20.742	5700	305.0
430	182.141	-17.031	11000	706.2
431	182.039	-18.297	9000	546.5
432	179.492	-19.008	6000	325.6
433	180.219	-20.469	4200	206.5
434	180.281	-21.234	3700	175.6
435	177.266	-22.313	4000	194.0
436	172.305	-19.313	7700	447.8
437	171.734	-17.781	3000	134.4
438	170.188	-17.688	3300	151.8
439	170.539	-19.852	4000	194.0
440	170.789	-20.742	3300	151.8
441	171.281	-20.781	3200	145.9
442	171.031	-22.906	3200	145.9

Crater #	***Longitude***	***Latitude***	***Diameter (m)***	***Impactor Diameter (m)***
443	172.867	-22.859	10400	657.4
444	176.633	-21.320	3000	134.4
445	176.633	-18.094	3000	134.4
446	180.867	-18.344	3600	169.6
447	180.250	-22.438	11100	714.4
448	178.453	-22.945	4000	194.0
449	178.180	-22.273	4000	194.0
450	171.750	-20.633	3000	134.4
451	172.281	-24.172	3000	134.4
452	171.789	-23.836	5000	258.0
453	171.789	-23.836	3000	134.4
454	171.203	-23.797	4000	194.0
455	175.281	-23.742	3000	134.4
457	180.445	-24.188	3000	134.4
458	180.063	-24.469	3300	151.8
459	176.039	-23.008	6400	353.6
460	176.234	-23.711	6000	325.6
461	176.766	-23.516	8000	470.2
462	178.609	-25.102	3000	134.4
463	178.922	-25.313	3500	163.6
464	179.758	-26.172	12200	806.0
465	181.867	-21.727	3500	163.6
466	181.844	-21.344	3000	134.4
467	180.836	-24.305	9000	546.5
468	181.477	-26.531	4600	231.9
469	170.984	-24.664	3000	134.4
470	171.070	-24.773	14000	960.9
471	172.273	-21.703	3000	134.4
473	177.359	-26.867	5000	258.0
474	175.609	-26.844	3000	134.4
475	175.633	-27.664	3000	134.4
476	173.492	-28.164	4000	194.0
477	174.305	-28.563	5000	258.0
478	179.680	-27.117	3000	134.4
479	180.250	-28.344	4000	194.0
480	175.141	-29.016	3000	134.4
481	176.219	-27.273	13000	874.1
482	172.195	-28.133	3000	134.4
483	171.500	-27.500	3000	134.4
484	170.477	-27.266	5000	258.0
485	172.234	-28.852	9000	546.5
486	180.852	-27.469	3000	134.4
487	181.031	-28.070	8400	500.4
488	182.477	-23.195	4000	194.0
489	182.852	-22.320	6000	325.6
490	183.539	-23.820	7000	396.5
491	184.289	-23.539	6000	325.6
492	182.617	-25.258	5100	264.6
493	184.617	-24.250	3000	134.4
494	185.742	-23.547	4300	212.8
495	187.203	-21.992	5000	258.0
496	187.313	-23.883	4600	231.9
497	187.391	-25.492	4900	251.4
498	184.250	-25.258	8000	470.2
499	183.742	-25.961	5300	277.9

Crater #	***Longitude***	***Latitude***	***Diameter (m)***	***Impactor Diameter (m)***
501	184.313	-28.063	5900	318.7
503	182.602	-27.742	3000	134.4
504	182.242	-27.430	5000	258.0
505	181.438	-29.039	3000	134.4
506	178.898	-27.391	3000	134.4
507	185.891	-25.555	3000	134.4
508	188.984	-25.063	3000	134.4
509	187.461	-29.648	3000	134.4
510	186.391	-21.680	5900	318.7
511	181.641	-19.813	5000	258.0
512	182.031	-20.031	4400	219.1
513	182.539	-21.352	3000	134.4
514	185.242	-18.898	8200	485.3
516	187.578	-19.523	5000	258.0
517	187.336	-19.000	5000	258.0
518	186.320	-17.516	5000	258.0
519	187.945	-16.086	3200	145.9
521	188.078	-14.430	3300	151.8
522	188.797	-13.445	6200	339.6
523	185.977	-12.445	3000	134.4
524	183.719	-12.891	3700	175.6
525	181.820	-12.297	3800	181.7
527	181.461	-14.406	7000	396.5
529	180.336	-14.930	3700	175.6
530	188.234	-10.234	3000	134.4
531	189.539	-11.875	3000	134.4
532	185.000	-10.914	4000	194.0
533	184.742	-10.414	4000	194.0
534	184.047	-10.297	4000	194.0
537	185.117	-12.344	3000	134.4
538	150.633	-11.734	4600	231.9
539	150.305	-11.469	10000	625.2
540	157.281	-11.547	3000	134.4
541	158.367	-11.625	4000	194.0
542	155.070	-12.359	3000	134.4
544	158.883	-12.406	3000	134.4
545	157.609	-13.008	4000	194.0
546	155.680	-12.203	3000	134.4
547	154.211	-13.570	3700	175.6
548	154.063	-14.313	5000	258.0
549	152.039	-12.633	3300	151.8
550	158.477	-10.203	3000	134.4
551	153.461	-15.180	4200	206.5
552	151.961	-15.289	4000	194.0
553	159.836	-15.531	5100	264.6
554	157.195	-16.398	3400	157.7
555	160.586	-13.367	6700	374.9
556	155.984	-16.297	4000	194.0
557	153.047	-17.094	4000	194.0
558	154.281	-17.508	4000	194.0
559	155.570	-18.180	3600	169.6
560	154.430	-19.242	3000	134.4
561	150.273	-18.477	5000	258.0
562	150.898	-18.742	4100	200.3
563	151.445	-18.297	4000	194.0

Crater #	*Longitude*	*Latitude*	*Diameter (m)*	*Impactor Diameter (m)*
564	151.211	-19.141	3300	151.8
566	158.328	-18.781	4900	251.4
567	157.031	-14.523	3000	134.4
568	160.281	-17.875	3800	181.7
569	160.695	-18.070	5000	258.0
570	160.609	-18.836	3200	145.9
571	161.352	-18.977	3000	134.4
572	162.039	-18.031	8900	538.8
573	161.742	-13.094	12400	822.9
574	155.266	-18.641	3000	134.4
575	159.953	-16.234	3000	134.4
576	160.305	-19.672	3000	134.4
577	153.688	-20.266	3000	134.4
578	151.203	-20.172	4000	194.0
579	151.586	-22.578	5400	284.7
580	154.086	-20.883	5000	258.0
581	153.836	-22.898	3700	175.6
583	153.367	-23.500	5000	258.0
584	154.977	-23.375	4000	194.0
585	152.891	-24.336	3200	145.9
586	155.492	-25.367	3000	134.4
587	159.070	-24.594	3000	134.4
588	162.016	-22.516	3600	169.6
589	153.813	-24.625	3200	145.9
590	156.664	-28.414	3200	145.9
591	157.234	-24.945	3000	134.4
592	151.063	-28.336	3000	134.4
593	151.766	-28.086	5000	258.0
594	154.906	-29.375	3200	145.9
595	154.930	-29.695	3000	134.4
596	158.063	-29.625	3600	169.6
597	157.563	-26.578	13000	874.1
598	160.266	-28.766	3000	134.4
599	157.656	-25.438	4000	194.0
600	158.102	-25.563	5100	264.6
601	160.148	-28.344	3000	134.4
602	163.008	-28.984	3000	134.4
603	164.922	-28.648	7000	396.5
604	164.266	-26.109	3000	134.4
605	165.180	-25.414	3300	151.8
606	165.625	-26.695	3600	169.6
607	163.203	-27.945	3000	134.4
608	167.109	-25.469	5000	258.0
609	168.633	-28.203	3000	134.4
610	169.383	-28.516	5700	305.0
611	169.242	-25.336	3200	145.9
612	164.500	-22.883	3300	151.8
613	163.625	-24.336	3300	151.8
614	163.703	-22.484	4200	206.5
615	163.500	-20.617	10200	641.3
616	161.250	-22.719	3000	134.4
617	165.484	-20.445	3000	134.4
618	167.133	-20.742	5000	258.0
620	166.164	-19.258	3200	145.9
621	165.398	-19.281	3200	145.9

Crater #	***Longitude***	***Latitude***	***Diameter (m)***	***Impactor Diameter (m)***
622	164.891	-14.898	5700	305.0
623	166.492	-13.141	3300	151.8
624	163.688	-13.141	3000	134.4
625	164.008	-13.453	3000	134.4
626	163.266	-13.328	4000	194.0
627	164.914	-17.617	4700	238.4
628	166.336	-17.875	3000	134.4
629	169.570	-14.828	5000	258.0
630	169.516	-13.563	4500	225.5
631	161.750	-11.008	3700	175.6
632	162.070	-11.195	3400	157.7
633	164.219	-11.266	3000	134.4
634	164.508	-10.992	4100	200.3
635	163.383	-12.297	3000	134.4
636	164.688	-12.094	3600	169.6
637	165.375	-10.664	3400	157.7
638	166.273	-10.148	3000	134.4
639	130.141	-12.773	3200	145.9
640	135.828	-10.438	6400	353.6
641	132.008	-13.336	3000	134.4
642	133.180	-14.680	3000	134.4
643	131.570	-15.367	4100	200.3
644	130.578	-16.453	4200	206.5
645	132.969	-16.086	5200	271.3
646	134.852	-16.234	6900	389.3
647	134.672	-11.766	5900	318.7
648	136.320	-11.820	3000	134.4
649	135.156	-12.742	6300	346.6
650	134.164	-13.406	13300	899.9
652	135.383	-15.102	3000	134.4
653	139.688	-12.242	4600	231.9
654	137.320	-13.992	4000	194.0
655	136.703	-10.523	3500	163.6
656	136.328	-16.531	7800	455.3
657	139.523	-14.234	3000	134.4
658	139.594	-14.586	3200	145.9
659	130.672	-17.688	4000	194.0
660	131.961	-17.953	8900	538.8
661	134.602	-18.094	5200	271.3
662	134.063	-20.234	5400	284.7
663	132.984	-20.555	3000	134.4
664	131.117	-22.367	4000	194.0
665	136.852	-18.945	3300	151.8
666	137.258	-20.008	13000	874.1
667	139.391	-17.313	3700	175.6
668	139.813	-19.234	4200	206.5
669	141.789	-19.328	3000	134.4
670	140.492	-20.391	5700	305.0
671	139.781	-20.953	6200	339.6
672	142.133	-20.961	13400	908.6
673	131.258	-19.594	3600	169.6
674	134.359	-21.352	4000	194.0
675	134.320	-23.148	3200	145.9
677	140.539	-25.344	9100	554.3
678	137.344	-25.508	3000	134.4

Crater #	*Longitude*	*Latitude*	*Diameter (m)*	*Impactor Diameter (m)*
679	136.727	-25.563	3000	134.4
680	139.133	-26.648	3000	134.4
681	132.273	-26.359	5200	271.3
682	132.016	-27.234	5200	271.3
683	134.211	-26.172	5000	258.0
684	137.938	-27.875	4200	206.5
685	140.742	-26.406	3600	169.6
686	138.547	-29.266	3300	151.8
687	140.477	-29.000	3200	145.9
688	140.008	-28.922	3000	134.4
690	137.820	-29.461	3000	134.4
691	140.414	-29.875	4000	194.0
692	144.102	-29.492	3000	134.4
694	143.219	-24.203	4500	225.5
695	143.219	-25.094	4700	238.4
696	144.703	-24.758	3000	134.4
697	146.406	-24.500	3100	140.1
698	149.211	-24.180	3200	145.9
699	145.359	-25.766	3000	134.4
700	147.125	-27.656	3100	140.1
701	145.898	-22.867	5700	305.0
702	148.203	-24.477	3000	134.4
703	143.734	-23.469	3300	151.8
704	141.359	-22.414	3000	134.4
705	144.805	-20.477	3000	134.4
706	144.711	-20.305	3800	181.7
707	145.609	-20.805	3000	134.4
708	146.641	-20.930	5000	258.0
709	147.711	-21.539	3700	175.6
710	148.164	-21.547	3300	151.8
711	149.281	-22.000	4300	212.8
712	149.625	-20.406	7300	418.3
713	147.969	-19.563	8400	500.4
714	149.305	-19.102	3000	134.4
715	142.922	-18.781	5700	305.0
716	145.156	-17.742	4400	219.1
717	145.258	-19.008	3000	134.4
718	146.102	-20.141	4000	194.0
719	144.266	-18.688	3300	151.8
720	141.586	-18.469	3400	157.7
721	140.984	-17.633	3000	134.4
722	147.031	-17.102	3000	134.4
723	143.484	-16.305	3000	134.4
724	143.016	-16.297	3400	157.7
725	143.297	-15.867	5200	271.3
726	144.258	-19.000	3000	134.4
727	147.531	-16.148	3000	134.4
728	147.602	-15.570	4000	194.0
729	141.164	-15.313	4800	244.9
730	145.281	-15.008	6000	325.6
731	147.430	-13.680	4000	194.0
732	149.063	-13.578	3000	134.4
734	144.539	-12.867	4000	194.0
735	145.555	-12.117	4000	194.0
736	143.945	-12.430	5100	264.6

Crater #	***Longitude***	***Latitude***	***Diameter (m)***	***Impactor Diameter (m)***
737	145.180	-11.039	3000	134.4
738	146.547	-11.047	3200	145.9
739	147.195	-10.852	5700	305.0
740	142.320	-10.750	9800	609.3
741	110.164	-10.852	7600	440.4
742	112.141	-10.977	4200	206.5
743	117.047	-10.328	5000	258.0
744	111.773	-12.477	4000	194.0
745	119.852	-13.328	5600	298.2
746	119.289	-16.281	3400	157.7
747	115.859	-16.016	4000	194.0
748	118.016	-16.844	3000	134.4
749	113.516	-17.867	3300	151.8
750	117.531	-19.125	3000	134.4
751	119.797	-18.469	3200	145.9
752	119.352	-18.008	6400	353.6
753	114.203	-17.156	3400	157.7
754	112.930	-17.883	13500	917.2
755	110.430	-21.664	3000	134.4
756	112.547	-20.766	3400	157.7
757	114.789	-20.344	6700	374.9
758	111.672	-20.094	4200	206.5
759	116.805	-22.250	3000	134.4
760	116.492	-22.047	3000	134.4
761	117.031	-24.281	3600	169.6
762	118.016	-23.727	3300	151.8
763	119.430	-24.250	6100	332.6
764	117.555	-22.539	3400	157.7
766	111.641	-28.602	3000	134.4
767	111.922	-28.453	5000	258.0
768	114.813	-25.453	3000	134.4
769	116.531	-27.313	5900	318.7
770	117.453	-28.367	3000	134.4
772	120.047	-27.297	9000	546.5
773	119.313	-29.211	5100	264.6
774	114.500	-29.148	4400	219.1
775	112.711	-29.594	4300	212.8
776	121.063	-27.109	3000	134.4
777	124.609	-27.234	3300	151.8
778	121.273	-28.711	3000	134.4
779	122.688	-29.063	4200	206.5
780	120.070	-25.641	13400	908.6
781	123.359	-29.563	3400	157.7
782	125.727	-24.117	4000	194.0
783	126.906	-25.852	3000	134.4
784	127.523	-25.672	3000	134.4
785	125.828	-28.164	3000	134.4
786	128.219	-23.344	5100	264.6
788	126.602	-22.641	5100	264.6
789	122.266	-21.711	4400	219.1
790	126.617	-20.172	3100	140.1
791	127.602	-20.016	7600	440.4
792	123.266	-19.805	3800	181.7
793	126.234	-17.570	5500	291.4
794	128.539	-17.344	4100	200.3

Crater #	***Longitude***	***Latitude***	***Diameter (m)***	***Impactor Diameter (m)***
795	128.992	-17.547	3500	163.6
796	126.102	-18.805	3000	134.4
797	127.078	-19.688	3000	134.4
798	125.258	-19.250	3700	175.6
799	122.516	-18.969	3000	134.4
800	121.023	-17.469	3200	145.9
801	125.016	-17.555	6300	346.6
802	126.953	-21.484	3000	134.4
803	127.203	-12.977	10400	657.4
804	124.250	-14.672	8000	470.2
805	126.203	-14.211	3000	134.4
806	126.164	-12.328	3000	134.4
807	129.352	-13.805	4000	194.0
808	129.375	-13.633	3300	151.8
809	129.297	-12.445	3000	134.4
811	116.375	-2.500	3400	157.7
812	118.320	-2.586	3500	163.6
813	117.477	-0.547	3300	151.8
814	111.719	-4.492	14700	1022.6
816	112.852	-6.195	10400	657.4
817	114.398	-3.969	3000	134.4
818	119.734	-1.641	3100	140.1
819	120.164	-4.063	8600	515.7
820	118.820	-6.617	4100	200.3
821	116.539	-7.297	13000	874.1
822	114.492	-7.055	5000	258.0
823	114.922	-9.367	4000	194.0
824	116.453	-9.414	4000	194.0
825	118.172	-9.438	5000	258.0
826	117.828	-9.188	3000	134.4
827	118.750	-7.852	4500	225.5
828	119.227	-7.961	4000	194.0
829	121.727	-3.719	3600	169.6
830	122.211	-4.328	5400	284.7
831	124.656	-5.492	7700	447.8
832	125.078	-4.563	3000	134.4
833	124.359	-8.383	4400	219.1
834	127.844	-9.016	4000	194.0
835	127.766	-9.859	3500	163.6
836	122.563	-9.758	3100	140.1
837	122.969	-0.570	12600	839.9
838	126.039	-1.188	4700	238.4
839	127.344	-3.313	3000	134.4
840	132.750	-2.133	4500	225.5
841	131.766	-4.563	4000	194.0
842	132.086	-4.938	4300	212.8
843	132.055	-5.672	4300	212.8
844	134.633	-4.117	4800	244.9
845	136.617	-4.391	4000	194.0
846	138.602	-3.102	3000	134.4
847	131.664	-6.547	3000	134.4
848	131.883	-7.492	4300	212.8
849	134.313	-7.438	5000	258.0
850	132.945	-8.047	9200	562.1
851	133.922	-8.672	3700	175.6

Crater #	***Longitude***	***Latitude***	***Diameter (m)***	***Impactor Diameter (m)***
852	139.711	-7.297	5000	258.0
853	139.008	-8.141	4000	194.0
854	137.719	-5.445	3800	181.7
855	135.375	-8.391	4600	231.9
856	139.773	-5.391	3000	134.4
857	140.172	-9.211	5600	298.2
858	140.375	-7.438	3000	134.4
859	141.867	-3.820	3200	145.9
860	142.141	-5.500	3200	145.9
861	143.750	-5.344	3000	134.4
862	142.961	-8.281	3300	151.8
863	144.188	-3.352	3000	134.4
864	145.422	-5.758	4400	219.1
865	145.625	-6.297	4800	244.9
866	146.430	-4.586	4200	206.5
867	147.422	-4.195	4100	200.3
868	149.078	-3.219	4000	194.0
869	148.453	-9.773	4300	212.8
870	147.492	-8.672	4300	212.8
871	143.117	-7.852	4400	219.1
872	142.313	-8.711	3500	163.6
873	149.875	-8.336	9400	577.7
875	149.961	-5.617	3600	169.6
876	147.172	-1.422	3100	140.1
877	143.625	-1.180	13600	925.9
878	193.555	7.641	5100	264.6
879	193.289	4.148	3000	134.4
881	191.994	3.702	11199.96345	722.6
882	191.974	2.664	9553.815081	589.8
883	199.024	8.506	13547.89405	921.4
884	198.914	5.733	3239.839863	148.2
886	198.844	4.188	3000	134.4
887	198.367	7.844	6700	374.9
888	200.438	4.578	3600	169.6
889	200.813	4.633	8200	485.3
890	197.719	2.844	3600	169.6
891	199.719	2.734	14300	987.2
892	193.141	-0.016	3800	181.7
893	194.055	-0.484	3200	145.9
895	201.125	1.547	3200	145.9
896	196.625	-0.633	3300	151.8
897	200.305	-0.234	8000	470.2
898	192.227	-4.516	3800	181.7
899	192.531	-4.891	8000	470.2
900	190.305	-5.484	5600	298.2
901	196.898	-7.055	3000	134.4
902	200.063	-5.430	9300	569.9
903	192.711	-6.773	3000	134.4
904	190.125	-6.625	5200	271.3
905	190.438	-7.453	3000	134.4
906	197.422	-9.703	4100	200.3
907	200.445	-7.430	5100	264.6
908	203.313	-5.648	8200	485.3
909	202.703	-8.852	4200	206.5
910	206.398	-7.609	3600	169.6

Crater #	***Longitude***	***Latitude***	***Diameter (m)***	***Impactor Diameter (m)***
911	207.703	-7.234	3200	145.9
912	207.648	-0.875	3000	134.4
913	208.094	-1.922	12800	857.0
914	206.102	3.367	6000	325.6
915	206.242	9.773	4900	251.4
916	200.063	8.727	3000	134.4
917	199.266	9.500	3000	134.4
922	176.781	-2.047	3000	134.4
923	177.992	6.086	3900	187.9
924	188.359	9.352	4000	194.0
925	184.094	5.852	4600	231.9
926	183.398	5.438	3800	181.7
927	181.852	4.109	5100	264.6
928	186.328	3.875	3600	169.6
929	186.352	3.141	12000	789.2
930	181.797	8.852	6300	346.6
931	186.945	1.906	4000	194.0
932	177.148	1.828	5200	271.3
933	174.602	6.234	5800	311.9
934	172.625	5.383	14700	1022.6
936	171.102	5.031	3000	134.4
937	170.625	6.563	5400	284.7
938	173.836	3.125	7200	411.0
939	177.273	3.141	3000	134.4
940	175.539	6.602	4100	200.3
941	178.773	9.813	3300	151.8
942	176.992	9.477	6800	382.1
943	172.656	8.773	3300	151.8
944	170.031	8.391	3200	145.9
945	170.487	9.613	10755.97544	686.2
946	171.366	10.539	13769.71506	940.7
947	170.914	-2.141	4000	194.0
948	172.375	-2.313	4000	194.0
949	179.875	-1.406	4200	206.5
950	179.602	-2.281	7800	455.3
951	180.531	-1.891	4000	194.0
952	180.477	-1.594	8200	485.3
953	174.711	-2.813	3000	134.4
954	177.023	-1.656	3200	145.9
955	173.578	-5.977	3100	140.1
957	178.938	-6.164	6000	325.6
959	183.359	-8.281	3100	140.1
960	186.180	-8.523	3000	134.4
961	187.000	-6.930	4200	206.5
962	186.477	-7.438	4200	206.5
963	189.070	-8.359	4100	200.3
964	188.891	-3.875	5400	284.7
965	189.375	-2.852	4800	244.9
966	188.891	-3.008	4100	200.3
967	187.914	-3.555	12600	839.9
968	183.953	-7.133	3000	134.4
969	188.555	-0.578	3800	181.7
970	184.602	-1.039	6700	374.9
971	185.414	-2.188	13700	934.6
972	182.828	-0.789	3000	134.4

Crater #	***Longitude***	***Latitude***	***Diameter (m)***	***Impactor Diameter (m)***
973	182.781	-0.430	3000	134.4
976	185.094	0.250	14000	960.9
978	184.188	-4.859	8800	531.1
979	164.844	6.531	6000	325.6
980	162.719	7.813	6100	332.6
981	169.016	5.078	6400	353.6
986	163.059	5.141	5310.004712	278.6
987	164.254	5.199	5566.608285	295.9
988	167.250	-2.750	4600	231.9
989	167.766	-6.344	3200	145.9
990	169.727	-8.484	3100	140.1
991	168.820	-4.758	3000	134.4
992	160.969	-3.883	7300	418.3
993	161.711	-6.320	6400	353.6
994	160.609	-6.977	4600	231.9
995	164.977	-8.430	3000	134.4
996	162.711	-9.109	4200	206.5
997	166.711	-5.883	5500	291.4
998	166.516	-8.602	3200	145.9
999	168.531	-8.820	3300	151.8
1000	160.961	-2.391	5200	271.3
1001	165.086	-4.781	4800	244.9
1002	165.063	-4.328	3300	151.8
1003	166.836	-2.188	3000	134.4
1004	162.531	-1.102	3000	134.4
1005	164.688	-1.133	3300	151.8
1006	166.359	-1.539	3300	151.8
1007	161.969	-0.523	5600	298.2
1008	160.797	-1.305	4500	225.5
1009	160.391	-1.953	5000	258.0
1010	165.469	1.055	3000	134.4
1011	169.633	3.289	6100	332.6
1012	160.891	6.094	4000	194.0
1013	162.500	6.109	3000	134.4
1014	151.641	4.008	6000	325.6
1015	151.516	4.188	4000	194.0
1016	152.563	3.422	5000	258.0
1017	156.102	5.117	3700	175.6
1018	155.328	4.914	3300	151.8
1019	155.008	9.211	5000	258.0
1020	159.633	2.094	3800	181.7
1021	153.680	1.906	3500	163.6
1022	151.469	3.016	3000	134.4
1023	152.102	3.219	3000	134.4
1024	153.773	-0.984	3000	134.4
1026	156.578	-1.406	3200	145.9
1027	159.336	-1.875	4700	238.4
1028	158.148	-2.875	4900	251.4
1029	156.719	-2.633	3800	181.7
1030	159.773	-0.609	3800	181.7
1031	158.875	-3.555	5700	305.0
1032	155.266	-3.648	4100	200.3
1033	150.313	-2.148	14000	960.9
1034	150.656	-7.102	8700	523.4
1035	153.945	-6.273	3000	134.4

Crater #	***Longitude***	***Latitude***	***Diameter (m)***	***Impactor Diameter (m)***
1036	153.891	-6.008	3700	175.6
1037	152.547	-5.422	3000	134.4
1038	151.445	-6.016	3800	181.7
1039	152.961	-3.758	11300	730.9
1040	157.398	-5.125	3500	163.6
1041	151.469	-4.531	4900	251.4
1042	153.461	-7.867	3000	134.4
1043	159.930	-6.422	3900	187.9
1044	155.914	-8.289	3000	134.4
1045	154.602	-8.000	3000	134.4
1046	154.117	-9.492	3000	134.4
1047	158.477	-9.898	3200	145.9
1048	159.984	-9.242	5000	258.0
1049	152.375	-6.023	3000	134.4
1050	159.227	-7.641	3000	134.4
1051	113.875	6.031	4200	206.5
1052	119.023	8.125	11000	706.2
1053	117.078	6.531	3000	134.4
1054	117.180	8.375	3000	134.4
1055	115.789	9.797	3000	134.4
1056	111.234	3.672	3400	157.7
1057	117.969	2.695	3000	134.4
1058	114.773	3.289	8800	531.1
1059	110.555	7.742	4000	194.0
1060	120.188	4.234	3000	134.4
1061	120.672	4.047	5100	264.6
1062	119.078	0.555	3000	134.4
1063	111.422	-0.008	3400	157.7
1064	123.516	3.883	3000	134.4
1065	127.711	2.938	3600	169.6
1066	129.719	1.234	4300	212.8
1068	121.344	4.219	3000	134.4
1070	129.414	9.273	3000	134.4
1072	133.656	8.875	3300	151.8
1073	137.313	2.602	9600	593.5
1074	136.742	0.008	4000	194.0
1075	137.320	0.742	3000	134.4
1076	137.773	0.070	5100	264.6
1077	138.656	3.086	3300	151.8
1078	140.445	3.539	3000	134.4
1079	140.477	3.117	4400	219.1
1080	139.703	5.234	4800	244.9
1081	139.867	0.742	3000	134.4
1082	149.734	2.984	3200	145.9
1083	148.586	5.219	3500	163.6
1084	148.211	5.680	3000	134.4

B STONY MAIN BELT ASTEROIDS

This appendix contains a list of 138 stony Main Belt asteroids and their physical characteristics. The quality column is an indication of the accuracy of the information, with "A" being the best.

#	Name	Mass (kg)	Diameter (km)	Density (g/cm^3)	Porosity (%)	Qual.
145	Adeona	2.08E+18	149.504	1.19	47	C
268	Adorea	3.25E+18	140.32	2.24	19	D
47	Aglaja	3.25E+18	141.901	2.17	22	D
702	Alauda	6.06E+18	191.655	1.64	41	D
259	Aletheia	7.79E+18	190.055	2.17	22	B
54	Alexandra	6.16E+18	149.686	3.51	0	D
516	Amherstia	1.43E+18	69.848	8.01	0	D
29	Amphitrite	1.29E+19	217.595	2.39	28	C
90	Antiope	8.3E+17	122.151	0.87	61	B
387	Aquitania	1.9E+18	103.514	3.27	0	C
404	Arsinoe	3.42E+18	96.974	7.16	0	D
105	Artemis	1.53E+18	119.102	1.73	23	C
5	Astraea	2.64E+18	113.415	3.45	0	B
111	Ate	1.76E+18	142.857	1.15	48	C
230	Athamantis	1.89E+18	110.17	2.7	19	B
419	Aurelia	1.72E+18	124.473	1.7	24	C
94	Aurora	6.23E+18	186.358	1.84	18	D
63	Ausonia	1.53E+18	94.457	3.47	0	C
324	Bamberga	1.03E+19	234.672	1.52	32	A
28	Bellona	2.62E+18	108.106	3.95	0	C
1313	Berna	2.25E+15	13.935	1.21	63	B
154	Bertha	9.19E+18	186.854	2.69	0	D
720	Bohlinia	5.97E+16	34.647	2.74	17	C
107	Camilla	1.12E+19	210.689	2.29	18	B
491	Carina	4.82E+18	97.37	9.97	0	C
505	Cava	3.99E+18	101.513	7.28	0	D
1	Ceres	9.44E+20	944.795	2.14	4	A
1669	Dagmar	3.98E+16	42.997	0.96	57	C
61	Danae	2.89E+18	82.53	9.82	0	D
41	Daphne	6.31E+18	181.05	2.03	9	B
511	Davida	3.38E+19	298.289	2.43	0	C
4492	Debussy	3.33E+14	15.786	0.9	60	B
349	Dembowska	3.58E+18	145.24	2.23	33	C
344	Desiderata	1.39E+18	129.203	1.23	45	C
78	Diana	1.27E+18	123.637	1.28	42	B
106	Dione	3.06E+18	147.178	1.83	18	D
423	Diotima	6.91E+18	211.644	1.39	38	C
48	Doris	6.12E+18	211.673	1.23	45	D
60	Echo	3.15E+17	60.005	2.78	16	B
13	Egeria	8.82E+18	214.735	1.7	24	D
442	Eichsfeldia	1.95E+17	65.584	1.32	41	B
130	Elektra	6.6E+18	189.628	1.85	17	B
59	Elpis	3E+18	163.617	1.31	53	C
481	Emita	5.78E+18	107.231	8.95	0	C

#	Name	Mass (kg)	Diameter (km)	Density (g/cm^3)	Porosity (%)	Qual.
283	Emma	1.38E+18	132.746	1.13	49	C
45	Eugenia	5.79E+18	201.817	1.35	40	C
185	Eunike	3.56E+18	160.616	1.64	27	D
15	Eunomia	3.14E+19	256.631	3.54	0	B
31	Euphrosyne	1.27E+19	272.925	1.19	47	D
52	Europa	2.38E+19	310.211	1.52	32	C
27	Euterpe	1.67E+18	105.803	2.7	19	D
164	Eva	9.29E+17	101.775	1.68	39	D
751	Faina	3.27E+18	107.318	5.05	0	B
19	Fortuna	8.6E+18	206.904	1.85	17	A
854	Frostia	1.06E+15	8.396	0.88	72	B
74	Galatea	6.13E+18	120.673	6.66	0	D
328	Gudrun	3.16E+18	122.599	3.27	1	B
444	Gyptis	1.06E+19	164.639	4.56	0	C
6	Hebe	1.39E+19	190.925	3.81	0	A
624	Hektor	9.95E+18	226.684	1.63	41	C
895	Helio	9.87E+18	148.432	5.77	0	D
532	Herculina	1.15E+19	217.494	2.13	36	C
121	Hermione	4.97E+18	195.368	1.27	43	B
804	Hispania	5E+18	148.252	2.93	0	C
379	Huenna	3.83E+17	87.282	1.1	51	C
10	Hygiea	8.63E+19	421.603	2.2	2	A
238	Hypatia	4.9E+18	146.133	3	0	C
98	Ianthe	8.93E+17	106.165	1.43	36	C
243	Ida	3.78E+16	31.3	2.35	29	A
173	Ino	4.79E+18	160.071	2.23	20	D
704	Interamnia	3.28E+19	317.195	1.96	0	A
85	Io	2.57E+18	155.005	1.32	41	D
14	Irene	2.91E+18	147.757	1.72	48	D
7	Iris	1.29E+19	225.896	2.14	35	C
42	Isis	1.58E+18	102.738	2.78	16	C
211	Isolda	4.49E+18	149.818	2.55	0	D
127	Johanna	3.08E+18	116.148	3.75	0	C
139	Juewa	5.54E+18	161.433	2.52	9	C
89	Julia	6.71E+18	147.573	3.98	0	C
3	Juno	2.73E+19	241.797	3.68	0	A
84	Klio	5.47E+17	79.402	2.09	7	D
179	Klytaemnestra	2.49E+17	75.02	1.13	66	C
488	Kreusa	2.48E+18	162.33	1.11	50	C
39	Laetitia	4.72E+18	153.81	2.48	25	C
187	Lamberta	1.8E+18	131.313	1.52	32	C
68	Leto	3.28E+18	124.961	3.21	3	D
117	Lomia	6.08E+18	146.783	3.67	0	B
809	Lundia	9.27E+14	10.26	1.64	49	B
21	Lutetia	1.7E+18	98	3.45	0	A
758	Mancunia	9.31E+17	87.088	2.69	3	B
20	Massalia	5E+18	137	3.71	0	C
760	Massinga	1.33E+18	70.821	7.15	0	D
253	Mathilde	1.03E+17	53	1.32	41	A
18	Melpomene	3.22E+18	141.721	2.16	35	C
9	Metis	8.39E+18	164.466	3.6	0	C
93	Minerva	3.5E+18	149.794	1.99	11	B
192	Nausikaa	1.79E+18	90.188	4.65	0	C
51	Nemausa	2.48E+18	148.852	1.44	36	C
128	Nemesis	5.97E+18	184.192	1.82	18	C

#	*Name*	*Mass (kg)*	*Diameter (km)*	*Density (g/cm³)*	*Porosity (%)*	*Qual.*
150	Nuwa	1.62E+18	146.546	0.98	56	C
3169	Ostro	1.86E+14	5.15	2.6	25	B
49	Pales	4.22E+18	150.825	2.35	0	D
2	Pallas	2.04E+20	514.417	2.87	0	A
372	Palma	5.15E+18	191.122	1.41	49	B
70	Panopaea	4.33E+18	133.431	3.48	0	C
471	Papagena	3.05E+18	124.555	3.02	9	D
11	Parthenope	5.91E+18	151.077	3.27	1	A
451	Patientia	1.09E+19	234.425	1.61	28	D
617	Patroclus	1.36E+18	143.15	0.89	68	B
679	Pax	7.14E+17	64.886	4.99	0	C
554	Peraga	6.59E+17	96.465	1.4	12	B
196	Philomela	4E+18	145.298	2.49	25	C
25	Phocaea	5.99E+17	80.191	2.22	33	C
189	Phthia	3.84E+16	40.919	1.07	67	C
790	Pretoria	4.58E+18	160.982	2.1	24	C
508	Princetonia	2.99E+18	139.695	2.09	25	C
194	Prokne	2.68E+18	170.336	1.04	53	B
762	Pulcova	1.4E+18	138.401	1.01	55	B
168	Sibylla	3.92E+18	149.062	2.26	0	C
386	Siegena	8.14E+18	170.357	3.14	0	C
87	Sylvia	1.48E+19	278.149	1.31	52	B
1089	Tama	8.9E+14	13.445	2.52	24	B
345	Tercidina	2.68E+18	98.788	5.31	0	C
81	Terpsichore	6.19E+18	121.776	6.55	0	D
23	Thalia	1.96E+18	106.814	3.08	7	B
24	Themis	5.89E+18	183.842	1.81	19	C
17	Thetis	1.33E+18	82.768	4.48	0	C
405	Thia	1.38E+18	122.148	1.45	35	C
88	Thisbe	1.53E+19	204.046	3.45	0	C
30	Urania	1.74E+18	94.489	3.93	0	C
240	Vanadis	1.1E+18	94.035	2.54	0	D
416	Vaticana	3.27E+18	87.109	9.45	0	D
490	Veritas	5.99E+18	110.965	8.38	0	C
4	Vesta	2.63E+20	519.337	3.59	0	A
144	Vibilia	5.3E+18	141.344	3.59	0	C
12	Victoria	2.45E+18	124.099	2.45	19	C
747	Winchester	3.81E+18	170.078	1.48	47	D
654	Zelinda	1.35E+18	127.831	1.23	45	B

C Candidate Crater Pairs

This appendix contains a list of 2037 pairs of impact craters from the study area whose separation is < 20 kilometers. The pairs are sorted by "Score", with the best scores at the top. The crater numbers correspond to crater numbers assigned in Appendix A.

Crater 1	*lon*	*lat*	*Crater 2*	*lon*	*lat*	*separation (km)*	*Score*
4	252.679	-13.583	37	252.938	-13.831	2.92	4
9	251.772	-21.941	77	252.054	-22.236	3.26	4
228	228.633	-9.703	229	228.367	-9.695	2.16	3
945	170.487	9.613	946	171.366	10.539	10.47	3
55	259.771	-26.107	64	259.332	-25.994	3.38	2
155	218.295	-21.601	156	218.063	-21.974	3.55	2
568	160.281	-17.875	569	160.695	-18.070	3.63	2
594	154.906	-29.375	595	154.930	-29.695	2.65	2
2	255.426	-16.152	57	255.199	-17.097	8.01	1
6	257.827	-16.434	69	258.159	-15.328	9.50	1
8	255.459	-20.777	11	256.429	-21.995	12.52	1
28	265.929	-15.805	30	266.929	-17.207	14.02	1
59	261.951	-27.115	71	260.451	-26.531	12.06	1
60	261.398	-27.557	71	260.451	-26.531	10.97	1
84	237.706	-13.735	85	238.662	-14.034	8.06	1
189	216.578	9.367	190	218.102	9.125	12.57	1
189	216.578	9.367	358	216.570	9.176	1.58	1
190	218.102	9.125	358	216.570	9.176	12.49	1
214	226.234	6.164	216	227.805	6.578	13.33	1
232	213.695	-3.711	234	211.406	-3.734	18.86	1
250	240.102	4.750	252	241.023	5.289	8.79	1
254	243.891	3.188	260	245.633	4.766	19.38	1
263	249.969	3.742	264	249.555	1.570	18.25	1
263	249.969	3.742	323	250.172	2.563	9.88	1
267	242.281	0.469	269	241.602	1.766	12.09	1
281	237.969	-2.125	294	236.273	-3.000	15.74	1
288	233.258	0.703	291	233.914	-1.023	15.25	1
320	257.508	2.961	351	259.352	3.555	15.97	1
323	250.172	2.563	324	251.297	1.742	11.49	1
337	261.172	-3.398	338	260.625	-3.875	5.98	1
365	190.163	-13.945	522	188.797	-13.445	11.71	1
408	170.320	-15.336	629	169.570	-14.828	7.30	1
408	170.320	-15.336	630	169.516	-13.563	15.99	1
413	172.641	-16.492	423	172.781	-17.320	6.93	1
423	172.781	-17.320	424	173.203	-17.344	3.33	1
465	181.867	-21.727	513	182.539	-21.352	6.02	1
478	179.680	-27.117	506	178.898	-27.391	6.16	1
523	185.977	-12.445	524	183.719	-12.891	18.55	1
523	185.977	-12.445	533	184.742	-10.414	19.52	1
540	157.281	-11.547	542	155.070	-12.359	19.07	1
542	155.070	-12.359	546	155.680	-12.203	5.08	1
554	157.195	-16.398	559	155.570	-18.180	19.50	1
562	150.898	-18.742	714	149.305	-19.102	12.79	1

Crater 1	***lon***	***lat***	***Crater 2***	***lon***	***lat***	***separation (km)***	***Score***
570	160.609	-18.836	571	161.352	-18.977	5.91	1
581	153.836	-22.898	583	153.367	-23.500	6.11	1
583	153.367	-23.500	584	154.977	-23.375	12.23	1
598	160.266	-28.766	602	163.008	-28.984	19.91	1
604	164.266	-26.109	605	165.180	-25.414	8.90	1
604	164.266	-26.109	606	165.625	-26.695	11.15	1
605	165.180	-25.414	606	165.625	-26.695	11.08	1
631	161.750	-11.008	996	162.711	-9.109	17.51	1
646	134.852	-16.234	652	135.383	-15.102	10.26	1
646	134.852	-16.234	656	136.328	-16.531	11.95	1
670	140.492	-20.391	671	139.781	-20.953	7.19	1
678	137.344	-25.508	679	136.727	-25.563	4.62	1
681	132.273	-26.359	682	132.016	-27.234	7.47	1
710	148.164	-21.547	711	149.281	-22.000	9.35	1
746	119.289	-16.281	751	119.797	-18.469	18.50	1
759	116.805	-22.250	760	116.492	-22.047	2.92	1
782	125.727	-24.117	783	126.906	-25.852	16.82	1
782	125.727	-24.117	784	127.523	-25.672	18.59	1
791	127.602	-20.016	802	126.953	-21.484	13.12	1
805	126.203	-14.211	806	126.164	-12.328	15.55	1
814	111.719	-4.492	816	112.852	-6.195	16.86	1
829	121.727	-3.719	830	122.211	-4.328	6.42	1
856	139.773	-5.391	858	140.375	-7.438	17.60	1
928	186.328	3.875	931	186.945	1.906	17.03	1
1004	162.531	-1.102	1005	164.688	-1.133	17.80	1
1005	164.688	-1.133	1006	166.359	-1.539	14.20	1
1035	153.945	-6.273	1042	153.461	-7.867	13.74	1
1047	158.477	-9.898	1048	159.984	-9.242	13.42	1
1	258.463	-17.341	33	259.162	-15.154	18.88	0
1	258.463	-17.341	51	258.482	-15.348	16.46	0
1	258.463	-17.341	69	258.159	-15.328	16.79	0
3	253.508	-16.685	39	253.317	-14.742	16.12	0
4	252.679	-13.583	34	254.118	-13.202	11.98	0
4	252.679	-13.583	36	252.900	-11.827	14.60	0
4	252.679	-13.583	38	251.078	-11.975	18.51	0
4	252.679	-13.583	66	254.925	-13.050	18.57	0
8	255.459	-20.777	17	254.645	-21.797	10.49	0
9	251.772	-21.941	16	251.662	-21.559	3.27	0
9	251.772	-21.941	58	252.719	-23.732	16.45	0
9	251.772	-21.941	65	252.699	-24.208	20.00	0
11	256.429	-21.995	17	254.645	-21.797	13.76	0
11	256.429	-21.995	18	255.086	-20.572	15.64	0
12	256.831	-24.793	46	258.755	-23.187	19.65	0
16	251.662	-21.559	43	250.785	-22.843	12.54	0
16	251.662	-21.559	58	252.719	-23.732	19.66	0
16	251.662	-21.559	77	252.054	-22.236	6.35	0
21	260.700	-24.108	46	258.755	-23.187	16.56	0
21	260.700	-24.108	64	259.332	-25.994	18.63	0
23	262.885	-27.650	47	264.955	-28.888	18.20	0
25	268.890	-25.130	35	267.191	-24.860	12.91	0
26	268.606	-24.971	48	267.537	-22.828	19.44	0
34	254.118	-13.202	36	252.900	-11.827	15.00	0
34	254.118	-13.202	39	253.317	-14.742	14.24	0
34	254.118	-13.202	66	254.925	-13.050	6.61	0
35	267.191	-24.860	48	267.537	-22.828	16.97	0

Crater 1	***lon***	***lat***	***Crater 2***	***lon***	***lat***	***separation (km)***	***Score***
35	267.191	-24.860	49	269.228	-25.301	15.66	0
35	267.191	-24.860	53	269.500	-25.804	18.91	0
36	252.900	-11.827	38	251.078	-11.975	14.77	0
36	252.900	-11.827	66	254.925	-13.050	19.19	0
36	252.900	-11.827	73	252.965	-12.413	4.86	0
37	252.938	-13.831	61	253.952	-12.410	14.28	0
37	252.938	-13.831	63	252.014	-12.463	13.52	0
38	251.078	-11.975	73	252.965	-12.413	15.66	0
39	253.317	-14.742	61	253.952	-12.410	19.91	0
39	253.317	-14.742	66	254.925	-13.050	19.00	0
40	250.236	-17.949	54	250.016	-17.516	3.97	0
40	250.236	-17.949	97	249.554	-17.733	5.65	0
43	250.785	-22.843	44	250.413	-22.422	4.49	0
44	250.413	-22.422	77	252.054	-22.236	12.63	0
45	256.439	-26.957	74	256.002	-25.332	13.80	0
46	258.755	-23.187	52	256.699	-24.483	18.85	0
49	269.228	-25.301	53	269.500	-25.804	4.62	0
50	259.953	-11.125	75	259.747	-10.249	7.42	0
54	250.016	-17.516	97	249.554	-17.733	4.06	0
55	259.771	-26.107	70	259.445	-25.366	6.58	0
55	259.771	-26.107	71	260.451	-26.531	6.13	0
58	252.719	-23.732	65	252.699	-24.208	3.94	0
61	253.952	-12.410	63	252.014	-12.463	15.63	0
61	253.952	-12.410	73	252.965	-12.413	7.96	0
62	256.281	-14.008	66	254.925	-13.050	13.46	0
62	256.281	-14.008	69	258.159	-15.328	18.53	0
63	252.014	-12.463	73	252.965	-12.413	7.68	0
64	259.332	-25.994	70	259.445	-25.366	5.25	0
65	252.699	-24.208	77	252.054	-22.236	17.00	0
72	257.001	-27.978	80	259.095	-28.744	16.48	0
75	259.747	-10.249	341	257.930	-9.125	17.46	0
89	238.775	-12.878	90	238.585	-11.916	8.09	0
96	248.483	-17.506	97	249.554	-17.733	8.63	0
96	248.483	-17.506	99	247.457	-18.358	10.69	0
97	249.554	-17.733	98	248.822	-18.898	11.20	0
97	249.554	-17.733	99	247.457	-18.358	17.25	0
99	247.457	-18.358	100	248.185	-20.008	14.75	0
101	243.393	-21.984	102	242.273	-20.782	13.14	0
101	243.393	-21.984	111	241.919	-23.310	15.69	0
101	243.393	-21.984	127	241.561	-20.603	18.13	0
102	242.273	-20.782	103	241.301	-22.542	16.33	0
102	242.273	-20.782	127	241.561	-20.603	5.70	0
103	241.301	-22.542	107	240.957	-24.232	14.19	0
105	237.993	-17.668	123	237.139	-17.774	6.77	0
106	240.153	-23.523	110	239.974	-25.297	14.70	0
107	240.957	-24.232	110	239.974	-25.297	11.47	0
108	238.070	-23.459	126	237.617	-23.102	4.53	0
109	238.802	-24.512	110	239.974	-25.297	10.91	0
109	238.802	-24.512	126	237.617	-23.102	14.68	0
112	242.103	-27.402	113	242.049	-27.903	4.15	0
115	235.400	-24.052	116	234.072	-23.943	10.05	0
115	235.400	-24.052	126	237.617	-23.102	18.52	0
118	233.159	-20.885	119	232.140	-20.844	7.87	0
133	214.115	-13.727	137	213.398	-14.632	9.42	0
146	213.820	-17.915	147	213.503	-18.639	6.47	0

Crater 1	***lon***	***lat***	***Crater 2***	***lon***	***lat***	***separation (km)***	***Score***
152	214.843	-21.840	158	216.527	-22.896	15.54	0
167	218.176	-26.679	171	220.819	-27.186	19.90	0
188	214.664	9.664	192	213.961	7.414	19.44	0
198	214.914	4.500	205	213.617	2.547	19.34	0
202	219.539	3.539	203	220.227	3.078	6.83	0
203	220.227	3.078	206	220.023	1.461	13.46	0
204	215.359	3.898	205	213.617	2.547	18.18	0
211	222.039	1.867	224	223.609	1.281	13.83	0
217	229.516	6.016	244	230.172	4.445	14.04	0
222	229.164	3.148	225	229.211	2.406	6.14	0
237	232.109	9.227	238	232.289	8.563	5.67	0
237	232.109	9.227	239	232.516	8.289	8.42	0
240	233.992	6.250	242	233.000	5.258	11.55	0
241	231.094	6.211	242	233.000	5.258	17.52	0
241	231.094	6.211	244	230.172	4.445	16.43	0
242	233.000	5.258	248	232.531	3.555	14.58	0
245	237.680	5.406	251	240.078	5.141	19.84	0
255	246.867	6.531	257	248.656	6.688	14.73	0
256	249.320	7.430	258	247.500	6.227	17.92	0
256	249.320	7.430	319	251.219	6.781	16.45	0
265	247.539	1.445	280	248.844	-0.250	17.66	0
269	241.602	1.766	270	241.141	0.477	11.30	0
270	241.141	0.477	276	240.523	-1.117	14.11	0
272	248.492	-1.656	273	246.375	-1.875	17.56	0
272	248.492	-1.656	280	248.844	-0.250	11.97	0
273	246.375	-1.875	274	245.672	-2.422	7.35	0
275	242.297	-1.578	277	240.305	-1.969	16.75	0
275	242.297	-1.578	278	241.102	-2.375	11.85	0
275	242.297	-1.578	279	241.516	-2.703	11.30	0
276	240.523	-1.117	277	240.305	-1.969	7.26	0
276	240.523	-1.117	278	241.102	-2.375	11.43	0
277	240.305	-1.969	278	241.102	-2.375	7.38	0
277	240.305	-1.969	296	239.563	-2.078	6.19	0
279	241.516	-2.703	296	239.563	-2.078	16.92	0
282	238.516	-3.000	305	239.750	-4.758	17.72	0
282	238.516	-3.000	306	239.703	-5.047	19.52	0
285	231.313	0.531	297	230.906	1.820	11.16	0
286	232.102	0.430	288	233.258	0.703	9.81	0
286	232.102	0.430	290	234.023	-0.672	18.29	0
286	232.102	0.430	291	233.914	-1.023	19.18	0
288	233.258	0.703	290	234.023	-0.672	12.99	0
299	238.398	-5.672	300	238.805	-6.859	10.35	0
300	238.805	-6.859	302	238.203	-8.664	15.69	0
304	242.555	-6.078	314	242.633	-5.391	5.71	0
308	248.430	-6.031	315	249.008	-4.063	16.93	0
309	245.383	-7.609	316	246.219	-9.719	18.70	0
311	244.461	-6.297	313	245.078	-6.148	5.21	0
311	244.461	-6.297	314	242.633	-5.391	16.77	0
312	245.617	-6.422	313	245.078	-6.148	4.97	0
321	255.461	1.930	322	254.078	2.320	11.85	0
321	255.461	1.930	329	256.258	-0.281	19.40	0
327	258.156	-0.164	328	257.625	-0.320	4.57	0
327	258.156	-0.164	329	256.258	-0.281	15.70	0
327	258.156	-0.164	330	256.648	-0.852	13.68	0
329	256.258	-0.281	330	256.648	-0.852	5.71	0

Crater 1	***lon***	***lat***	***Crater 2***	***lon***	***lat***	***separation (km)***	***Score***
330	256.648	-0.852	331	256.211	-1.180	4.51	0
362	195.861	-10.215	368	194.372	-11.844	18.07	0
377	200.168	-14.031	381	201.102	-15.942	17.44	0
391	197.192	-29.565	392	199.026	-29.568	13.17	0
394	202.908	-27.962	395	203.902	-28.436	8.22	0
421	179.375	-16.727	422	179.906	-16.484	4.65	0
425	174.547	-17.703	445	176.633	-18.094	16.70	0
430	182.141	-17.031	431	182.039	-18.297	10.48	0
433	180.219	-20.469	511	181.641	-19.813	12.28	0
433	180.219	-20.469	512	182.031	-20.031	14.50	0
447	180.250	-22.438	458	180.063	-24.469	16.83	0
448	178.453	-22.945	449	178.180	-22.273	5.93	0
448	178.453	-22.945	463	178.922	-25.313	19.86	0
452	171.789	-23.836	453	171.789	-23.836	0.00	0
452	171.789	-23.836	454	171.203	-23.797	4.44	0
453	171.789	-23.836	454	171.203	-23.797	4.44	0
453	171.789	-23.836	469	170.984	-24.664	9.13	0
453	171.789	-23.836	470	171.070	-24.773	9.44	0
453	171.789	-23.836	471	172.273	-21.703	17.99	0
453	171.789	-23.836	472	170.836	-26.031	19.48	0
453	171.789	-23.836	619	169.695	-22.492	19.38	0
466	181.844	-21.344	512	182.031	-20.031	10.93	0
487	181.031	-28.070	504	182.242	-27.430	10.31	0
488	182.477	-23.195	489	182.852	-22.320	7.77	0
488	182.477	-23.195	490	183.539	-23.820	9.56	0
488	182.477	-23.195	491	184.289	-23.539	14.03	0
489	182.852	-22.320	490	183.539	-23.820	13.44	0
489	182.852	-22.320	512	182.031	-20.031	19.92	0
490	183.539	-23.820	491	184.289	-23.539	6.13	0
490	183.539	-23.820	494	185.742	-23.547	16.81	0
490	183.539	-23.820	498	184.250	-25.258	13.01	0
490	183.539	-23.820	499	183.742	-25.961	17.74	0
491	184.289	-23.539	493	184.617	-24.250	6.37	0
491	184.289	-23.539	498	184.250	-25.258	14.19	0
495	187.203	-21.992	510	186.391	-21.680	6.74	0
511	181.641	-19.813	512	182.031	-20.031	3.53	0
532	185.000	-10.914	537	185.117	-12.344	11.84	0
551	153.461	-15.180	557	153.047	-17.094	16.14	0
552	151.961	-15.289	557	153.047	-17.094	17.21	0
557	153.047	-17.094	558	154.281	-17.508	10.31	0
557	153.047	-17.094	563	151.445	-18.297	16.04	0
561	150.273	-18.477	562	150.898	-18.742	5.36	0
563	151.445	-18.297	578	151.203	-20.172	15.59	0
563	151.445	-18.297	714	149.305	-19.102	18.01	0
564	151.211	-19.141	712	149.625	-20.406	16.15	0
566	158.328	-18.781	568	160.281	-17.875	17.04	0
574	155.266	-18.641	577	153.688	-20.266	18.19	0
577	153.688	-20.266	578	151.203	-20.172	19.26	0
577	153.688	-20.266	580	154.086	-20.883	5.95	0
588	162.016	-22.516	612	164.500	-22.883	19.16	0
588	162.016	-22.516	613	163.625	-24.336	19.35	0
608	167.109	-25.469	611	169.242	-25.336	15.94	0
617	165.484	-20.445	618	167.133	-20.742	12.97	0
617	165.484	-20.445	620	166.164	-19.258	11.13	0
617	165.484	-20.445	621	165.398	-19.281	9.63	0

Crater 1	***lon***	***lat***	***Crater 2***	***lon***	***lat***	***separation (km)***	***Score***
618	167.133	-20.742	620	166.164	-19.258	14.37	0
618	167.133	-20.742	621	165.398	-19.281	18.07	0
620	166.164	-19.258	621	165.398	-19.281	5.97	0
623	166.492	-13.141	636	164.688	-12.094	16.91	0
624	163.688	-13.141	625	164.008	-13.453	3.64	0
624	163.688	-13.141	626	163.266	-13.328	3.73	0
624	163.688	-13.141	635	163.383	-12.297	7.38	0
625	164.008	-13.453	626	163.266	-13.328	6.05	0
625	164.008	-13.453	633	164.219	-11.266	18.14	0
625	164.008	-13.453	635	163.383	-12.297	10.79	0
626	163.266	-13.328	635	163.383	-12.297	8.57	0
629	169.570	-14.828	630	169.516	-13.563	10.46	0
632	162.070	-11.195	633	164.219	-11.266	17.41	0
637	165.375	-10.664	638	166.273	-10.148	8.45	0
637	165.375	-10.664	995	164.977	-8.430	18.73	0
638	166.273	-10.148	995	164.977	-8.430	17.69	0
639	130.141	-12.773	808	129.375	-13.633	9.39	0
643	131.570	-15.367	644	130.578	-16.453	11.93	0
647	134.672	-11.766	655	136.703	-10.523	19.39	0
653	139.688	-12.242	658	139.594	-14.586	19.36	0
658	139.594	-14.586	729	141.164	-15.313	13.89	0
659	130.672	-17.688	794	128.539	-17.344	17.03	0
659	130.672	-17.688	795	128.992	-17.547	13.27	0
661	134.602	-18.094	665	136.852	-18.945	18.96	0
667	139.391	-17.313	668	139.813	-19.234	16.21	0
667	139.391	-17.313	720	141.586	-18.469	19.71	0
668	139.813	-19.234	670	140.492	-20.391	10.91	0
680	139.133	-26.648	685	140.742	-26.406	12.05	0
686	138.547	-29.266	688	140.008	-28.922	10.91	0
695	143.219	-25.094	703	143.734	-23.469	13.96	0
698	149.211	-24.180	711	149.281	-22.000	18.00	0
706	144.711	-20.305	717	145.258	-19.008	11.52	0
708	146.641	-20.930	718	146.102	-20.141	7.73	0
709	147.711	-21.539	718	146.102	-20.141	16.95	0
715	142.922	-18.781	716	145.156	-17.742	19.50	0
717	145.258	-19.008	718	146.102	-20.141	11.42	0
718	146.102	-20.141	719	144.266	-18.688	18.66	0
719	144.266	-18.688	726	144.258	-19.000	2.58	0
734	144.539	-12.867	736	143.945	-12.430	5.99	0
735	145.555	-12.117	738	146.547	-11.047	11.94	0
736	143.945	-12.430	737	145.180	-11.039	15.21	0
742	112.141	-10.977	744	111.773	-12.477	12.73	0
743	117.047	-10.328	825	118.172	-9.438	11.74	0
760	116.492	-22.047	762	118.016	-23.727	18.07	0
760	116.492	-22.047	764	117.555	-22.539	9.08	0
761	117.031	-24.281	764	117.555	-22.539	14.92	0
761	117.031	-24.281	768	114.813	-25.453	19.23	0
762	118.016	-23.727	764	117.555	-22.539	10.41	0
767	111.922	-28.453	774	114.500	-29.148	19.51	0
772	120.047	-27.297	773	119.313	-29.211	16.68	0
778	121.273	-28.711	779	122.688	-29.063	10.63	0
778	121.273	-28.711	781	123.359	-29.563	16.60	0
786	128.219	-23.344	788	126.602	-22.641	13.59	0
789	122.266	-21.711	792	123.266	-19.805	17.53	0
792	123.266	-19.805	798	125.258	-19.250	16.16	0

Crater 1	***lon***	***lat***	***Crater 2***	***lon***	***lat***	***separation (km)***	***Score***
792	123.266	-19.805	799	122.516	-18.969	9.04	0
796	126.102	-18.805	797	127.078	-19.688	10.54	0
796	126.102	-18.805	798	125.258	-19.250	7.54	0
796	126.102	-18.805	801	125.016	-17.555	13.38	0
797	127.078	-19.688	798	125.258	-19.250	14.62	0
812	118.320	-2.586	813	117.477	-0.547	18.22	0
812	118.320	-2.586	818	119.734	-1.641	14.04	0
822	114.492	-7.055	823	114.922	-9.367	19.41	0
826	117.828	-9.188	827	118.750	-7.852	13.35	0
827	118.750	-7.852	828	119.227	-7.961	4.00	0
843	132.055	-5.672	848	131.883	-7.492	15.09	0
852	139.711	-7.297	853	139.008	-8.141	9.03	0
864	145.422	-5.758	865	145.625	-6.297	4.75	0
864	145.422	-5.758	866	146.430	-4.586	12.74	0
865	145.625	-6.297	866	146.430	-4.586	15.60	0
866	146.430	-4.586	867	147.422	-4.195	8.78	0
871	143.117	-7.852	872	142.313	-8.711	9.67	0
875	149.961	-5.617	1038	151.445	-6.016	12.63	0
900	190.305	-5.484	904	190.125	-6.625	9.53	0
904	190.125	-6.625	963	189.070	-8.359	16.72	0
910	206.398	-7.609	911	207.703	-7.234	11.12	0
936	171.102	5.031	937	170.625	6.563	13.23	0
941	178.773	9.813	942	176.992	9.477	14.76	0
949	179.875	-1.406	950	179.602	-2.281	7.57	0
961	187.000	-6.930	962	186.477	-7.438	6.00	0
995	164.977	-8.430	998	166.516	-8.602	12.65	0
1000	160.961	-2.391	1007	161.969	-0.523	17.51	0
1000	160.961	-2.391	1008	160.797	-1.305	9.07	0
1001	165.086	-4.781	1002	165.063	-4.328	3.75	0
1004	162.531	-1.102	1009	160.391	-1.953	19.01	0
1005	164.688	-1.133	1010	165.469	1.055	19.18	0
1007	161.969	-0.523	1008	160.797	-1.305	11.63	0
1007	161.969	-0.523	1009	160.391	-1.953	17.58	0
1008	160.797	-1.305	1009	160.391	-1.953	6.32	0
1008	160.797	-1.305	1027	159.336	-1.875	12.94	0
1008	160.797	-1.305	1030	159.773	-0.609	10.21	0
1009	160.391	-1.953	1027	159.336	-1.875	8.73	0
1009	160.391	-1.953	1028	158.148	-2.875	20.00	0
1009	160.391	-1.953	1030	159.773	-0.609	12.21	0
1009	160.391	-1.953	1031	158.875	-3.555	18.19	0
1012	160.891	6.094	1013	162.500	6.109	13.21	0
1016	152.563	3.422	1022	151.469	3.016	9.62	0
1021	153.680	1.906	1023	152.102	3.219	16.93	0
1027	159.336	-1.875	1028	158.148	-2.875	12.81	0
1027	159.336	-1.875	1030	159.773	-0.609	11.05	0
1027	159.336	-1.875	1031	158.875	-3.555	14.38	0
1028	158.148	-2.875	1029	156.719	-2.633	11.96	0
1028	158.148	-2.875	1031	158.875	-3.555	8.21	0
1029	156.719	-2.633	1032	155.266	-3.648	14.62	0
1036	153.891	-6.008	1049	152.375	-6.023	12.44	0
1041	151.469	-4.531	1049	152.375	-6.023	14.40	0
1043	159.930	-6.422	1050	159.227	-7.641	11.59	0
1045	154.602	-8.000	1046	154.117	-9.492	12.94	0
1054	117.180	8.375	1055	115.789	9.797	16.32	0
1060	120.188	4.234	1068	121.344	4.219	9.52	0

Crater 1	***lon***	***lat***	***Crater 2***	***lon***	***lat***	***separation (km)***	***Score***
1077	138.656	3.086	1079	140.477	3.117	15.01	0
1079	140.477	3.117	1080	139.703	5.234	18.60	0
4	252.679	-13.583	73	252.965	-12.413	9.93	-1
6	257.827	-16.434	51	258.482	-15.348	10.37	-1
9	251.772	-21.941	44	250.413	-22.422	11.12	-1
26	268.606	-24.971	35	267.191	-24.860	10.63	-1
36	252.900	-11.827	61	253.952	-12.410	9.76	-1
40	250.236	-17.949	98	248.822	-18.898	13.56	-1
43	250.785	-22.843	77	252.054	-22.236	10.89	-1
45	256.439	-26.957	72	257.001	-27.978	9.38	-1
51	258.482	-15.348	69	258.159	-15.328	2.58	-1
52	256.699	-24.483	74	256.002	-25.332	8.74	-1
54	250.016	-17.516	98	248.822	-18.898	14.76	-1
59	261.951	-27.115	60	261.398	-27.557	5.46	-1
70	259.445	-25.366	71	260.451	-26.531	12.18	-1
81	230.239	-11.093	82	231.721	-10.781	12.29	-1
98	248.822	-18.898	99	247.457	-18.358	11.57	-1
98	248.822	-18.898	100	248.185	-20.008	10.42	-1
130	215.520	-13.238	133	214.115	-13.727	11.98	-1
134	218.853	-15.363	141	219.496	-16.390	9.89	-1
134	218.853	-15.363	142	219.451	-17.616	19.19	-1
135	220.623	-13.475	138	220.692	-14.881	11.62	-1
141	219.496	-16.390	142	219.451	-17.616	10.13	-1
142	219.451	-17.616	143	219.983	-19.203	13.75	-1
142	219.451	-17.616	144	220.265	-19.539	17.10	-1
142	219.451	-17.616	160	220.923	-18.669	14.45	-1
143	219.983	-19.203	144	220.265	-19.539	3.54	-1
143	219.983	-19.203	145	217.999	-19.809	16.23	-1
143	219.983	-19.203	160	220.923	-18.669	8.56	-1
144	220.265	-19.539	145	217.999	-19.809	17.76	-1
144	220.265	-19.539	160	220.923	-18.669	8.82	-1
144	220.265	-19.539	161	222.599	-18.817	19.15	-1
145	217.999	-19.809	148	216.096	-18.832	16.87	-1
145	217.999	-19.809	154	217.354	-20.613	8.31	-1
146	213.820	-17.915	148	216.096	-18.832	19.37	-1
146	213.820	-17.915	150	214.380	-19.974	17.55	-1
147	213.503	-18.639	150	214.380	-19.974	12.97	-1
148	216.096	-18.832	150	214.380	-19.974	16.36	-1
148	216.096	-18.832	154	217.354	-20.613	17.66	-1
149	211.476	-16.581	186	210.724	-15.361	11.71	-1
159	212.314	-22.243	185	211.491	-23.552	12.49	-1
160	220.923	-18.669	161	222.599	-18.817	13.16	-1
164	221.111	-23.153	165	222.845	-24.244	15.90	-1
166	222.052	-25.621	168	221.197	-26.488	9.56	-1
174	225.538	-24.487	176	226.505	-25.675	12.18	-1
176	226.505	-25.675	177	228.357	-26.993	17.49	-1
179	225.129	-18.175	180	225.483	-18.415	3.40	-1
179	225.129	-18.175	181	225.635	-19.927	14.99	-1
180	225.483	-18.415	181	225.635	-19.927	12.54	-1
188	214.664	9.664	191	213.406	7.719	19.06	-1
191	213.406	7.719	192	213.961	7.414	5.19	-1
197	217.086	4.320	198	214.914	4.500	17.94	-1
197	217.086	4.320	209	216.461	2.047	19.46	-1
198	214.914	4.500	200	212.922	4.719	16.49	-1
198	214.914	4.500	204	215.359	3.898	6.17	-1

Crater 1	***lon***	***lat***	***Crater 2***	***lon***	***lat***	***separation (km)***	***Score***
199	212.484	5.328	200	212.922	4.719	6.18	-1
200	212.922	4.719	205	213.617	2.547	18.82	-1
202	219.539	3.539	226	221.867	3.234	19.35	-1
203	220.227	3.078	211	222.039	1.867	17.98	-1
204	215.359	3.898	209	216.461	2.047	17.78	-1
205	213.617	2.547	207	212.172	1.766	13.56	-1
207	212.172	1.766	208	211.727	1.422	4.64	-1
220	226.242	3.492	221	228.344	3.906	17.65	-1
221	228.344	3.906	222	229.164	3.148	9.21	-1
221	228.344	3.906	225	229.211	2.406	14.30	-1
222	229.164	3.148	244	230.172	4.445	13.55	-1
222	229.164	3.148	297	230.906	1.820	18.07	-1
225	229.211	2.406	297	230.906	1.820	14.80	-1
255	246.867	6.531	260	245.633	4.766	17.76	-1
367	196.794	-12.509	373	197.997	-13.449	12.40	-1
396	205.136	-22.724	397	205.805	-22.735	5.10	-1
403	205.587	-10.446	404	205.760	-11.347	7.57	-1
407	170.664	-14.102	410	172.375	-15.859	19.92	-1
407	170.664	-14.102	412	170.984	-16.297	18.30	-1
411	170.914	-16.641	412	170.984	-16.297	2.89	-1
411	170.914	-16.641	438	170.188	-17.688	10.37	-1
412	170.984	-16.297	437	171.734	-17.781	13.61	-1
412	170.984	-16.297	438	170.188	-17.688	13.09	-1
414	175.844	-11.313	415	176.656	-11.602	6.99	-1
416	178.188	-16.148	421	179.375	-16.727	10.54	-1
416	178.188	-16.148	529	180.336	-14.930	19.83	-1
418	181.305	-12.273	419	179.430	-11.953	15.36	-1
418	181.305	-12.273	527	181.461	-14.406	17.65	-1
419	179.430	-11.953	420	179.469	-11.273	5.62	-1
421	179.375	-16.727	446	180.867	-18.344	17.78	-1
422	179.906	-16.484	430	182.141	-17.031	18.23	-1
422	179.906	-16.484	446	180.867	-18.344	17.11	-1
427	178.867	-17.680	446	180.867	-18.344	16.63	-1
428	174.586	-20.742	471	172.273	-21.703	19.48	-1
432	179.492	-19.008	433	180.219	-20.469	13.32	-1
432	179.492	-19.008	434	180.281	-21.234	19.37	-1
434	180.281	-21.234	448	178.453	-22.945	19.88	-1
434	180.281	-21.234	449	178.180	-22.273	18.25	-1
434	180.281	-21.234	511	181.641	-19.813	15.76	-1
435	177.266	-22.313	444	176.633	-21.320	9.52	-1
436	172.305	-19.313	441	171.281	-20.781	14.49	-1
437	171.734	-17.781	438	170.188	-17.688	12.19	-1
439	170.539	-19.852	441	171.281	-20.781	9.59	-1
441	171.281	-20.781	471	172.273	-21.703	10.78	-1
446	180.867	-18.344	511	181.641	-19.813	13.54	-1
446	180.867	-18.344	512	182.031	-20.031	16.63	-1
447	180.250	-22.438	466	181.844	-21.344	15.18	-1
448	178.453	-22.945	460	176.234	-23.711	17.97	-1
449	178.180	-22.273	459	176.039	-23.008	17.40	-1
449	178.180	-22.273	460	176.234	-23.711	18.96	-1
449	178.180	-22.273	461	176.766	-23.516	14.86	-1
452	171.789	-23.836	469	170.984	-24.664	9.13	-1
454	171.203	-23.797	469	170.984	-24.664	7.35	-1
454	171.203	-23.797	471	172.273	-21.703	19.11	-1
457	180.445	-24.188	462	178.609	-25.102	15.71	-1

Crater 1	*lon*	*lat*	*Crater 2*	*lon*	*lat*	*separation (km)*	*Score*
459	176.039	-23.008	460	176.234	-23.711	5.99	-1
459	176.039	-23.008	461	176.766	-23.516	6.92	-1
460	176.234	-23.711	461	176.766	-23.516	4.33	-1
462	178.609	-25.102	478	179.680	-27.117	18.43	-1
462	178.609	-25.102	506	178.898	-27.391	19.02	-1
463	178.922	-25.313	467	180.836	-24.305	16.58	-1
464	179.758	-26.172	487	181.031	-28.070	18.25	-1
466	181.844	-21.344	489	182.852	-22.320	11.16	-1
467	180.836	-24.305	468	181.477	-26.531	18.99	-1
467	180.836	-24.305	488	182.477	-23.195	15.41	-1
468	181.477	-26.531	487	181.031	-28.070	13.12	-1
468	181.477	-26.531	499	183.742	-25.961	17.42	-1
468	181.477	-26.531	504	182.242	-27.430	9.31	-1
472	170.836	-26.031	484	170.477	-27.266	10.53	-1
476	173.492	-28.164	477	174.305	-28.563	6.76	-1
476	173.492	-28.164	480	175.141	-29.016	13.86	-1
476	173.492	-28.164	482	172.195	-28.133	9.44	-1
478	179.680	-27.117	486	180.852	-27.469	9.07	-1
480	175.141	-29.016	481	176.219	-27.273	16.38	-1
482	172.195	-28.133	483	171.500	-27.500	7.28	-1
482	172.195	-28.133	484	170.477	-27.266	14.46	-1
484	170.477	-27.266	485	172.234	-28.852	18.31	-1
493	184.617	-24.250	499	183.742	-25.961	15.57	-1
494	185.742	-23.547	498	184.250	-25.258	18.04	-1
499	183.742	-25.961	504	182.242	-27.430	16.41	-1
516	187.578	-19.523	518	186.320	-17.516	19.28	-1
533	184.742	-10.414	534	184.047	-10.297	5.73	-1
536	183.156	-10.523	959	183.359	-8.281	18.58	-1
541	158.367	-11.625	543	159.984	-10.969	14.17	-1
541	158.367	-11.625	545	157.609	-13.008	12.95	-1
556	155.984	-16.297	567	157.031	-14.523	16.84	-1
559	155.570	-18.180	560	154.430	-19.242	12.51	-1
561	150.273	-18.477	712	149.625	-20.406	16.71	-1
599	157.656	-25.438	600	158.102	-25.563	3.47	-1
646	134.852	-16.234	651	134.555	-14.313	16.04	-1
772	120.047	-27.297	778	121.273	-28.711	14.70	-1
783	126.906	-25.852	784	127.523	-25.672	4.82	-1
790	126.617	-20.172	791	127.602	-20.016	7.74	-1
993	161.711	-6.320	994	160.609	-6.977	10.53	-1
1034	150.656	-7.102	1038	151.445	-6.016	11.06	-1
7	254.448	-19.573	17	254.645	-21.797	18.42	-2
37	252.938	-13.831	73	252.965	-12.413	11.71	-2
96	248.483	-17.506	98	248.822	-18.898	11.79	-2
101	243.393	-21.984	103	241.301	-22.542	16.64	-2
103	241.301	-22.542	111	241.919	-23.310	7.89	-2
103	241.301	-22.542	127	241.561	-20.603	16.14	-2
106	240.153	-23.523	109	238.802	-24.512	13.05	-2
106	240.153	-23.523	111	241.919	-23.310	13.50	-2
107	240.957	-24.232	109	238.802	-24.512	16.37	-2
108	238.070	-23.459	109	238.802	-24.512	10.30	-2
120	234.287	-19.330	121	235.840	-19.451	12.14	-2
120	234.287	-19.330	122	235.278	-18.875	8.60	-2
121	235.840	-19.451	125	235.344	-17.743	14.63	-2
129	213.444	-16.862	136	215.762	-16.214	19.10	-2
130	215.520	-13.238	131	217.438	-13.934	16.43	-2

Crater 1	***lon***	***lat***	***Crater 2***	***lon***	***lat***	***separation (km)***	***Score***
150	214.380	-19.974	152	214.843	-21.840	15.82	-2
151	215.387	-21.355	152	214.843	-21.840	5.79	-2
166	222.052	-25.621	171	220.819	-27.186	15.81	-2
190	218.102	9.125	194	219.219	9.797	10.65	-2
202	219.539	3.539	206	220.023	1.461	17.61	-2
223	227.766	4.242	244	230.172	4.445	19.88	-2
247	237.406	3.109	249	236.398	3.320	8.49	-2
248	232.531	3.555	284	233.156	1.984	13.95	-2
253	246.516	5.961	255	246.867	6.531	5.52	-2
253	246.516	5.961	260	245.633	4.766	12.25	-2
254	243.891	3.188	262	244.852	3.063	7.99	-2
256	249.320	7.430	257	248.656	6.688	8.19	-2
257	248.656	6.688	258	247.500	6.227	10.22	-2
258	247.500	6.227	260	245.633	4.766	19.52	-2
261	248.375	3.656	265	247.539	1.445	19.51	-2
263	249.969	3.742	324	251.297	1.742	19.81	-2
264	249.555	1.570	265	247.539	1.445	16.67	-2
264	249.555	1.570	280	248.844	-0.250	16.13	-2
271	248.813	-1.383	272	248.492	-1.656	3.48	-2
271	248.813	-1.383	280	248.844	-0.250	9.36	-2
276	240.523	-1.117	279	241.516	-2.703	15.44	-2
277	240.305	-1.969	279	241.516	-2.703	11.68	-2
277	240.305	-1.969	282	238.516	-3.000	17.04	-2
281	237.969	-2.125	293	236.898	-2.320	8.98	-2
283	231.875	1.625	286	232.102	0.430	10.04	-2
283	231.875	1.625	288	233.258	0.703	13.72	-2
284	233.156	1.984	285	231.313	0.531	19.38	-2
284	233.156	1.984	288	233.258	0.703	10.61	-2
285	231.313	0.531	286	232.102	0.430	6.57	-2
285	231.313	0.531	288	233.258	0.703	16.12	-2
286	232.102	0.430	289	232.227	-0.617	8.70	-2
289	232.227	-0.617	290	234.023	-0.672	14.84	-2
289	232.227	-0.617	291	233.914	-1.023	14.33	-2
293	236.898	-2.320	294	236.273	-3.000	7.62	-2
295	231.273	-2.984	298	233.039	-3.680	15.64	-2
304	242.555	-6.078	311	244.461	-6.297	15.75	-2
307	248.273	-6.695	308	248.430	-6.031	5.63	-2
309	245.383	-7.609	313	245.078	-6.148	12.32	-2
310	247.086	-8.734	316	246.219	-9.719	10.77	-2
317	255.680	9.758	318	256.820	9.273	10.11	-2
320	257.508	2.961	321	255.461	1.930	18.91	-2
327	258.156	-0.164	332	259.047	-1.391	12.51	-2
334	258.570	-2.602	339	257.242	-3.898	15.31	-2
363	199.070	-11.388	906	197.422	-9.703	19.30	-2
364	192.133	-12.013	368	194.372	-11.844	18.14	-2
369	195.070	-13.867	370	197.439	-13.895	18.98	-2
369	195.070	-13.867	372	193.398	-14.037	13.47	-2
383	202.763	-21.088	384	200.501	-20.702	17.73	-2
413	172.641	-16.492	424	173.203	-17.344	8.32	-2
430	182.141	-17.031	528	182.133	-14.758	18.77	-2
441	171.281	-20.781	619	169.695	-22.492	18.64	-2
447	180.250	-22.438	448	178.453	-22.945	14.31	-2
447	180.250	-22.438	449	178.180	-22.273	15.86	-2
454	171.203	-23.797	470	171.070	-24.773	8.12	-2
456	174.336	-25.383	474	175.609	-26.844	15.32	-2

Crater 1	*lon*	*lat*	*Crater 2*	*lon*	*lat*	*separation (km)*	*Score*
462	178.609	-25.102	464	179.758	-26.172	12.29	-2
462	178.609	-25.102	473	177.359	-26.867	17.28	-2
464	179.758	-26.172	468	181.477	-26.531	13.06	-2
468	181.477	-26.531	492	182.617	-25.258	13.50	-2
473	177.359	-26.867	506	178.898	-27.391	12.11	-2
497	187.391	-25.492	507	185.891	-25.555	11.19	-2
500	184.461	-26.570	504	182.242	-27.430	17.80	-2
501	184.313	-28.063	503	182.602	-27.742	12.76	-2
502	186.016	-28.094	509	187.461	-29.648	16.55	-2
514	185.242	-18.898	515	184.617	-20.438	13.60	-2
514	185.242	-18.898	518	186.320	-17.516	14.21	-2
518	186.320	-17.516	520	186.039	-15.453	17.17	-2
519	187.945	-16.086	520	186.039	-15.453	16.02	-2
527	181.461	-14.406	529	180.336	-14.930	9.97	-2
528	182.133	-14.758	529	180.336	-14.930	14.41	-2
533	184.742	-10.414	960	186.180	-8.523	19.51	-2
540	157.281	-11.547	546	155.680	-12.203	14.03	-2
543	159.984	-10.969	544	158.883	-12.406	14.84	-2
543	159.984	-10.969	631	161.750	-11.008	14.31	-2
543	159.984	-10.969	632	162.070	-11.195	17.00	-2
543	159.984	-10.969	1047	158.477	-9.898	15.10	-2
572	162.039	-18.031	576	160.305	-19.672	19.16	-2
635	163.383	-12.297	636	164.688	-12.094	10.66	-2
651	134.555	-14.313	652	135.383	-15.102	9.28	-2
659	130.672	-17.688	673	131.258	-19.594	16.39	-2
687	140.477	-29.000	688	140.008	-28.922	3.45	-2
735	145.555	-12.117	739	147.195	-10.852	16.89	-2
883	199.024	8.506	887	198.367	7.844	7.66	-2
1	258.463	-17.341	6	257.827	-16.434	9.02	-3
1	258.463	-17.341	42	257.898	-17.972	6.84	-3
4	252.679	-13.583	61	253.952	-12.410	14.09	-3
4	252.679	-13.583	63	252.014	-12.463	10.68	-3
20	263.060	-23.443	24	265.089	-24.617	18.11	-3
26	268.606	-24.971	49	269.228	-25.301	5.39	-3
30	266.929	-17.207	76	269.025	-17.816	17.25	-3
33	259.162	-15.154	51	258.482	-15.348	5.65	-3
33	259.162	-15.154	69	258.159	-15.328	8.12	-3
34	254.118	-13.202	37	252.938	-13.831	10.80	-3
34	254.118	-13.202	73	252.965	-12.413	11.34	-3
36	252.900	-11.827	37	252.938	-13.831	16.54	-3
40	250.236	-17.949	96	248.483	-17.506	14.26	-3
43	250.785	-22.843	67	250.910	-23.100	2.33	-3
47	264.955	-28.888	68	265.570	-29.293	5.56	-3
54	250.016	-17.516	96	248.483	-17.506	12.07	-3
55	259.771	-26.107	59	261.951	-27.115	18.12	-3
58	252.719	-23.732	77	252.054	-22.236	13.34	-3
66	254.925	-13.050	73	252.965	-12.413	16.64	-3
75	259.747	-10.249	340	258.453	-9.063	14.38	-3
84	237.706	-13.735	89	238.775	-12.878	11.13	-3
84	237.706	-13.735	90	238.585	-11.916	16.60	-3
85	238.662	-14.034	89	238.775	-12.878	9.58	-3
85	238.662	-14.034	90	238.585	-11.916	17.50	-3
93	242.624	-16.832	128	241.412	-17.955	13.31	-3
94	248.510	-14.173	95	247.117	-14.079	11.18	-3
103	241.301	-22.542	106	240.153	-23.523	11.90	-3

Crater 1	*lon*	*lat*	*Crater 2*	*lon*	*lat*	*separation (km)*	*Score*
106	240.153	-23.523	107	240.957	-24.232	8.43	-3
106	240.153	-23.523	108	238.070	-23.459	15.78	-3
106	240.153	-23.523	126	237.617	-23.102	19.54	-3
112	242.103	-27.402	114	243.246	-28.957	15.29	-3
113	242.049	-27.903	114	243.246	-28.957	12.29	-3
118	233.159	-20.885	120	234.287	-19.330	15.53	-3
120	234.287	-19.330	125	235.344	-17.743	15.50	-3
121	235.840	-19.451	122	235.278	-18.875	6.48	-3
122	235.278	-18.875	123	237.139	-17.774	17.19	-3
123	237.139	-17.774	125	235.344	-17.743	14.11	-3
124	240.777	-19.178	127	241.561	-20.603	13.24	-3
124	240.777	-19.178	128	241.412	-17.955	11.25	-3
129	213.444	-16.862	146	213.820	-17.915	9.19	-3
129	213.444	-16.862	147	213.503	-18.639	14.68	-3
131	217.438	-13.934	134	218.853	-15.363	16.34	-3
132	213.044	-13.695	133	214.115	-13.727	8.59	-3
132	213.044	-13.695	137	213.398	-14.632	8.23	-3
134	218.853	-15.363	138	220.692	-14.881	15.19	-3
143	219.983	-19.203	157	220.971	-20.990	16.61	-3
144	220.265	-19.539	157	220.971	-20.990	13.16	-3
145	217.999	-19.809	155	218.295	-21.601	14.97	-3
145	217.999	-19.809	156	218.063	-21.974	17.88	-3
150	214.380	-19.974	151	215.387	-21.355	13.80	-3
151	215.387	-21.355	158	216.527	-22.896	15.43	-3
152	214.843	-21.840	162	214.642	-23.992	17.83	-3
153	212.067	-21.302	159	212.314	-22.243	8.00	-3
153	212.067	-21.302	185	211.491	-23.552	19.09	-3
154	217.354	-20.613	156	218.063	-21.974	12.49	-3
154	217.354	-20.613	158	216.527	-22.896	19.89	-3
155	218.295	-21.601	158	216.527	-22.896	17.23	-3
156	218.063	-21.974	158	216.527	-22.896	13.98	-3
158	216.527	-22.896	162	214.642	-23.992	16.90	-3
165	222.845	-24.244	166	222.052	-25.621	12.83	-3
165	222.845	-24.244	169	223.789	-25.774	14.47	-3
166	222.052	-25.621	169	223.789	-25.774	12.98	-3
167	218.176	-26.679	172	220.123	-28.211	19.06	-3
167	218.176	-26.679	173	219.631	-28.586	19.00	-3
168	221.197	-26.488	171	220.819	-27.186	6.39	-3
168	221.197	-26.488	172	220.123	-28.211	16.26	-3
169	223.789	-25.774	174	225.538	-24.487	16.84	-3
171	220.819	-27.186	172	220.123	-28.211	9.88	-3
171	220.819	-27.186	173	219.631	-28.586	14.45	-3
172	220.123	-28.211	173	219.631	-28.586	4.73	-3
174	225.538	-24.487	175	225.036	-23.282	10.64	-3
184	227.420	-10.899	228	228.633	-9.703	13.95	-3
184	227.420	-10.899	229	228.367	-9.695	12.57	-3
188	214.664	9.664	189	216.578	9.367	15.78	-3
188	214.664	9.664	358	216.570	9.176	16.04	-3
190	218.102	9.125	193	217.344	6.883	19.52	-3
190	218.102	9.125	195	220.508	9.172	19.62	-3
193	217.344	6.883	358	216.570	9.176	19.96	-3
194	219.219	9.797	195	220.508	9.172	11.70	-3
195	220.508	9.172	212	222.352	8.133	17.32	-3
196	220.594	6.250	213	223.000	5.953	19.90	-3
197	217.086	4.320	204	215.359	3.898	14.64	-3

Crater 1	***lon***	***lat***	***Crater 2***	***lon***	***lat***	***separation (km)***	***Score***
201	220.211	3.617	203	220.227	3.078	4.45	-3
203	220.227	3.078	226	221.867	3.234	13.58	-3
205	213.617	2.547	208	211.727	1.422	18.15	-3
206	220.023	1.461	211	222.039	1.867	16.97	-3
211	222.039	1.867	226	221.867	3.234	11.38	-3
214	226.234	6.164	215	226.609	6.102	3.12	-3
215	226.609	6.102	216	227.805	6.578	10.57	-3
215	226.609	6.102	223	227.766	4.242	18.06	-3
216	227.805	6.578	217	229.516	6.016	14.79	-3
216	227.805	6.578	218	228.141	8.555	16.55	-3
216	227.805	6.578	223	227.766	4.242	19.29	-3
217	229.516	6.016	221	228.344	3.906	19.90	-3
217	229.516	6.016	241	231.094	6.211	13.05	-3
220	226.242	3.492	223	227.766	4.242	13.99	-3
221	228.344	3.906	244	230.172	4.445	15.70	-3
222	229.164	3.148	223	227.766	4.242	14.64	-3
223	227.766	4.242	225	229.211	2.406	19.28	-3
225	229.211	2.406	244	230.172	4.445	18.60	-3
230	218.141	-9.531	357	219.641	-10.250	13.57	-3
234	211.406	-3.734	236	210.469	-1.969	16.50	-3
240	233.992	6.250	243	235.180	7.086	11.93	-3
245	237.680	5.406	246	238.094	4.711	6.67	-3
245	237.680	5.406	247	237.406	3.109	19.09	-3
246	238.094	4.711	247	237.406	3.109	14.38	-3
246	238.094	4.711	249	236.398	3.320	18.07	-3
246	238.094	4.711	250	240.102	4.750	16.52	-3
246	238.094	4.711	251	240.078	5.141	16.70	-3
248	232.531	3.555	283	231.875	1.625	16.82	-3
248	232.531	3.555	297	230.906	1.820	19.61	-3
250	240.102	4.750	251	240.078	5.141	3.23	-3
251	240.078	5.141	252	241.023	5.289	7.87	-3
253	246.516	5.961	257	248.656	6.688	18.56	-3
253	246.516	5.961	258	247.500	6.227	8.37	-3
254	243.891	3.188	266	245.109	2.359	12.15	-3
255	246.867	6.531	258	247.500	6.227	5.77	-3
261	248.375	3.656	263	249.969	3.742	13.15	-3
261	248.375	3.656	264	249.555	1.570	19.78	-3
261	248.375	3.656	323	250.172	2.563	17.35	-3
264	249.555	1.570	323	250.172	2.563	9.64	-3
264	249.555	1.570	324	251.297	1.742	14.45	-3
267	242.281	0.469	268	241.516	0.141	6.88	-3
267	242.281	0.469	270	241.141	0.477	9.42	-3
267	242.281	0.469	275	242.297	-1.578	16.90	-3
267	242.281	0.469	276	240.523	-1.117	19.54	-3
268	241.516	0.141	269	241.602	1.766	13.43	-3
268	241.516	0.141	270	241.141	0.477	4.16	-3
268	241.516	0.141	275	242.297	-1.578	15.59	-3
270	241.141	0.477	275	242.297	-1.578	19.46	-3
275	242.297	-1.578	276	240.523	-1.117	15.12	-3
276	240.523	-1.117	296	239.563	-2.078	11.22	-3
277	240.305	-1.969	281	237.969	-2.125	19.31	-3
278	241.102	-2.375	279	241.516	-2.703	4.36	-3
278	241.102	-2.375	296	239.563	-2.078	12.93	-3
282	238.516	-3.000	293	236.898	-2.320	14.47	-3
283	231.875	1.625	285	231.313	0.531	10.15	-3

Crater 1	***lon***	***lat***	***Crater 2***	***lon***	***lat***	***separation (km)***	***Score***
283	231.875	1.625	289	232.227	-0.617	18.74	-3
283	231.875	1.625	297	230.906	1.820	8.15	-3
284	233.156	1.984	286	232.102	0.430	15.51	-3
284	233.156	1.984	297	230.906	1.820	18.61	-3
285	231.313	0.531	289	232.227	-0.617	12.12	-3
286	232.102	0.430	297	230.906	1.820	15.14	-3
287	237.156	0.328	292	236.695	-0.250	6.10	-3
288	233.258	0.703	289	232.227	-0.617	13.83	-3
290	234.023	-0.672	291	233.914	-1.023	3.04	-3
292	236.695	-0.250	293	236.898	-2.320	17.17	-3
299	238.398	-5.672	305	239.750	-4.758	13.43	-3
299	238.398	-5.672	306	239.703	-5.047	11.90	-3
300	238.805	-6.859	305	239.750	-4.758	19.01	-3
300	238.805	-6.859	306	239.703	-5.047	16.68	-3
301	236.180	-8.641	302	238.203	-8.664	16.52	-3
303	243.938	-6.789	304	242.555	-6.078	12.77	-3
303	243.938	-6.789	309	245.383	-7.609	13.64	-3
303	243.938	-6.789	311	244.461	-6.297	5.91	-3
303	243.938	-6.789	312	245.617	-6.422	14.10	-3
303	243.938	-6.789	313	245.078	-6.148	10.75	-3
303	243.938	-6.789	314	242.633	-5.391	15.75	-3
305	239.750	-4.758	306	239.703	-5.047	2.42	-3
307	248.273	-6.695	310	247.086	-8.734	19.44	-3
309	245.383	-7.609	311	244.461	-6.297	13.21	-3
309	245.383	-7.609	312	245.617	-6.422	9.99	-3
311	244.461	-6.297	312	245.617	-6.422	9.54	-3
321	255.461	1.930	333	255.141	-0.336	18.89	-3
324	251.297	1.742	325	252.195	-0.031	16.41	-3
327	258.156	-0.164	331	256.211	-1.180	18.12	-3
328	257.625	-0.320	329	256.258	-0.281	11.29	-3
328	257.625	-0.320	330	256.648	-0.852	9.18	-3
328	257.625	-0.320	331	256.211	-1.180	13.66	-3
329	256.258	-0.281	331	256.211	-1.180	7.43	-3
330	256.648	-0.852	333	255.141	-0.336	13.15	-3
331	256.211	-1.180	333	255.141	-0.336	11.25	-3
332	259.047	-1.391	334	258.570	-2.602	10.74	-3
337	261.172	-3.398	344	262.680	-4.281	14.40	-3
338	260.625	-3.875	344	262.680	-4.281	17.25	-3
340	258.453	-9.063	341	257.930	-9.125	4.30	-3
340	258.453	-9.063	343	258.055	-7.695	11.75	-3
342	256.836	-6.406	343	258.055	-7.695	14.59	-3
359	191.761	-10.611	364	192.133	-12.013	11.96	-3
360	193.133	-12.721	368	194.372	-11.844	12.34	-3
360	193.133	-12.721	372	193.398	-14.037	11.07	-3
361	194.255	-10.245	362	195.861	-10.215	13.05	-3
361	194.255	-10.245	368	194.372	-11.844	13.23	-3
362	195.861	-10.215	906	197.422	-9.703	13.37	-3
363	199.070	-11.388	373	197.997	-13.449	19.09	-3
363	199.070	-11.388	376	200.808	-10.607	15.48	-3
365	190.163	-13.945	366	190.518	-15.976	17.00	-3
365	190.163	-13.945	375	191.595	-15.101	14.90	-3
365	190.163	-13.945	521	188.078	-14.430	17.16	-3
365	190.163	-13.945	531	189.539	-11.875	17.81	-3
367	196.794	-12.509	370	197.439	-13.895	12.56	-3
368	194.372	-11.844	369	195.070	-13.867	17.62	-3

Crater 1	*lon*	*lat*	*Crater 2*	*lon*	*lat*	*separation (km)*	*Score*
368	194.372	-11.844	372	193.398	-14.037	19.73	-3
369	195.070	-13.867	371	196.537	-15.293	16.61	-3
370	197.439	-13.895	371	196.537	-15.293	13.61	-3
370	197.439	-13.895	373	197.997	-13.449	5.79	-3
371	196.537	-15.293	373	197.997	-13.449	19.19	-3
374	192.841	-15.947	380	194.229	-17.952	19.86	-3
379	195.616	-18.571	380	194.229	-17.952	12.01	-3
390	194.939	-29.667	391	197.192	-29.565	16.20	-3
393	200.834	-28.248	394	202.908	-27.962	15.29	-3
394	202.908	-27.962	398	204.003	-27.957	7.98	-3
395	203.902	-28.436	398	204.003	-27.957	4.02	-3
402	204.804	-13.425	404	205.760	-11.347	18.80	-3
405	170.250	-11.328	630	169.516	-13.563	19.37	-3
407	170.664	-14.102	629	169.570	-14.828	10.60	-3
407	170.664	-14.102	630	169.516	-13.563	10.22	-3
408	170.320	-15.336	410	172.375	-15.859	16.90	-3
408	170.320	-15.336	411	170.914	-16.641	11.76	-3
408	170.320	-15.336	412	170.984	-16.297	9.53	-3
408	170.320	-15.336	438	170.188	-17.688	19.44	-3
409	173.188	-15.391	410	172.375	-15.859	7.53	-3
409	173.188	-15.391	412	170.984	-16.297	19.03	-3
409	173.188	-15.391	413	172.641	-16.492	10.08	-3
409	173.188	-15.391	423	172.781	-17.320	16.25	-3
409	173.188	-15.391	424	173.203	-17.344	16.12	-3
410	172.375	-15.859	412	170.984	-16.297	11.61	-3
410	172.375	-15.859	423	172.781	-17.320	12.48	-3
410	172.375	-15.859	424	173.203	-17.344	13.90	-3
411	170.914	-16.641	413	172.641	-16.492	13.72	-3
411	170.914	-16.641	423	172.781	-17.320	15.77	-3
411	170.914	-16.641	424	173.203	-17.344	18.98	-3
411	170.914	-16.641	629	169.570	-14.828	18.38	-3
412	170.984	-16.297	413	172.641	-16.492	13.22	-3
412	170.984	-16.297	423	172.781	-17.320	16.52	-3
412	170.984	-16.297	424	173.203	-17.344	19.55	-3
412	170.984	-16.297	629	169.570	-14.828	16.54	-3
416	178.188	-16.148	422	179.906	-16.484	13.90	-3
416	178.188	-16.148	426	177.367	-17.125	10.35	-3
416	178.188	-16.148	427	178.867	-17.680	13.73	-3
417	180.141	-13.750	418	181.305	-12.273	15.37	-3
418	181.305	-12.273	420	179.469	-11.273	16.98	-3
418	181.305	-12.273	525	181.820	-12.297	4.16	-3
419	179.430	-11.953	525	181.820	-12.297	19.50	-3
421	179.375	-16.727	426	177.367	-17.125	16.19	-3
421	179.375	-16.727	427	178.867	-17.680	8.83	-3
421	179.375	-16.727	432	179.492	-19.008	18.86	-3
422	179.906	-16.484	427	178.867	-17.680	12.83	-3
422	179.906	-16.484	529	180.336	-14.930	13.28	-3
423	172.781	-17.320	425	174.547	-17.703	14.26	-3
423	172.781	-17.320	436	172.305	-19.313	16.87	-3
423	172.781	-17.320	437	171.734	-17.781	9.08	-3
424	173.203	-17.344	425	174.547	-17.703	10.99	-3
424	173.203	-17.344	436	172.305	-19.313	17.71	-3
424	173.203	-17.344	437	171.734	-17.781	12.11	-3
426	177.367	-17.125	427	178.867	-17.680	12.67	-3
426	177.367	-17.125	445	176.633	-18.094	9.87	-3

Crater 1	*lon*	*lat*	*Crater 2*	*lon*	*lat*	*separation (km)*	*Score*
427	178.867	-17.680	432	179.492	-19.008	12.01	-3
427	178.867	-17.680	445	176.633	-18.094	17.88	-3
428	174.586	-20.742	444	176.633	-21.320	16.48	-3
431	182.039	-18.297	511	181.641	-19.813	12.89	-3
431	182.039	-18.297	512	182.031	-20.031	14.32	-3
433	180.219	-20.469	465	181.867	-21.727	16.40	-3
433	180.219	-20.469	466	181.844	-21.344	14.46	-3
433	180.219	-20.469	513	182.539	-21.352	19.32	-3
434	180.281	-21.234	465	181.867	-21.727	12.84	-3
434	180.281	-21.234	466	181.844	-21.344	12.05	-3
434	180.281	-21.234	512	182.031	-20.031	16.78	-3
434	180.281	-21.234	513	182.539	-21.352	17.39	-3
435	177.266	-22.313	449	178.180	-22.273	6.99	-3
435	177.266	-22.313	455	175.281	-23.742	19.15	-3
435	177.266	-22.313	459	176.039	-23.008	10.97	-3
435	177.266	-22.313	460	176.234	-23.711	13.95	-3
435	177.266	-22.313	461	176.766	-23.516	10.64	-3
436	172.305	-19.313	437	171.734	-17.781	13.41	-3
436	172.305	-19.313	439	170.539	-19.852	14.44	-3
436	172.305	-19.313	440	170.789	-20.742	16.66	-3
436	172.305	-19.313	450	171.750	-20.633	11.72	-3
436	172.305	-19.313	471	172.273	-21.703	19.74	-3
437	171.734	-17.781	439	170.539	-19.852	19.48	-3
438	170.188	-17.688	439	170.539	-19.852	18.08	-3
439	170.539	-19.852	440	170.789	-20.742	7.60	-3
439	170.539	-19.852	450	171.750	-20.633	11.38	-3
440	170.789	-20.742	441	171.281	-20.781	3.81	-3
440	170.789	-20.742	442	171.031	-22.906	17.96	-3
440	170.789	-20.742	450	171.750	-20.633	7.48	-3
440	170.789	-20.742	471	172.273	-21.703	13.91	-3
441	171.281	-20.781	442	171.031	-22.906	17.65	-3
442	171.031	-22.906	443	172.867	-22.859	13.97	-3
442	171.031	-22.906	450	171.750	-20.633	19.56	-3
442	171.031	-22.906	451	172.281	-24.172	14.09	-3
442	171.031	-22.906	452	171.789	-23.836	9.59	-3
442	171.031	-22.906	453	171.789	-23.836	9.59	-3
442	171.031	-22.906	470	171.070	-24.773	15.42	-3
442	171.031	-22.906	471	172.273	-21.703	13.74	-3
442	171.031	-22.906	619	169.695	-22.492	10.73	-3
443	172.867	-22.859	451	172.281	-24.172	11.71	-3
443	172.867	-22.859	453	171.789	-23.836	11.48	-3
443	172.867	-22.859	454	171.203	-23.797	14.80	-3
444	176.633	-21.320	448	178.453	-22.945	19.33	-3
444	176.633	-21.320	449	178.180	-22.273	14.23	-3
444	176.633	-21.320	459	176.039	-23.008	14.65	-3
447	180.250	-22.438	465	181.867	-21.727	13.69	-3
447	180.250	-22.438	467	180.836	-24.305	16.04	-3
447	180.250	-22.438	488	182.477	-23.195	18.06	-3
447	180.250	-22.438	489	182.852	-22.320	19.88	-3
447	180.250	-22.438	513	182.539	-21.352	19.69	-3
448	178.453	-22.945	457	180.445	-24.188	18.23	-3
448	178.453	-22.945	458	180.063	-24.469	17.50	-3
448	178.453	-22.945	462	178.609	-25.102	17.84	-3
450	171.750	-20.633	471	172.273	-21.703	9.71	-3
451	172.281	-24.172	452	171.789	-23.836	4.63	-3

Crater 1	*lon*	*lat*	*Crater 2*	*lon*	*lat*	*separation (km)*	*Score*
451	172.281	-24.172	453	171.789	-23.836	4.63	-3
451	172.281	-24.172	454	171.203	-23.797	8.70	-3
451	172.281	-24.172	469	170.984	-24.664	10.56	-3
451	172.281	-24.172	470	171.070	-24.773	10.37	-3
451	172.281	-24.172	472	170.836	-26.031	18.77	-3
452	171.789	-23.836	470	171.070	-24.773	9.44	-3
452	171.789	-23.836	471	172.273	-21.703	17.99	-3
452	171.789	-23.836	619	169.695	-22.492	19.38	-3
454	171.203	-23.797	472	170.836	-26.031	18.65	-3
454	171.203	-23.797	611	169.242	-25.336	19.45	-3
454	171.203	-23.797	619	169.695	-22.492	15.72	-3
455	175.281	-23.742	456	174.336	-25.383	15.29	-3
455	175.281	-23.742	459	176.039	-23.008	8.35	-3
455	175.281	-23.742	460	176.234	-23.711	7.21	-3
455	175.281	-23.742	461	176.766	-23.516	11.38	-3
456	174.336	-25.383	460	176.234	-23.711	19.84	-3
457	180.445	-24.188	458	180.063	-24.469	3.70	-3
457	180.445	-24.188	467	180.836	-24.305	3.10	-3
457	180.445	-24.188	488	182.477	-23.195	17.40	-3
457	180.445	-24.188	492	182.617	-25.258	18.53	-3
458	180.063	-24.469	462	178.609	-25.102	12.08	-3
458	180.063	-24.469	463	178.922	-25.313	11.02	-3
458	180.063	-24.469	464	179.758	-26.172	14.24	-3
458	180.063	-24.469	467	180.836	-24.305	5.97	-3
461	176.766	-23.516	462	178.609	-25.102	19.07	-3
462	178.609	-25.102	467	180.836	-24.305	17.95	-3
463	178.922	-25.313	478	179.680	-27.117	15.92	-3
463	178.922	-25.313	506	178.898	-27.391	17.16	-3
464	179.758	-26.172	473	177.359	-26.867	18.62	-3
464	179.758	-26.172	478	179.680	-27.117	7.83	-3
464	179.758	-26.172	479	180.250	-28.344	18.29	-3
464	179.758	-26.172	506	178.898	-27.391	11.89	-3
465	181.867	-21.727	466	181.844	-21.344	3.17	-3
465	181.867	-21.727	488	182.477	-23.195	12.99	-3
465	181.867	-21.727	489	182.852	-22.320	8.99	-3
465	181.867	-21.727	511	181.641	-19.813	15.90	-3
465	181.867	-21.727	512	182.031	-20.031	14.05	-3
466	181.844	-21.344	488	182.477	-23.195	16.03	-3
466	181.844	-21.344	511	181.641	-19.813	12.74	-3
466	181.844	-21.344	513	182.539	-21.352	5.35	-3
467	180.836	-24.305	492	182.617	-25.258	15.50	-3
468	181.477	-26.531	478	179.680	-27.117	14.09	-3
468	181.477	-26.531	479	180.250	-28.344	17.45	-3
468	181.477	-26.531	486	180.852	-27.469	9.00	-3
468	181.477	-26.531	503	182.602	-27.742	12.97	-3
469	170.984	-24.664	470	171.070	-24.773	1.11	-3
469	170.984	-24.664	472	170.836	-26.031	11.34	-3
469	170.984	-24.664	611	169.242	-25.336	14.17	-3
470	171.070	-24.773	472	170.836	-26.031	10.53	-3
470	171.070	-24.773	611	169.242	-25.336	14.44	-3
472	170.836	-26.031	483	171.500	-27.500	13.08	-3
472	170.836	-26.031	611	169.242	-25.336	13.17	-3
473	177.359	-26.867	474	175.609	-26.844	12.89	-3
473	177.359	-26.867	475	175.633	-27.664	14.28	-3
473	177.359	-26.867	478	179.680	-27.117	17.19	-3

Crater 1	*lon*	*lat*	*Crater 2*	*lon*	*lat*	*separation (km)*	*Score*
473	177.359	-26.867	481	176.219	-27.273	9.03	-3
474	175.609	-26.844	475	175.633	-27.664	6.77	-3
474	175.609	-26.844	476	173.492	-28.164	18.95	-3
474	175.609	-26.844	477	174.305	-28.563	17.10	-3
474	175.609	-26.844	480	175.141	-29.016	18.25	-3
474	175.609	-26.844	481	176.219	-27.273	5.71	-3
475	175.633	-27.664	476	173.492	-28.164	16.15	-3
475	175.633	-27.664	477	174.305	-28.563	12.19	-3
475	175.633	-27.664	480	175.141	-29.016	11.72	-3
475	175.633	-27.664	481	176.219	-27.273	5.37	-3
476	173.492	-28.164	483	171.500	-27.500	15.54	-3
476	173.492	-28.164	485	172.234	-28.852	10.75	-3
477	174.305	-28.563	480	175.141	-29.016	7.11	-3
477	174.305	-28.563	481	176.219	-27.273	17.55	-3
477	174.305	-28.563	482	172.195	-28.133	15.73	-3
477	174.305	-28.563	485	172.234	-28.852	15.18	-3
478	179.680	-27.117	479	180.250	-28.344	10.95	-3
478	179.680	-27.117	487	181.031	-28.070	12.64	-3
478	179.680	-27.117	504	182.242	-27.430	18.98	-3
479	180.250	-28.344	486	180.852	-27.469	8.45	-3
479	180.250	-28.344	487	181.031	-28.070	6.12	-3
479	180.250	-28.344	503	182.602	-27.742	17.84	-3
479	180.250	-28.344	504	182.242	-27.430	16.38	-3
479	180.250	-28.344	505	181.438	-29.039	10.34	-3
479	180.250	-28.344	506	178.898	-27.391	12.62	-3
481	176.219	-27.273	506	178.898	-27.391	19.68	-3
482	172.195	-28.133	485	172.234	-28.852	5.94	-3
483	171.500	-27.500	484	170.477	-27.266	7.75	-3
483	171.500	-27.500	485	172.234	-28.852	12.37	-3
484	170.477	-27.266	609	168.633	-28.203	15.54	-3
484	170.477	-27.266	610	169.383	-28.516	13.04	-3
484	170.477	-27.266	611	169.242	-25.336	18.36	-3
486	180.852	-27.469	487	181.031	-28.070	5.14	-3
486	180.852	-27.469	503	182.602	-27.742	13.00	-3
486	180.852	-27.469	504	182.242	-27.430	10.19	-3
486	180.852	-27.469	505	181.438	-29.039	13.65	-3
486	180.852	-27.469	506	178.898	-27.391	14.33	-3
487	181.031	-28.070	503	182.602	-27.742	11.77	-3
487	181.031	-28.070	505	181.438	-29.039	8.52	-3
487	181.031	-28.070	506	178.898	-27.391	16.56	-3
488	182.477	-23.195	492	182.617	-25.258	17.06	-3
488	182.477	-23.195	493	184.617	-24.250	18.37	-3
488	182.477	-23.195	513	182.539	-21.352	15.23	-3
489	182.852	-22.320	491	184.289	-23.539	14.86	-3
489	182.852	-22.320	513	182.539	-21.352	8.35	-3
490	183.539	-23.820	492	182.617	-25.258	13.74	-3
490	183.539	-23.820	493	184.617	-24.250	8.87	-3
491	184.289	-23.539	492	182.617	-25.258	18.96	-3
491	184.289	-23.539	494	185.742	-23.547	11.00	-3
492	182.617	-25.258	493	184.617	-24.250	17.15	-3
492	182.617	-25.258	498	184.250	-25.258	12.19	-3
492	182.617	-25.258	499	183.742	-25.961	10.19	-3
492	182.617	-25.258	500	184.461	-26.570	17.46	-3
492	182.617	-25.258	504	182.242	-27.430	18.14	-3
493	184.617	-24.250	494	185.742	-23.547	10.29	-3

Crater 1	***lon***	***lat***	***Crater 2***	***lon***	***lat***	***separation (km)***	***Score***
493	184.617	-24.250	498	184.250	-25.258	8.76	-3
493	184.617	-24.250	500	184.461	-26.570	19.19	-3
493	184.617	-24.250	507	185.891	-25.555	14.38	-3
494	185.742	-23.547	495	187.203	-21.992	16.98	-3
494	185.742	-23.547	496	187.313	-23.883	12.19	-3
494	185.742	-23.547	507	185.891	-25.555	16.61	-3
495	187.203	-21.992	496	187.313	-23.883	15.63	-3
496	187.313	-23.883	497	187.391	-25.492	13.30	-3
496	187.313	-23.883	507	185.891	-25.555	17.44	-3
496	187.313	-23.883	508	188.984	-25.063	15.89	-3
496	187.313	-23.883	510	186.391	-21.680	19.49	-3
497	187.391	-25.492	508	188.984	-25.063	12.41	-3
498	184.250	-25.258	499	183.742	-25.961	6.93	-3
498	184.250	-25.258	500	184.461	-26.570	10.95	-3
498	184.250	-25.258	507	185.891	-25.555	12.48	-3
499	183.742	-25.961	500	184.461	-26.570	7.32	-3
499	183.742	-25.961	501	184.313	-28.063	17.85	-3
499	183.742	-25.961	503	182.602	-27.742	16.94	-3
499	183.742	-25.961	507	185.891	-25.555	16.32	-3
500	184.461	-26.570	501	184.313	-28.063	12.37	-3
500	184.461	-26.570	503	182.602	-27.742	16.74	-3
500	184.461	-26.570	507	185.891	-25.555	13.52	-3
501	184.313	-28.063	502	186.016	-28.094	12.41	-3
501	184.313	-28.063	504	182.242	-27.430	16.00	-3
503	182.602	-27.742	504	182.242	-27.430	3.68	-3
503	182.602	-27.742	505	181.438	-29.039	13.64	-3
504	182.242	-27.430	505	181.438	-29.039	14.52	-3
510	186.391	-21.680	515	184.617	-20.438	17.08	-3
511	181.641	-19.813	513	182.539	-21.352	14.48	-3
512	182.031	-20.031	513	182.539	-21.352	11.58	-3
513	182.539	-21.352	515	184.617	-20.438	17.71	-3
514	185.242	-18.898	516	187.578	-19.523	18.93	-3
514	185.242	-18.898	517	187.336	-19.000	16.37	-3
516	187.578	-19.523	517	187.336	-19.000	4.72	-3
517	187.336	-19.000	518	186.320	-17.516	14.61	-3
519	187.945	-16.086	521	188.078	-14.430	13.71	-3
520	186.039	-15.453	521	188.078	-14.430	18.33	-3
520	186.039	-15.453	526	185.148	-14.148	12.90	-3
521	188.078	-14.430	522	188.797	-13.445	9.96	-3
522	188.797	-13.445	531	189.539	-11.875	14.28	-3
523	185.977	-12.445	526	185.148	-14.148	15.55	-3
523	185.977	-12.445	532	185.000	-10.914	14.90	-3
523	185.977	-12.445	537	185.117	-12.344	6.98	-3
524	183.719	-12.891	525	181.820	-12.297	16.06	-3
524	183.719	-12.891	526	185.148	-14.148	15.48	-3
524	183.719	-12.891	528	182.133	-14.758	19.98	-3
524	183.719	-12.891	532	185.000	-10.914	19.32	-3
524	183.719	-12.891	537	185.117	-12.344	12.14	-3
525	181.820	-12.297	527	181.461	-14.406	17.65	-3
525	181.820	-12.297	536	183.156	-10.523	18.20	-3
527	181.461	-14.406	528	182.133	-14.758	6.10	-3
530	188.234	-10.234	531	189.539	-11.875	17.18	-3
530	188.234	-10.234	535	188.078	-10.883	5.50	-3
530	188.234	-10.234	963	189.070	-8.359	16.91	-3
531	189.539	-11.875	535	188.078	-10.883	14.38	-3

Crater 1	*lon*	*lat*	*Crater 2*	*lon*	*lat*	*separation (km)*	*Score*
532	185.000	-10.914	533	184.742	-10.414	4.63	-3
532	185.000	-10.914	534	184.047	-10.297	9.26	-3
532	185.000	-10.914	536	183.156	-10.523	15.30	-3
533	184.742	-10.414	536	183.156	-10.523	12.91	-3
533	184.742	-10.414	537	185.117	-12.344	16.22	-3
534	184.047	-10.297	536	183.156	-10.523	7.47	-3
534	184.047	-10.297	537	185.117	-12.344	18.99	-3
534	184.047	-10.297	959	183.359	-8.281	17.56	-3
538	150.633	-11.734	539	150.305	-11.469	3.44	-3
538	150.633	-11.734	549	152.039	-12.633	13.56	-3
538	150.633	-11.734	732	149.063	-13.578	19.79	-3
539	150.305	-11.469	549	152.039	-12.633	16.98	-3
540	157.281	-11.547	541	158.367	-11.625	8.81	-3
540	157.281	-11.547	544	158.883	-12.406	14.75	-3
540	157.281	-11.547	545	157.609	-13.008	12.35	-3
540	157.281	-11.547	550	158.477	-10.203	14.73	-3
540	157.281	-11.547	1047	158.477	-9.898	16.71	-3
541	158.367	-11.625	544	158.883	-12.406	7.68	-3
541	158.367	-11.625	550	158.477	-10.203	11.77	-3
541	158.367	-11.625	1047	158.477	-9.898	14.28	-3
542	155.070	-12.359	547	154.211	-13.570	12.15	-3
542	155.070	-12.359	548	154.063	-14.313	18.04	-3
543	159.984	-10.969	550	158.477	-10.203	13.77	-3
543	159.984	-10.969	1048	159.984	-9.242	14.25	-3
544	158.883	-12.406	545	157.609	-13.008	11.39	-3
545	157.609	-13.008	546	155.680	-12.203	16.91	-3
545	157.609	-13.008	567	157.031	-14.523	13.34	-3
546	155.680	-12.203	547	154.211	-13.570	16.34	-3
548	154.063	-14.313	551	153.461	-15.180	8.62	-3
548	154.063	-14.313	552	151.961	-15.289	18.61	-3
550	158.477	-10.203	1047	158.477	-9.898	2.52	-3
550	158.477	-10.203	1048	159.984	-9.242	14.61	-3
553	159.836	-15.531	555	160.586	-13.367	18.84	-3
553	159.836	-15.531	575	159.953	-16.234	5.88	-3
554	157.195	-16.398	556	155.984	-16.297	9.63	-3
554	157.195	-16.398	565	158.070	-16.867	7.93	-3
554	157.195	-16.398	567	157.031	-14.523	15.53	-3
556	155.984	-16.297	558	154.281	-17.508	16.76	-3
556	155.984	-16.297	559	155.570	-18.180	15.88	-3
556	155.984	-16.297	565	158.070	-16.867	17.16	-3
558	154.281	-17.508	559	155.570	-18.180	11.55	-3
558	154.281	-17.508	560	154.430	-19.242	14.37	-3
558	154.281	-17.508	574	155.266	-18.641	12.13	-3
559	155.570	-18.180	574	155.266	-18.641	4.49	-3
560	154.430	-19.242	574	155.266	-18.641	8.20	-3
560	154.430	-19.242	577	153.688	-20.266	10.23	-3
560	154.430	-19.242	580	154.086	-20.883	13.80	-3
561	150.273	-18.477	563	151.445	-18.297	9.30	-3
561	150.273	-18.477	564	151.211	-19.141	9.15	-3
561	150.273	-18.477	578	151.203	-20.172	15.76	-3
561	150.273	-18.477	714	149.305	-19.102	9.16	-3
562	150.898	-18.742	563	151.445	-18.297	5.64	-3
562	150.898	-18.742	564	151.211	-19.141	4.10	-3
562	150.898	-18.742	578	151.203	-20.172	12.04	-3
562	150.898	-18.742	712	149.625	-20.406	16.94	-3

Crater 1	*lon*	*lat*	*Crater 2*	*lon*	*lat*	*separation (km)*	*Score*
563	151.445	-18.297	564	151.211	-19.141	7.20	-3
564	151.211	-19.141	578	151.203	-20.172	8.51	-3
564	151.211	-19.141	714	149.305	-19.102	14.87	-3
565	158.070	-16.867	566	158.328	-18.781	15.93	-3
565	158.070	-16.867	568	160.281	-17.875	19.30	-3
565	158.070	-16.867	575	159.953	-16.234	15.79	-3
566	158.328	-18.781	570	160.609	-18.836	17.83	-3
566	158.328	-18.781	576	160.305	-19.672	17.07	-3
568	160.281	-17.875	570	160.609	-18.836	8.34	-3
568	160.281	-17.875	571	161.352	-18.977	12.37	-3
568	160.281	-17.875	576	160.305	-19.672	14.84	-3
569	160.695	-18.070	570	160.609	-18.836	6.36	-3
569	160.695	-18.070	571	161.352	-18.977	9.08	-3
569	160.695	-18.070	576	160.305	-19.672	13.57	-3
570	160.609	-18.836	576	160.305	-19.672	7.30	-3
571	161.352	-18.977	576	160.305	-19.672	9.97	-3
578	151.203	-20.172	712	149.625	-20.406	12.37	-3
578	151.203	-20.172	714	149.305	-19.102	17.20	-3
579	151.586	-22.578	581	153.836	-22.898	17.33	-3
579	151.586	-22.578	583	153.367	-23.500	15.53	-3
579	151.586	-22.578	585	152.891	-24.336	17.56	-3
579	151.586	-22.578	711	149.281	-22.000	18.24	-3
580	154.086	-20.883	581	153.836	-22.898	16.75	-3
581	153.836	-22.898	584	154.977	-23.375	9.51	-3
581	153.836	-22.898	585	152.891	-24.336	13.85	-3
581	153.836	-22.898	589	153.813	-24.625	14.25	-3
583	153.367	-23.500	585	152.891	-24.336	7.78	-3
583	153.367	-23.500	589	153.813	-24.625	9.88	-3
584	154.977	-23.375	585	152.891	-24.336	17.63	-3
584	154.977	-23.375	586	155.492	-25.367	16.90	-3
584	154.977	-23.375	589	153.813	-24.625	13.55	-3
585	152.891	-24.336	589	153.813	-24.625	7.33	-3
586	155.492	-25.367	589	153.813	-24.625	13.98	-3
586	155.492	-25.367	591	157.234	-24.945	13.48	-3
586	155.492	-25.367	597	157.563	-26.578	18.33	-3
586	155.492	-25.367	599	157.656	-25.438	16.15	-3
586	155.492	-25.367	600	158.102	-25.563	19.52	-3
587	159.070	-24.594	591	157.234	-24.945	14.06	-3
587	159.070	-24.594	597	157.563	-26.578	19.86	-3
587	159.070	-24.594	599	157.656	-25.438	12.67	-3
587	159.070	-24.594	600	158.102	-25.563	10.79	-3
588	162.016	-22.516	614	163.703	-22.484	12.87	-3
588	162.016	-22.516	615	163.500	-20.617	19.38	-3
588	162.016	-22.516	616	161.250	-22.719	6.07	-3
590	156.664	-28.414	594	154.906	-29.375	14.98	-3
590	156.664	-28.414	595	154.930	-29.695	16.39	-3
590	156.664	-28.414	596	158.063	-29.625	14.21	-3
590	156.664	-28.414	597	157.563	-26.578	16.52	-3
591	157.234	-24.945	597	157.563	-26.578	13.70	-3
591	157.234	-24.945	599	157.656	-25.438	5.14	-3
591	157.234	-24.945	600	158.102	-25.563	8.24	-3
592	151.063	-28.336	593	151.766	-28.086	5.52	-3
596	158.063	-29.625	598	160.266	-28.766	17.39	-3
596	158.063	-29.625	601	160.148	-28.344	18.41	-3
597	157.563	-26.578	600	158.102	-25.563	9.29	-3

Crater 1	*lon*	*lat*	*Crater 2*	*lon*	*lat*	*separation (km)*	*Score*
598	160.266	-28.766	601	160.148	-28.344	3.58	-3
602	163.008	-28.984	603	164.922	-28.648	14.12	-3
602	163.008	-28.984	607	163.203	-27.945	8.69	-3
603	164.922	-28.648	607	163.203	-27.945	13.78	-3
604	164.266	-26.109	607	163.203	-27.945	17.05	-3
604	164.266	-26.109	613	163.625	-24.336	15.40	-3
605	165.180	-25.414	608	167.109	-25.469	14.39	-3
605	165.180	-25.414	613	163.625	-24.336	14.66	-3
606	165.625	-26.695	608	167.109	-25.469	14.96	-3
609	168.633	-28.203	610	169.383	-28.516	6.03	-3
612	164.500	-22.883	614	163.703	-22.484	6.90	-3
613	163.625	-24.336	614	163.703	-22.484	15.30	-3
614	163.703	-22.484	615	163.500	-20.617	15.49	-3
614	163.703	-22.484	616	161.250	-22.719	18.80	-3
615	163.500	-20.617	617	165.484	-20.445	15.41	-3
615	163.500	-20.617	621	165.398	-19.281	18.40	-3
620	166.164	-19.258	627	164.914	-17.617	16.71	-3
620	166.164	-19.258	628	166.336	-17.875	11.49	-3
621	165.398	-19.281	627	164.914	-17.617	14.25	-3
621	165.398	-19.281	628	166.336	-17.875	13.73	-3
622	164.891	-14.898	623	166.492	-13.141	19.37	-3
622	164.891	-14.898	624	163.688	-13.141	17.42	-3
622	164.891	-14.898	626	163.266	-13.328	18.37	-3
624	163.688	-13.141	633	164.219	-11.266	16.06	-3
624	163.688	-13.141	634	164.508	-10.992	18.93	-3
624	163.688	-13.141	636	164.688	-12.094	11.81	-3
625	164.008	-13.453	636	164.688	-12.094	12.49	-3
626	163.266	-13.328	633	164.219	-11.266	18.68	-3
626	163.266	-13.328	636	164.688	-12.094	15.33	-3
627	164.914	-17.617	628	166.336	-17.875	11.38	-3
631	161.750	-11.008	632	162.070	-11.195	3.02	-3
631	161.750	-11.008	635	163.383	-12.297	16.96	-3
632	162.070	-11.195	634	164.508	-10.992	19.82	-3
632	162.070	-11.195	635	163.383	-12.297	13.97	-3
632	162.070	-11.195	996	162.711	-9.109	17.99	-3
633	164.219	-11.266	634	164.508	-10.992	3.25	-3
633	164.219	-11.266	635	163.383	-12.297	10.87	-3
633	164.219	-11.266	636	164.688	-12.094	7.82	-3
633	164.219	-11.266	637	165.375	-10.664	10.61	-3
633	164.219	-11.266	638	166.273	-10.148	19.05	-3
634	164.508	-10.992	635	163.383	-12.297	14.10	-3
634	164.508	-10.992	636	164.688	-12.094	9.21	-3
634	164.508	-10.992	637	165.375	-10.664	7.54	-3
634	164.508	-10.992	638	166.273	-10.148	15.93	-3
636	164.688	-12.094	637	165.375	-10.664	13.05	-3
637	165.375	-10.664	998	166.516	-8.602	19.39	-3
638	166.273	-10.148	998	166.516	-8.602	12.92	-3
639	130.141	-12.773	641	132.008	-13.336	15.72	-3
639	130.141	-12.773	807	129.352	-13.805	10.61	-3
639	130.141	-12.773	809	129.297	-12.445	7.32	-3
640	135.828	-10.438	647	134.672	-11.766	14.42	-3
640	135.828	-10.438	648	136.320	-11.820	12.09	-3
640	135.828	-10.438	649	135.156	-12.742	19.79	-3
640	135.828	-10.438	655	136.703	-10.523	7.14	-3
640	135.828	-10.438	855	135.375	-8.391	17.30	-3

Crater 1	***lon***	***lat***	***Crater 2***	***lon***	***lat***	***separation (km)***	***Score***
641	132.008	-13.336	642	133.180	-14.680	14.53	-3
642	133.180	-14.680	643	131.570	-15.367	14.03	-3
642	133.180	-14.680	645	132.969	-16.086	11.73	-3
642	133.180	-14.680	646	134.852	-16.234	18.48	-3
642	133.180	-14.680	650	134.164	-13.406	13.14	-3
642	133.180	-14.680	651	134.555	-14.313	11.40	-3
642	133.180	-14.680	652	135.383	-15.102	17.92	-3
643	131.570	-15.367	645	132.969	-16.086	12.60	-3
644	130.578	-16.453	645	132.969	-16.086	19.19	-3
644	130.578	-16.453	659	130.672	-17.688	10.22	-3
644	130.578	-16.453	660	131.961	-17.953	16.50	-3
644	130.578	-16.453	794	128.539	-17.344	17.71	-3
644	130.578	-16.453	795	128.992	-17.547	15.44	-3
645	132.969	-16.086	646	134.852	-16.234	14.98	-3
645	132.969	-16.086	651	134.555	-14.313	19.34	-3
645	132.969	-16.086	660	131.961	-17.953	17.35	-3
646	134.852	-16.234	661	134.602	-18.094	15.48	-3
647	134.672	-11.766	648	136.320	-11.820	13.33	-3
647	134.672	-11.766	649	135.156	-12.742	8.96	-3
647	134.672	-11.766	650	134.164	-13.406	14.15	-3
648	136.320	-11.820	649	135.156	-12.742	12.09	-3
648	136.320	-11.820	654	137.320	-13.992	19.65	-3
648	136.320	-11.820	655	136.703	-10.523	11.15	-3
649	135.156	-12.742	650	134.164	-13.406	9.68	-3
649	135.156	-12.742	651	134.555	-14.313	13.83	-3
649	135.156	-12.742	652	135.383	-15.102	19.56	-3
650	134.164	-13.406	652	135.383	-15.102	17.06	-3
652	135.383	-15.102	654	137.320	-13.992	17.99	-3
652	135.383	-15.102	656	136.328	-16.531	13.99	-3
653	139.688	-12.242	657	139.523	-14.234	16.50	-3
654	137.320	-13.992	657	139.523	-14.234	17.75	-3
654	137.320	-13.992	658	139.594	-14.586	18.84	-3
656	136.328	-16.531	661	134.602	-18.094	18.75	-3
657	139.523	-14.234	658	139.594	-14.586	2.96	-3
657	139.523	-14.234	729	141.164	-15.313	15.83	-3
659	130.672	-17.688	660	131.961	-17.953	10.37	-3
660	131.961	-17.953	673	131.258	-19.594	14.62	-3
661	134.602	-18.094	662	134.063	-20.234	18.16	-3
662	134.063	-20.234	663	132.984	-20.555	8.75	-3
662	134.063	-20.234	674	134.359	-21.352	9.50	-3
663	132.984	-20.555	673	131.258	-19.594	15.56	-3
663	132.984	-20.555	674	134.359	-21.352	12.48	-3
665	136.852	-18.945	666	137.258	-20.008	9.32	-3
667	139.391	-17.313	721	140.984	-17.633	12.83	-3
668	139.813	-19.234	669	141.789	-19.328	15.42	-3
668	139.813	-19.234	671	139.781	-20.953	14.19	-3
668	139.813	-19.234	720	141.586	-18.469	15.23	-3
668	139.813	-19.234	721	140.984	-17.633	16.09	-3
669	141.789	-19.328	670	140.492	-20.391	13.35	-3
669	141.789	-19.328	672	142.133	-20.961	13.74	-3
669	141.789	-19.328	715	142.922	-18.781	9.93	-3
669	141.789	-19.328	720	141.586	-18.469	7.27	-3
669	141.789	-19.328	721	140.984	-17.633	15.35	-3
669	141.789	-19.328	726	144.258	-19.000	19.44	-3
670	140.492	-20.391	672	142.133	-20.961	13.52	-3

Crater 1	***lon***	***lat***	***Crater 2***	***lon***	***lat***	***separation (km)***	***Score***
670	140.492	-20.391	704	141.359	-22.414	17.98	-3
670	140.492	-20.391	720	141.586	-18.469	18.01	-3
671	139.781	-20.953	672	142.133	-20.961	18.13	-3
671	139.781	-20.953	704	141.359	-22.414	17.09	-3
672	142.133	-20.961	704	141.359	-22.414	13.38	-3
672	142.133	-20.961	715	142.922	-18.781	19.01	-3
674	134.359	-21.352	675	134.320	-23.148	14.84	-3
677	140.539	-25.344	680	139.133	-26.648	15.00	-3
677	140.539	-25.344	685	140.742	-26.406	8.90	-3
677	140.539	-25.344	693	140.680	-26.453	9.22	-3
678	137.344	-25.508	680	139.133	-26.648	16.27	-3
679	136.727	-25.563	680	139.133	-26.648	19.96	-3
679	136.727	-25.563	683	134.211	-26.172	19.35	-3
680	139.133	-26.648	684	137.938	-27.875	13.40	-3
680	139.133	-26.648	688	140.008	-28.922	19.83	-3
680	139.133	-26.648	693	140.680	-26.453	11.54	-3
681	132.273	-26.359	683	134.211	-26.172	14.43	-3
682	132.016	-27.234	683	134.211	-26.172	18.41	-3
682	132.016	-27.234	689	131.953	-29.039	14.91	-3
684	137.938	-27.875	686	138.547	-29.266	12.30	-3
684	137.938	-27.875	688	140.008	-28.922	17.34	-3
684	137.938	-27.875	690	137.820	-29.461	13.12	-3
685	140.742	-26.406	693	140.680	-26.453	0.60	-3
686	138.547	-29.266	687	140.477	-29.000	14.09	-3
686	138.547	-29.266	690	137.820	-29.461	5.47	-3
686	138.547	-29.266	691	140.414	-29.875	14.32	-3
687	140.477	-29.000	690	137.820	-29.461	19.51	-3
687	140.477	-29.000	691	140.414	-29.875	7.24	-3
688	140.008	-28.922	690	137.820	-29.461	16.38	-3
688	140.008	-28.922	691	140.414	-29.875	8.39	-3
690	137.820	-29.461	691	140.414	-29.875	18.92	-3
694	143.219	-24.203	695	143.219	-25.094	7.35	-3
694	143.219	-24.203	696	144.703	-24.758	12.06	-3
694	143.219	-24.203	703	143.734	-23.469	7.21	-3
695	143.219	-25.094	696	144.703	-24.758	11.45	-3
696	144.703	-24.758	697	146.406	-24.500	12.96	-3
696	144.703	-24.758	699	145.359	-25.766	9.66	-3
696	144.703	-24.758	701	145.898	-22.867	18.03	-3
696	144.703	-24.758	703	143.734	-23.469	12.90	-3
697	146.406	-24.500	699	145.359	-25.766	13.05	-3
697	146.406	-24.500	701	145.898	-22.867	14.02	-3
697	146.406	-24.500	702	148.203	-24.477	13.50	-3
698	149.211	-24.180	702	148.203	-24.477	7.97	-3
701	145.898	-22.867	703	143.734	-23.469	17.16	-3
701	145.898	-22.867	707	145.609	-20.805	17.17	-3
701	145.898	-22.867	708	146.641	-20.930	16.97	-3
701	145.898	-22.867	709	147.711	-21.539	17.67	-3
705	144.805	-20.477	706	144.711	-20.305	1.59	-3
705	144.805	-20.477	707	145.609	-20.805	6.78	-3
705	144.805	-20.477	708	146.641	-20.930	14.66	-3
705	144.805	-20.477	717	145.258	-19.008	12.63	-3
705	144.805	-20.477	718	146.102	-20.141	10.42	-3
705	144.805	-20.477	719	144.266	-18.688	15.35	-3
705	144.805	-20.477	726	144.258	-19.000	12.91	-3
706	144.711	-20.305	707	145.609	-20.805	8.08	-3

Crater 1	*lon*	*lat*	*Crater 2*	*lon*	*lat*	*separation (km)*	*Score*
706	144.711	-20.305	708	146.641	-20.930	15.78	-3
706	144.711	-20.305	715	142.922	-18.781	18.76	-3
706	144.711	-20.305	718	146.102	-20.141	10.86	-3
706	144.711	-20.305	719	144.266	-18.688	13.79	-3
706	144.711	-20.305	726	144.258	-19.000	11.33	-3
707	145.609	-20.805	708	146.641	-20.930	8.02	-3
707	145.609	-20.805	709	147.711	-21.539	17.28	-3
707	145.609	-20.805	717	145.258	-19.008	15.08	-3
707	145.609	-20.805	718	146.102	-20.141	6.67	-3
707	145.609	-20.805	726	144.258	-19.000	18.22	-3
708	146.641	-20.930	709	147.711	-21.539	9.65	-3
708	146.641	-20.930	710	148.164	-21.547	12.78	-3
708	146.641	-20.930	713	147.969	-19.563	15.27	-3
708	146.641	-20.930	717	145.258	-19.008	19.15	-3
709	147.711	-21.539	710	148.164	-21.547	3.48	-3
709	147.711	-21.539	711	149.281	-22.000	12.63	-3
709	147.711	-21.539	712	149.625	-20.406	17.47	-3
709	147.711	-21.539	713	147.969	-19.563	16.44	-3
710	148.164	-21.547	712	149.625	-20.406	14.68	-3
710	148.164	-21.547	713	147.969	-19.563	16.45	-3
710	148.164	-21.547	718	146.102	-20.141	19.70	-3
711	149.281	-22.000	712	149.625	-20.406	13.42	-3
712	149.625	-20.406	713	147.969	-19.563	14.62	-3
712	149.625	-20.406	714	149.305	-19.102	11.05	-3
713	147.969	-19.563	714	149.305	-19.102	11.08	-3
713	147.969	-19.563	718	146.102	-20.141	15.26	-3
715	142.922	-18.781	717	145.258	-19.008	18.34	-3
715	142.922	-18.781	719	144.266	-18.688	10.53	-3
715	142.922	-18.781	720	141.586	-18.469	10.76	-3
715	142.922	-18.781	721	140.984	-17.633	17.91	-3
715	142.922	-18.781	726	144.258	-19.000	10.59	-3
716	145.156	-17.742	717	145.258	-19.008	10.48	-3
716	145.156	-17.742	719	144.266	-18.688	10.47	-3
716	145.156	-17.742	722	147.031	-17.102	15.69	-3
716	145.156	-17.742	723	143.484	-16.305	17.75	-3
716	145.156	-17.742	726	144.258	-19.000	12.54	-3
717	145.258	-19.008	719	144.266	-18.688	8.19	-3
717	145.258	-19.008	726	144.258	-19.000	7.81	-3
718	146.102	-20.141	726	144.258	-19.000	17.16	-3
720	141.586	-18.469	721	140.984	-17.633	8.36	-3
721	140.984	-17.633	724	143.016	-16.297	19.46	-3
721	140.984	-17.633	729	141.164	-15.313	19.21	-3
722	147.031	-17.102	727	147.531	-16.148	8.81	-3
722	147.031	-17.102	728	147.602	-15.570	13.42	-3
723	143.484	-16.305	724	143.016	-16.297	3.71	-3
723	143.484	-16.305	725	143.297	-15.867	3.91	-3
723	143.484	-16.305	730	145.281	-15.008	17.85	-3
724	143.016	-16.297	725	143.297	-15.867	4.19	-3
724	143.016	-16.297	729	141.164	-15.313	16.80	-3
725	143.297	-15.867	729	141.164	-15.313	17.57	-3
725	143.297	-15.867	730	145.281	-15.008	17.31	-3
727	147.531	-16.148	728	147.602	-15.570	4.81	-3
728	147.602	-15.570	730	145.281	-15.008	19.05	-3
728	147.602	-15.570	731	147.430	-13.680	15.67	-3
728	147.602	-15.570	733	148.789	-14.047	15.75	-3

Crater 1	*lon*	*lat*	*Crater 2*	*lon*	*lat*	*separation (km)*	*Score*
730	145.281	-15.008	734	144.539	-12.867	18.65	-3
731	147.430	-13.680	732	149.063	-13.578	13.13	-3
731	147.430	-13.680	733	148.789	-14.047	11.31	-3
731	147.430	-13.680	735	145.555	-12.117	19.85	-3
732	149.063	-13.578	733	148.789	-14.047	4.45	-3
734	144.539	-12.867	735	145.555	-12.117	10.26	-3
734	144.539	-12.867	737	145.180	-11.039	15.95	-3
735	145.555	-12.117	736	143.945	-12.430	13.24	-3
735	145.555	-12.117	737	145.180	-11.039	9.40	-3
736	143.945	-12.430	740	142.320	-10.750	19.10	-3
737	145.180	-11.039	738	146.547	-11.047	11.08	-3
737	145.180	-11.039	739	147.195	-10.852	16.41	-3
738	146.547	-11.047	739	147.195	-10.852	5.50	-3
738	146.547	-11.047	869	148.453	-9.773	18.71	-3
739	147.195	-10.852	869	148.453	-9.773	13.55	-3
739	147.195	-10.852	870	147.492	-8.672	18.16	-3
740	142.320	-10.750	872	142.313	-8.711	16.83	-3
741	110.164	-10.852	742	112.141	-10.977	16.06	-3
741	110.164	-10.852	744	111.773	-12.477	18.69	-3
743	117.047	-10.328	823	114.922	-9.367	19.02	-3
743	117.047	-10.328	824	116.453	-9.414	8.96	-3
743	117.047	-10.328	826	117.828	-9.188	11.36	-3
746	119.289	-16.281	748	118.016	-16.844	11.10	-3
746	119.289	-16.281	752	119.352	-18.008	14.26	-3
746	119.289	-16.281	800	121.023	-17.469	16.85	-3
747	115.859	-16.016	748	118.016	-16.844	18.39	-3
747	115.859	-16.016	753	114.203	-17.156	16.14	-3
748	118.016	-16.844	750	117.531	-19.125	19.21	-3
748	118.016	-16.844	751	119.797	-18.469	19.40	-3
748	118.016	-16.844	752	119.352	-18.008	14.25	-3
749	113.516	-17.867	753	114.203	-17.156	7.98	-3
749	113.516	-17.867	754	112.930	-17.883	4.61	-3
750	117.531	-19.125	751	119.797	-18.469	18.52	-3
750	117.531	-19.125	752	119.352	-18.008	16.97	-3
751	119.797	-18.469	752	119.352	-18.008	5.16	-3
751	119.797	-18.469	800	121.023	-17.469	12.69	-3
752	119.352	-18.008	800	121.023	-17.469	13.88	-3
753	114.203	-17.156	754	112.930	-17.883	11.68	-3
755	110.430	-21.664	756	112.547	-20.766	17.90	-3
755	110.430	-21.664	758	111.672	-20.094	16.12	-3
756	112.547	-20.766	757	114.789	-20.344	17.68	-3
756	112.547	-20.766	758	111.672	-20.094	8.75	-3
757	114.789	-20.344	760	116.492	-22.047	19.22	-3
759	116.805	-22.250	761	117.031	-24.281	16.86	-3
759	116.805	-22.250	762	118.016	-23.727	15.27	-3
759	116.805	-22.250	764	117.555	-22.539	6.20	-3
759	116.805	-22.250	765	118.375	-23.055	13.68	-3
760	116.492	-22.047	761	117.031	-24.281	18.89	-3
760	116.492	-22.047	765	118.375	-23.055	16.59	-3
761	117.031	-24.281	762	118.016	-23.727	8.72	-3
761	117.031	-24.281	763	119.430	-24.250	18.05	-3
761	117.031	-24.281	765	118.375	-23.055	14.34	-3
762	118.016	-23.727	763	119.430	-24.250	11.51	-3
762	118.016	-23.727	765	118.375	-23.055	6.18	-3
763	119.430	-24.250	765	118.375	-23.055	12.69	-3

Crater 1	*lon*	*lat*	*Crater 2*	*lon*	*lat*	*separation (km)*	*Score*
763	119.430	-24.250	771	119.109	-26.531	18.98	-3
763	119.430	-24.250	780	120.070	-25.641	12.44	-3
764	117.555	-22.539	765	118.375	-23.055	7.56	-3
766	111.641	-28.602	767	111.922	-28.453	2.38	-3
766	111.641	-28.602	775	112.711	-29.594	11.26	-3
767	111.922	-28.453	775	112.711	-29.594	11.00	-3
768	114.813	-25.453	769	116.531	-27.313	19.93	-3
769	116.531	-27.313	770	117.453	-28.367	11.00	-3
770	117.453	-28.367	771	119.109	-26.531	19.41	-3
770	117.453	-28.367	773	119.313	-29.211	15.15	-3
771	119.109	-26.531	772	120.047	-27.297	9.36	-3
771	119.109	-26.531	776	121.063	-27.109	15.16	-3
772	120.047	-27.297	776	121.063	-27.109	7.62	-3
772	120.047	-27.297	780	120.070	-25.641	13.67	-3
773	119.313	-29.211	778	121.273	-28.711	14.75	-3
774	114.500	-29.148	775	112.711	-29.594	13.39	-3
776	121.063	-27.109	778	121.273	-28.711	13.31	-3
776	121.063	-27.109	780	120.070	-25.641	14.17	-3
777	124.609	-27.234	785	125.828	-28.164	11.76	-3
779	122.688	-29.063	781	123.359	-29.563	6.36	-3
782	125.727	-24.117	786	128.219	-23.344	19.89	-3
782	125.727	-24.117	788	126.602	-22.641	13.88	-3
784	127.523	-25.672	786	128.219	-23.344	19.92	-3
786	128.219	-23.344	802	126.953	-21.484	18.14	-3
788	126.602	-22.641	802	126.953	-21.484	9.92	-3
790	126.617	-20.172	796	126.102	-18.805	11.98	-3
790	126.617	-20.172	797	127.078	-19.688	5.37	-3
790	126.617	-20.172	798	125.258	-19.250	13.02	-3
790	126.617	-20.172	802	126.953	-21.484	11.14	-3
791	127.602	-20.016	796	126.102	-18.805	15.37	-3
791	127.602	-20.016	798	125.258	-19.250	19.29	-3
793	126.234	-17.570	794	128.539	-17.344	18.25	-3
793	126.234	-17.570	796	126.102	-18.805	10.24	-3
793	126.234	-17.570	797	127.078	-19.688	18.68	-3
793	126.234	-17.570	798	125.258	-19.250	15.84	-3
793	126.234	-17.570	801	125.016	-17.555	9.59	-3
797	127.078	-19.688	802	126.953	-21.484	14.87	-3
798	125.258	-19.250	801	125.016	-17.555	14.12	-3
799	122.516	-18.969	800	121.023	-17.469	17.04	-3
803	127.203	-12.977	805	126.203	-14.211	12.97	-3
803	127.203	-12.977	806	126.164	-12.328	9.93	-3
803	127.203	-12.977	807	129.352	-13.805	18.56	-3
803	127.203	-12.977	808	129.375	-13.633	18.27	-3
803	127.203	-12.977	809	129.297	-12.445	17.42	-3
804	124.250	-14.672	805	126.203	-14.211	16.07	-3
806	126.164	-12.328	810	124.898	-10.750	16.57	-3
807	129.352	-13.805	809	129.297	-12.445	11.23	-3
808	129.375	-13.633	809	129.297	-12.445	9.82	-3
811	116.375	-2.500	812	118.320	-2.586	16.06	-3
811	116.375	-2.500	813	117.477	-0.547	18.51	-3
812	118.320	-2.586	819	120.164	-4.063	19.48	-3
813	117.477	-0.547	1062	119.078	0.555	16.05	-3
815	115.844	-5.492	817	114.398	-3.969	17.31	-3
815	115.844	-5.492	821	116.539	-7.297	15.95	-3
815	115.844	-5.492	822	114.492	-7.055	17.01	-3

Crater 1	*lon*	*lat*	*Crater 2*	*lon*	*lat*	*separation (km)*	*Score*
816	112.852	-6.195	822	114.492	-7.055	15.21	-3
818	119.734	-1.641	1062	119.078	0.555	18.92	-3
819	120.164	-4.063	829	121.727	-3.719	13.18	-3
819	120.164	-4.063	830	122.211	-4.328	16.99	-3
820	118.820	-6.617	821	116.539	-7.297	19.52	-3
820	118.820	-6.617	827	118.750	-7.852	10.21	-3
820	118.820	-6.617	828	119.227	-7.961	11.58	-3
821	116.539	-7.297	822	114.492	-7.055	16.88	-3
821	116.539	-7.297	824	116.453	-9.414	17.49	-3
821	116.539	-7.297	826	117.828	-9.188	18.83	-3
821	116.539	-7.297	827	118.750	-7.852	18.66	-3
823	114.922	-9.367	824	116.453	-9.414	12.48	-3
824	116.453	-9.414	825	118.172	-9.438	14.00	-3
824	116.453	-9.414	826	117.828	-9.188	11.36	-3
825	118.172	-9.438	826	117.828	-9.188	3.48	-3
825	118.172	-9.438	827	118.750	-7.852	13.92	-3
825	118.172	-9.438	828	119.227	-7.961	14.92	-3
826	117.828	-9.188	828	119.227	-7.961	15.26	-3
831	124.656	-5.492	832	125.078	-4.563	8.42	-3
833	124.359	-8.383	836	122.563	-9.758	18.53	-3
834	127.844	-9.016	835	127.766	-9.859	6.99	-3
841	131.766	-4.563	842	132.086	-4.938	4.07	-3
841	131.766	-4.563	843	132.055	-5.672	9.46	-3
841	131.766	-4.563	847	131.664	-6.547	16.40	-3
842	132.086	-4.938	843	132.055	-5.672	6.07	-3
842	132.086	-4.938	847	131.664	-6.547	13.73	-3
843	132.055	-5.672	847	131.664	-6.547	7.90	-3
844	134.633	-4.117	845	136.617	-4.391	16.49	-3
845	136.617	-4.391	846	138.602	-3.102	19.51	-3
845	136.617	-4.391	854	137.719	-5.445	12.57	-3
847	131.664	-6.547	848	131.883	-7.492	8.01	-3
847	131.664	-6.547	850	132.945	-8.047	16.23	-3
848	131.883	-7.492	849	134.313	-7.438	19.89	-3
848	131.883	-7.492	850	132.945	-8.047	9.82	-3
848	131.883	-7.492	851	133.922	-8.672	19.30	-3
849	134.313	-7.438	850	132.945	-8.047	12.26	-3
849	134.313	-7.438	851	133.922	-8.672	10.68	-3
849	134.313	-7.438	855	135.375	-8.391	11.72	-3
850	132.945	-8.047	851	133.922	-8.672	9.50	-3
851	133.922	-8.672	855	135.375	-8.391	12.09	-3
852	139.711	-7.297	856	139.773	-5.391	15.75	-3
852	139.711	-7.297	857	140.172	-9.211	16.24	-3
852	139.711	-7.297	858	140.375	-7.438	5.56	-3
853	139.008	-8.141	857	140.172	-9.211	12.97	-3
853	139.008	-8.141	858	140.375	-7.438	12.60	-3
854	137.719	-5.445	856	139.773	-5.391	16.89	-3
856	139.773	-5.391	860	142.141	-5.500	19.47	-3
857	140.172	-9.211	858	140.375	-7.438	14.73	-3
857	140.172	-9.211	872	142.313	-8.711	17.94	-3
858	140.375	-7.438	872	142.313	-8.711	19.01	-3
859	141.867	-3.820	860	142.141	-5.500	14.05	-3
859	141.867	-3.820	861	143.750	-5.344	19.96	-3
859	141.867	-3.820	863	144.188	-3.352	19.51	-3
860	142.141	-5.500	861	143.750	-5.344	13.29	-3
861	143.750	-5.344	863	144.188	-3.352	16.84	-3

Crater 1	*lon*	*lat*	*Crater 2*	*lon*	*lat*	*separation (km)*	*Score*
861	143.750	-5.344	864	145.422	-5.758	14.16	-3
861	143.750	-5.344	865	145.625	-6.297	17.29	-3
862	142.961	-8.281	871	143.117	-7.852	3.77	-3
862	142.961	-8.281	872	142.313	-8.711	6.37	-3
867	147.422	-4.195	868	149.078	-3.219	15.85	-3
868	149.078	-3.219	1033	150.313	-2.148	13.48	-3
869	148.453	-9.773	870	147.492	-8.672	12.00	-3
869	148.453	-9.773	873	149.875	-8.336	16.59	-3
869	148.453	-9.773	874	147.789	-8.117	14.71	-3
870	147.492	-8.672	873	149.875	-8.336	19.65	-3
870	147.492	-8.672	874	147.789	-8.117	5.18	-3
873	149.875	-8.336	874	147.789	-8.117	17.14	-3
873	149.875	-8.336	1034	150.656	-7.102	12.03	-3
875	149.961	-5.617	1034	150.656	-7.102	13.52	-3
875	149.961	-5.617	1041	151.469	-4.531	15.30	-3
879	193.289	4.148	881	191.994	3.702	11.29	-3
879	193.289	4.148	882	191.974	2.664	16.36	-3
880	191.666	6.028	881	191.994	3.702	19.39	-3
881	191.994	3.702	882	191.974	2.664	8.57	-3
882	191.974	2.664	894	193.195	0.938	17.45	-3
883	199.024	8.506	916	200.063	8.727	8.67	-3
883	199.024	8.506	917	199.266	9.500	8.44	-3
884	198.914	5.733	886	198.844	4.188	12.77	-3
884	198.914	5.733	887	198.367	7.844	17.99	-3
884	198.914	5.733	888	200.438	4.578	15.74	-3
884	198.914	5.733	889	200.813	4.633	18.06	-3
886	198.844	4.188	888	200.438	4.578	13.51	-3
886	198.844	4.188	889	200.813	4.633	16.62	-3
886	198.844	4.188	890	197.719	2.844	14.46	-3
886	198.844	4.188	891	199.719	2.734	14.00	-3
887	198.367	7.844	916	200.063	8.727	15.65	-3
887	198.367	7.844	917	199.266	9.500	15.51	-3
888	200.438	4.578	889	200.813	4.633	3.12	-3
888	200.438	4.578	891	199.719	2.734	16.33	-3
889	200.813	4.633	891	199.719	2.734	18.08	-3
890	197.719	2.844	891	199.719	2.734	16.52	-3
891	199.719	2.734	895	201.125	1.547	15.19	-3
892	193.141	-0.016	893	194.055	-0.484	8.48	-3
892	193.141	-0.016	894	193.195	0.938	7.88	-3
892	193.141	-0.016	921	193.746	-1.388	12.39	-3
893	194.055	-0.484	894	193.195	0.938	13.72	-3
893	194.055	-0.484	921	193.746	-1.388	7.89	-3
894	193.195	0.938	921	193.746	-1.388	19.73	-3
895	201.125	1.547	897	200.305	-0.234	16.19	-3
897	200.305	-0.234	918	200.868	-2.489	19.18	-3
898	192.227	-4.516	899	192.531	-4.891	3.98	-3
898	192.227	-4.516	900	190.305	-5.484	17.71	-3
898	192.227	-4.516	903	192.711	-6.773	19.06	-3
899	192.531	-4.891	900	190.305	-5.484	18.95	-3
899	192.531	-4.891	903	192.711	-6.773	15.61	-3
900	190.305	-5.484	905	190.438	-7.453	16.29	-3
900	190.305	-5.484	964	188.891	-3.875	17.66	-3
902	200.063	-5.430	907	200.445	-7.430	16.81	-3
903	192.711	-6.773	905	190.438	-7.453	19.45	-3
904	190.125	-6.625	905	190.438	-7.453	7.30	-3

Crater 1	***lon***	***lat***	***Crater 2***	***lon***	***lat***	***separation (km)***	***Score***
905	190.438	-7.453	963	189.070	-8.359	13.45	-3
912	207.648	-0.875	913	208.094	-1.922	9.39	-3
916	200.063	8.727	917	199.266	9.500	9.11	-3
922	176.781	-2.047	953	174.711	-2.813	18.21	-3
922	176.781	-2.047	954	177.023	-1.656	3.79	-3
925	184.094	5.852	926	183.398	5.438	6.66	-3
926	183.398	5.438	927	181.852	4.109	16.80	-3
928	186.328	3.875	929	186.352	3.141	6.07	-3
928	186.328	3.875	977	186.938	3.563	5.64	-3
929	186.352	3.141	931	186.945	1.906	11.31	-3
929	186.352	3.141	977	186.938	3.563	5.95	-3
931	186.945	1.906	977	186.938	3.563	13.67	-3
932	177.148	1.828	939	177.273	3.141	10.88	-3
933	174.602	6.234	934	172.625	5.383	17.69	-3
933	174.602	6.234	935	173.695	5.445	9.89	-3
933	174.602	6.234	940	175.539	6.602	8.27	-3
934	172.625	5.383	935	173.695	5.445	8.81	-3
934	172.625	5.383	936	171.102	5.031	12.86	-3
934	172.625	5.383	937	170.625	6.563	19.09	-3
935	173.695	5.445	938	173.836	3.125	19.19	-3
935	173.695	5.445	940	175.539	6.602	17.89	-3
936	171.102	5.031	981	169.016	5.078	17.16	-3
936	171.102	5.031	1011	169.633	3.289	18.79	-3
937	170.625	6.563	944	170.031	8.391	15.86	-3
937	170.625	6.563	981	169.016	5.078	18.02	-3
942	176.992	9.477	975	176.375	9.219	5.46	-3
943	172.656	8.773	945	170.487	9.613	18.99	-3
943	172.656	8.773	946	171.366	10.539	17.97	-3
944	170.031	8.391	945	170.487	9.613	10.75	-3
947	170.914	-2.141	948	172.375	-2.313	12.13	-3
948	172.375	-2.313	953	174.711	-2.813	19.70	-3
949	179.875	-1.406	951	180.531	-1.891	6.73	-3
949	179.875	-1.406	952	180.477	-1.594	5.20	-3
950	179.602	-2.281	951	180.531	-1.891	8.32	-3
950	179.602	-2.281	952	180.477	-1.594	9.18	-3
951	180.531	-1.891	952	180.477	-1.594	2.49	-3
955	173.578	-5.977	958	173.484	-8.352	19.62	-3
956	171.664	-7.586	958	173.484	-8.352	16.17	-3
956	171.664	-7.586	990	169.727	-8.484	17.49	-3
959	183.359	-8.281	968	183.953	-7.133	10.65	-3
960	186.180	-8.523	961	187.000	-6.930	14.77	-3
960	186.180	-8.523	962	186.477	-7.438	9.29	-3
964	188.891	-3.875	965	189.375	-2.852	9.34	-3
964	188.891	-3.875	966	188.891	-3.008	7.16	-3
964	188.891	-3.875	967	187.914	-3.555	8.47	-3
965	189.375	-2.852	966	188.891	-3.008	4.20	-3
965	189.375	-2.852	967	187.914	-3.555	13.37	-3
965	189.375	-2.852	969	188.555	-0.578	19.95	-3
968	183.953	-7.133	978	184.188	-4.859	18.87	-3
970	184.602	-1.039	971	185.414	-2.188	11.61	-3
970	184.602	-1.039	972	182.828	-0.789	14.78	-3
970	184.602	-1.039	973	182.781	-0.430	15.85	-3
970	184.602	-1.039	976	185.094	0.250	11.39	-3
972	182.828	-0.789	973	182.781	-0.430	2.99	-3
973	182.781	-0.430	976	185.094	0.250	19.90	-3

Crater 1	***lon***	***lat***	***Crater 2***	***lon***	***lat***	***separation (km)***	***Score***
979	164.844	6.531	984	166.567	7.102	14.89	-3
979	164.844	6.531	987	164.254	5.199	12.02	-3
979	164.844	6.531	1013	162.500	6.109	19.54	-3
980	162.719	7.813	982	162.818	9.306	12.35	-3
980	162.719	7.813	1013	162.500	6.109	14.17	-3
981	169.016	5.078	1011	169.633	3.289	15.62	-3
983	164.148	3.332	986	163.059	5.141	17.42	-3
983	164.148	3.332	987	164.254	5.199	15.44	-3
986	163.059	5.141	987	164.254	5.199	9.84	-3
986	163.059	5.141	1012	160.891	6.094	19.47	-3
986	163.059	5.141	1013	162.500	6.109	9.22	-3
987	164.254	5.199	1013	162.500	6.109	16.25	-3
988	167.250	-2.750	1003	166.836	-2.188	5.76	-3
988	167.250	-2.750	1006	166.359	-1.539	12.41	-3
989	167.766	-6.344	991	168.820	-4.758	15.70	-3
989	167.766	-6.344	997	166.711	-5.883	9.46	-3
990	169.727	-8.484	999	168.531	-8.820	10.14	-3
991	168.820	-4.758	997	166.711	-5.883	19.67	-3
992	160.969	-3.883	1000	160.961	-2.391	12.32	-3
992	160.969	-3.883	1009	160.391	-1.953	16.63	-3
992	160.969	-3.883	1031	158.875	-3.555	17.46	-3
993	161.711	-6.320	1043	159.930	-6.422	14.64	-3
994	160.609	-6.977	1043	159.930	-6.422	7.21	-3
994	160.609	-6.977	1048	159.984	-9.242	19.39	-3
994	160.609	-6.977	1050	159.227	-7.641	12.58	-3
995	164.977	-8.430	996	162.711	-9.109	19.32	-3
997	166.711	-5.883	1001	165.086	-4.781	16.16	-3
997	166.711	-5.883	1002	165.063	-4.328	18.67	-3
998	166.516	-8.602	999	168.531	-8.820	16.55	-3
1000	160.961	-2.391	1004	162.531	-1.102	16.77	-3
1000	160.961	-2.391	1009	160.391	-1.953	5.93	-3
1000	160.961	-2.391	1027	159.336	-1.875	14.07	-3
1000	160.961	-2.391	1030	159.773	-0.609	17.67	-3
1000	160.961	-2.391	1031	158.875	-3.555	19.70	-3
1003	166.836	-2.188	1005	164.688	-1.133	19.75	-3
1003	166.836	-2.188	1006	166.359	-1.539	6.64	-3
1004	162.531	-1.102	1007	161.969	-0.523	6.66	-3
1004	162.531	-1.102	1008	160.797	-1.305	14.41	-3
1007	161.969	-0.523	1030	159.773	-0.609	18.14	-3
1014	151.641	4.008	1015	151.516	4.188	1.81	-3
1014	151.641	4.008	1016	152.563	3.422	9.00	-3
1014	151.641	4.008	1022	151.469	3.016	8.31	-3
1014	151.641	4.008	1023	152.102	3.219	7.54	-3
1014	151.641	4.008	1082	149.734	2.984	17.84	-3
1015	151.516	4.188	1016	152.563	3.422	10.69	-3
1015	151.516	4.188	1022	151.469	3.016	9.68	-3
1015	151.516	4.188	1023	152.102	3.219	9.34	-3
1015	151.516	4.188	1082	149.734	2.984	17.72	-3
1016	152.563	3.422	1021	153.680	1.906	15.54	-3
1016	152.563	3.422	1023	152.102	3.219	4.15	-3
1017	156.102	5.117	1018	155.328	4.914	6.58	-3
1022	151.469	3.016	1023	152.102	3.219	5.48	-3
1022	151.469	3.016	1082	149.734	2.984	14.30	-3
1023	152.102	3.219	1082	149.734	2.984	19.61	-3
1024	153.773	-0.984	1025	155.391	-0.391	14.22	-3

Crater 1	*lon*	*lat*	*Crater 2*	*lon*	*lat*	*separation (km)*	*Score*
1025	155.391	-0.391	1026	156.578	-1.406	12.90	-3
1026	156.578	-1.406	1028	158.148	-2.875	17.74	-3
1026	156.578	-1.406	1029	156.719	-2.633	10.19	-3
1028	158.148	-2.875	1040	157.398	-5.125	19.57	-3
1029	156.719	-2.633	1031	158.875	-3.555	19.34	-3
1031	158.875	-3.555	1040	157.398	-5.125	17.77	-3
1032	155.266	-3.648	1039	152.961	-3.758	19.01	-3
1034	150.656	-7.102	1049	152.375	-6.023	16.67	-3
1035	153.945	-6.273	1036	153.891	-6.008	2.24	-3
1035	153.945	-6.273	1037	152.547	-5.422	13.47	-3
1035	153.945	-6.273	1045	154.602	-8.000	15.23	-3
1035	153.945	-6.273	1049	152.375	-6.023	13.05	-3
1036	153.891	-6.008	1037	152.547	-5.422	12.05	-3
1036	153.891	-6.008	1042	153.461	-7.867	15.75	-3
1036	153.891	-6.008	1045	154.602	-8.000	17.45	-3
1037	152.547	-5.422	1038	151.445	-6.016	10.29	-3
1037	152.547	-5.422	1039	152.961	-3.758	14.15	-3
1037	152.547	-5.422	1041	151.469	-4.531	11.52	-3
1037	152.547	-5.422	1049	152.375	-6.023	5.16	-3
1038	151.445	-6.016	1041	151.469	-4.531	12.26	-3
1038	151.445	-6.016	1049	152.375	-6.023	7.63	-3
1039	152.961	-3.758	1041	151.469	-4.531	13.85	-3
1039	152.961	-3.758	1049	152.375	-6.023	19.31	-3
1042	153.461	-7.867	1045	154.602	-8.000	9.39	-3
1042	153.461	-7.867	1046	154.117	-9.492	14.44	-3
1042	153.461	-7.867	1049	152.375	-6.023	17.63	-3
1044	155.914	-8.289	1045	154.602	-8.000	10.99	-3
1044	155.914	-8.289	1046	154.117	-9.492	17.70	-3
1047	158.477	-9.898	1050	159.227	-7.641	19.62	-3
1048	159.984	-9.242	1050	159.227	-7.641	14.60	-3
1052	119.023	8.125	1054	117.180	8.375	15.20	-3
1057	117.969	2.695	1062	119.078	0.555	19.90	-3
1060	120.188	4.234	1061	120.672	4.047	4.28	-3
1061	120.672	4.047	1068	121.344	4.219	5.71	-3
1064	123.516	3.883	1068	121.344	4.219	18.10	-3
1065	127.711	2.938	1067	128.953	1.492	15.73	-3
1066	129.719	1.234	1067	128.953	1.492	6.67	-3
1073	137.313	2.602	1075	137.320	0.742	15.35	-3
1073	137.313	2.602	1077	138.656	3.086	11.78	-3
1074	136.742	0.008	1075	137.320	0.742	7.72	-3
1074	136.742	0.008	1076	137.773	0.070	8.53	-3
1075	137.320	0.742	1076	137.773	0.070	6.69	-3
1076	137.773	0.070	1081	139.867	0.742	18.15	-3
1077	138.656	3.086	1078	140.445	3.539	15.21	-3
1077	138.656	3.086	1080	139.703	5.234	19.72	-3
1078	140.445	3.539	1079	140.477	3.117	3.49	-3
1078	140.445	3.539	1080	139.703	5.234	15.27	-3
1083	148.586	5.219	1084	148.211	5.680	4.90	-3
3	253.508	-16.685	41	253.515	-18.099	11.67	-4
4	252.679	-13.583	39	253.317	-14.742	10.84	-4
5	256.622	-11.029	341	257.930	-9.125	18.97	-4
8	255.459	-20.777	18	255.086	-20.572	3.34	-4
9	251.772	-21.941	43	250.785	-22.843	10.59	-4
12	256.831	-24.793	52	256.699	-24.483	2.74	-4
16	251.662	-21.559	44	250.413	-22.422	11.93	-4

Crater 1	*lon*	*lat*	*Crater 2*	*lon*	*lat*	*separation (km)*	*Score*
17	254.645	-21.797	18	255.086	-20.572	10.67	-4
25	268.890	-25.130	26	268.606	-24.971	2.50	-4
25	268.890	-25.130	49	269.228	-25.301	2.89	-4
25	268.890	-25.130	53	269.500	-25.804	7.19	-4
26	268.606	-24.971	53	269.500	-25.804	9.58	-4
157	220.971	-20.990	164	221.111	-23.153	17.89	-4
219	223.195	4.086	226	221.867	3.234	13.01	-4
221	228.344	3.906	223	227.766	4.242	5.51	-4
238	232.289	8.563	239	232.516	8.289	2.92	-4
282	238.516	-3.000	296	239.563	-2.078	11.51	-4
360	193.133	-12.721	364	192.133	-12.013	9.96	-4
360	193.133	-12.721	369	195.070	-13.867	18.21	-4
364	192.133	-12.013	372	193.398	-14.037	19.56	-4
372	193.398	-14.037	375	191.595	-15.101	16.87	-4
373	197.997	-13.449	377	200.168	-14.031	18.06	-4
392	199.026	-29.568	393	200.834	-28.248	17.01	-4
407	170.664	-14.102	408	170.320	-15.336	10.55	-4
410	172.375	-15.859	411	170.914	-16.641	13.25	-4
410	172.375	-15.859	437	171.734	-17.781	16.65	-4
421	179.375	-16.727	529	180.336	-14.930	16.68	-4
430	182.141	-17.031	446	180.867	-18.344	14.76	-4
431	182.039	-18.297	446	180.867	-18.344	9.19	-4
432	179.492	-19.008	446	180.867	-18.344	12.07	-4
432	179.492	-19.008	511	181.641	-19.813	18.00	-4
433	180.219	-20.469	434	180.281	-21.234	6.34	-4
433	180.219	-20.469	446	180.867	-18.344	18.25	-4
435	177.266	-22.313	448	178.453	-22.945	10.45	-4
441	171.281	-20.781	450	171.750	-20.633	3.82	-4
443	172.867	-22.859	452	171.789	-23.836	11.48	-4
443	172.867	-22.859	455	175.281	-23.742	19.70	-4
443	172.867	-22.859	471	172.273	-21.703	10.57	-4
444	176.633	-21.320	460	176.234	-23.711	19.97	-4
444	176.633	-21.320	461	176.766	-23.516	18.15	-4
447	180.250	-22.438	457	180.445	-24.188	14.52	-4
448	178.453	-22.945	459	176.039	-23.008	18.36	-4
448	178.453	-22.945	461	176.766	-23.516	13.64	-4
462	178.609	-25.102	463	178.922	-25.313	2.91	-4
483	171.500	-27.500	610	169.383	-28.516	17.56	-4
494	185.742	-23.547	510	186.391	-21.680	16.19	-4
500	184.461	-26.570	502	186.016	-28.094	16.98	-4
518	186.320	-17.516	519	187.945	-16.086	17.44	-4
544	158.883	-12.406	550	158.477	-10.203	18.48	-4
544	158.883	-12.406	555	160.586	-13.367	15.84	-4
547	154.211	-13.570	549	152.039	-12.633	19.10	-4
547	154.211	-13.570	551	153.461	-15.180	14.58	-4
551	153.461	-15.180	552	151.961	-15.289	11.98	-4
553	159.836	-15.531	568	160.281	-17.875	19.67	-4
566	158.328	-18.781	569	160.695	-18.070	19.45	-4
597	157.563	-26.578	599	157.656	-25.438	9.44	-4
612	164.500	-22.883	613	163.625	-24.336	13.70	-4
641	132.008	-13.336	643	131.570	-15.367	17.13	-4
641	132.008	-13.336	650	134.164	-13.406	17.33	-4
695	143.219	-25.094	699	145.359	-25.766	16.90	-4
794	128.539	-17.344	795	128.992	-17.547	3.94	-4
807	129.352	-13.805	808	129.375	-13.633	1.43	-4

Crater 1	*lon*	*lat*	*Crater 2*	*lon*	*lat*	*separation (km)*	*Score*
966	188.891	-3.008	967	187.914	-3.555	9.23	-4
1053	117.078	6.531	1054	117.180	8.375	15.24	-4
2	255.426	-16.152	3	253.508	-16.685	15.82	-5
2	255.426	-16.152	6	257.827	-16.434	19.17	-5
2	255.426	-16.152	32	256.003	-15.443	7.43	-5
2	255.426	-16.152	62	256.281	-14.008	18.97	-5
3	253.508	-16.685	57	255.199	-17.097	13.79	-5
6	257.827	-16.434	32	256.003	-15.443	16.63	-5
6	257.827	-16.434	33	259.162	-15.154	14.97	-5
6	257.827	-16.434	42	257.898	-17.972	12.71	-5
7	254.448	-19.573	8	255.459	-20.777	12.66	-5
7	254.448	-19.573	18	255.086	-20.572	9.62	-5
7	254.448	-19.573	41	253.515	-18.099	14.18	-5
9	251.772	-21.941	67	250.910	-23.100	11.61	-5
10	251.215	-24.928	43	250.785	-22.843	17.51	-5
10	251.215	-24.928	58	252.719	-23.732	15.01	-5
10	251.215	-24.928	65	252.699	-24.208	12.62	-5
10	251.215	-24.928	67	250.910	-23.100	15.26	-5
11	256.429	-21.995	15	255.089	-23.205	14.28	-5
12	256.831	-24.793	15	255.089	-23.205	18.56	-5
12	256.831	-24.793	45	256.439	-26.957	18.10	-5
12	256.831	-24.793	74	256.002	-25.332	7.63	-5
13	257.207	-29.123	45	256.439	-26.957	18.73	-5
13	257.207	-29.123	72	257.001	-27.978	9.57	-5
13	257.207	-29.123	80	259.095	-28.744	14.00	-5
14	252.002	-28.994	78	251.144	-27.787	11.75	-5
15	255.089	-23.205	17	254.645	-21.797	12.11	-5
15	255.089	-23.205	52	256.699	-24.483	16.09	-5
15	255.089	-23.205	58	252.719	-23.732	18.47	-5
15	255.089	-23.205	65	252.699	-24.208	19.88	-5
15	255.089	-23.205	74	256.002	-25.332	18.85	-5
16	251.662	-21.559	67	250.910	-23.100	13.97	-5
19	261.189	-23.371	20	263.060	-23.443	14.18	-5
19	261.189	-23.371	21	260.700	-24.108	7.12	-5
19	261.189	-23.371	22	260.536	-21.280	17.97	-5
19	261.189	-23.371	46	258.755	-23.187	18.53	-5
20	263.060	-23.443	21	260.700	-24.108	18.66	-5
21	260.700	-24.108	55	259.771	-26.107	17.91	-5
21	260.700	-24.108	70	259.445	-25.366	14.01	-5
23	262.885	-27.650	59	261.951	-27.115	8.15	-5
23	262.885	-27.650	60	261.398	-27.557	10.90	-5
24	265.089	-24.617	35	267.191	-24.860	15.89	-5
31	253.087	-10.138	36	252.900	-11.827	14.03	-5
31	253.087	-10.138	73	252.965	-12.413	18.80	-5
32	256.003	-15.443	51	258.482	-15.348	19.75	-5
32	256.003	-15.443	57	255.199	-17.097	15.07	-5
32	256.003	-15.443	62	256.281	-14.008	12.05	-5
32	256.003	-15.443	69	258.159	-15.328	17.18	-5
34	254.118	-13.202	62	256.281	-14.008	18.59	-5
34	254.118	-13.202	63	252.014	-12.463	18.00	-5
36	252.900	-11.827	63	252.014	-12.463	8.87	-5
37	252.938	-13.831	66	254.925	-13.050	17.21	-5
38	251.078	-11.975	63	252.014	-12.463	8.57	-5
39	253.317	-14.742	73	252.965	-12.413	19.43	-5
41	253.515	-18.099	57	255.199	-17.097	15.62	-5

Crater 1	***lon***	***lat***	***Crater 2***	***lon***	***lat***	***separation (km)***	***Score***
43	250.785	-22.843	58	252.719	-23.732	16.40	-5
43	250.785	-22.843	65	252.699	-24.208	18.35	-5
46	258.755	-23.187	70	259.445	-25.366	18.72	-5
55	259.771	-26.107	60	261.398	-27.557	16.94	-5
58	252.719	-23.732	67	250.910	-23.100	14.66	-5
60	261.398	-27.557	64	259.332	-25.994	19.96	-5
60	261.398	-27.557	80	259.095	-28.744	19.41	-5
61	253.952	-12.410	66	254.925	-13.050	9.45	-5
64	259.332	-25.994	71	260.451	-26.531	9.39	-5
65	252.699	-24.208	67	250.910	-23.100	16.33	-5
67	250.910	-23.100	77	252.054	-22.236	11.26	-5
81	230.239	-11.093	228	228.633	-9.703	17.37	-5
81	230.239	-11.093	229	228.367	-9.695	19.08	-5
82	231.721	-10.781	88	233.824	-11.505	18.05	-5
87	241.385	-14.924	93	242.624	-16.832	18.57	-5
92	247.797	-13.377	94	248.510	-14.173	8.70	-5
92	247.797	-13.377	95	247.117	-14.079	7.96	-5
102	242.273	-20.782	124	240.777	-19.178	17.61	-5
104	238.001	-21.630	108	238.070	-23.459	15.11	-5
104	238.001	-21.630	126	237.617	-23.102	12.50	-5
107	240.957	-24.232	111	241.919	-23.310	10.52	-5
121	235.840	-19.451	123	237.139	-17.774	17.18	-5
122	235.278	-18.875	125	235.344	-17.743	9.36	-5
129	213.444	-16.862	137	213.398	-14.632	18.41	-5
129	213.444	-16.862	149	211.476	-16.581	15.73	-5
138	220.692	-14.881	141	219.496	-16.390	15.67	-5
139	223.265	-15.868	140	223.136	-16.737	7.25	-5
140	223.136	-16.737	161	222.599	-18.817	17.68	-5
140	223.136	-16.737	179	225.129	-18.175	19.68	-5
151	215.387	-21.355	154	217.354	-20.613	16.35	-5
152	214.843	-21.840	159	212.314	-22.243	19.63	-5
154	217.354	-20.613	155	218.295	-21.601	10.91	-5
157	220.971	-20.990	160	220.923	-18.669	19.16	-5
163	217.390	-25.482	167	218.176	-26.679	11.47	-5
165	222.845	-24.244	175	225.036	-23.282	18.35	-5
201	220.211	3.617	202	219.539	3.539	5.57	-5
201	220.211	3.617	206	220.023	1.461	17.87	-5
201	220.211	3.617	226	221.867	3.234	14.01	-5
212	222.352	8.133	213	223.000	5.953	18.76	-5
213	223.000	5.953	219	223.195	4.086	15.50	-5
236	210.469	-1.969	913	208.094	-1.922	19.60	-5
255	246.867	6.531	259	246.609	8.383	15.43	-5
258	247.500	6.227	259	246.609	8.383	19.24	-5
260	245.633	4.766	262	244.852	3.063	15.46	-5
262	244.852	3.063	266	245.109	2.359	6.18	-5
268	241.516	0.141	276	240.523	-1.117	13.23	-5
281	237.969	-2.125	282	238.516	-3.000	8.52	-5
281	237.969	-2.125	292	236.695	-0.250	18.71	-5
281	237.969	-2.125	296	239.563	-2.078	13.15	-5
282	238.516	-3.000	294	236.273	-3.000	18.48	-5
283	231.875	1.625	284	233.156	1.984	10.98	-5
309	245.383	-7.609	310	247.086	-8.734	16.73	-5
325	252.195	-0.031	335	251.938	-2.359	19.34	-5
328	257.625	-0.320	332	259.047	-1.391	14.69	-5
329	256.258	-0.281	333	255.141	-0.336	9.23	-5

Crater 1	*lon*	*lat*	*Crater 2*	*lon*	*lat*	*separation (km)*	*Score*
334	258.570	-2.602	338	260.625	-3.875	19.93	-5
341	257.930	-9.125	343	258.055	-7.695	11.85	-5
347	269.305	-2.867	348	269.266	-1.727	9.42	-5
352	268.898	7.086	353	267.320	8.789	19.08	-5
353	267.320	8.789	354	266.156	8.172	10.78	-5
366	190.518	-15.976	374	192.841	-15.947	18.44	-5
366	190.518	-15.976	375	191.595	-15.101	11.21	-5
367	196.794	-12.509	369	195.070	-13.867	17.82	-5
372	193.398	-14.037	374	192.841	-15.947	16.38	-5
374	192.841	-15.947	375	191.595	-15.101	12.12	-5
377	200.168	-14.031	378	201.049	-15.286	12.52	-5
378	201.049	-15.286	381	201.102	-15.942	5.43	-5
386	191.537	-25.791	388	193.119	-27.475	18.15	-5
386	191.537	-25.791	508	188.984	-25.063	19.96	-5
410	172.375	-15.859	413	172.641	-16.492	5.63	-5
413	172.641	-16.492	425	174.547	-17.703	18.06	-5
413	172.641	-16.492	437	171.734	-17.781	12.82	-5
417	180.141	-13.750	419	179.430	-11.953	15.90	-5
417	180.141	-13.750	525	181.820	-12.297	18.07	-5
417	180.141	-13.750	527	181.461	-14.406	11.88	-5
417	180.141	-13.750	528	182.133	-14.758	17.98	-5
417	180.141	-13.750	529	180.336	-14.930	9.86	-5
428	174.586	-20.742	429	176.688	-19.922	17.62	-5
429	176.688	-19.922	444	176.633	-21.320	11.55	-5
429	176.688	-19.922	445	176.633	-18.094	15.10	-5
433	180.219	-20.469	447	180.250	-22.438	16.25	-5
434	180.281	-21.234	447	180.250	-22.438	9.94	-5
440	170.789	-20.742	619	169.695	-22.492	16.71	-5
442	171.031	-22.906	454	171.203	-23.797	7.47	-5
442	171.031	-22.906	469	170.984	-24.664	14.52	-5
451	172.281	-24.172	456	174.336	-25.383	18.36	-5
452	171.789	-23.836	472	170.836	-26.031	19.48	-5
457	180.445	-24.188	463	178.922	-25.313	14.72	-5
457	180.445	-24.188	464	179.758	-26.172	17.17	-5
463	178.922	-25.313	464	179.758	-26.172	9.43	-5
463	178.922	-25.313	473	177.359	-26.867	17.29	-5
464	179.758	-26.172	467	180.836	-24.305	17.39	-5
464	179.758	-26.172	486	180.852	-27.469	13.40	-5
526	185.148	-14.148	537	185.117	-12.344	14.90	-5
547	154.211	-13.570	548	154.063	-14.313	6.24	-5
555	160.586	-13.367	573	161.742	-13.094	9.56	-5
568	160.281	-17.875	572	162.039	-18.031	13.86	-5
568	160.281	-17.875	575	159.953	-16.234	13.79	-5
569	160.695	-18.070	572	162.039	-18.031	10.55	-5
569	160.695	-18.070	575	159.953	-16.234	16.25	-5
570	160.609	-18.836	572	162.039	-18.031	13.02	-5
571	161.352	-18.977	572	162.039	-18.031	9.48	-5
573	161.742	-13.094	624	163.688	-13.141	15.65	-5
573	161.742	-13.094	625	164.008	-13.453	18.44	-5
573	161.742	-13.094	626	163.266	-13.328	12.40	-5
573	161.742	-13.094	631	161.750	-11.008	17.22	-5
573	161.742	-13.094	632	162.070	-11.195	15.89	-5
573	161.742	-13.094	635	163.383	-12.297	14.76	-5
576	160.305	-19.672	582	159.430	-21.359	15.49	-5
582	159.430	-21.359	616	161.250	-22.719	17.89	-5

Crater 1	***lon***	***lat***	***Crater 2***	***lon***	***lat***	***separation (km)***	***Score***
603	164.922	-28.648	606	165.625	-26.695	16.92	-5
622	164.891	-14.898	625	164.008	-13.453	13.87	-5
791	127.602	-20.016	797	127.078	-19.688	4.88	-5
863	144.188	-3.352	877	143.625	-1.180	18.52	-5
34	254.118	-13.202	61	253.952	-12.410	6.67	-6
37	252.938	-13.831	39	253.317	-14.742	8.11	-6
44	250.413	-22.422	67	250.910	-23.100	6.76	-6
411	170.914	-16.641	437	171.734	-17.781	11.42	-6
553	159.836	-15.531	565	158.070	-16.867	17.82	-6
650	134.164	-13.406	651	134.555	-14.313	8.11	-6
676	137.188	-23.984	678	137.344	-25.508	12.63	-6
676	137.188	-23.984	679	136.727	-25.563	13.48	-6
979	164.844	6.531	986	163.059	5.141	18.62	-6
771	119.109	-26.531	780	120.070	-25.641	10.24	-8

D SOFTWARE TOOLS

This appendix provides details on both the off-the-shelf and custom software applications used in this study.

D.1 JMARS

JMARS (Java Mission-planning and Analysis for Remote Sensing) is a planetary Geographic Information System (GIS) application developed by ASU's Mars Space Flight Facility to provide mission planning and data analysis tools for NASA missions, researchers, students of all ages, and the general public (Christensen et al., 2009). It is an open-source, free application.

JMARS distinguishes itself from other GIS applications by providing servers that host pre-processed maps and individual remote-sensing images. Official NASA/ESA/DLR/JAXA/USGS data products for Mars, the Moon, and many other planetary bodies (including Ceres) are readily available and searchable.

JMARS provides a wide variety of tools to remote sensing analysis. This study will make use of the following features:

- **Map Layer** – for displaying a high-resolution global mosaic of Ceres.
- **Stamp Layer** – used to display individual images captured by the Dawn Framing Camera.

- **Crater Counting Layer** – provides easy-to-use tools for marking and labeling impact craters. Crater data (latitude, longitude, and diameter in meters) can be saved to a CSV file.
- **Custom Shape Layer** – used to draw shapes around objects or regions on a planetary surface. Underlying numeric data maps (e.g., Digital Elevation Models) can be sampled to determine max, min, and mean values within a shape. An entire shape layer can be exported to an ArcGIS-compatible shape file. This study uses the Custom Shape Layer for two things: analyzing the morphology of impact craters, and creating graphics to easily locate and evaluate individual crater pairs.

D.2 Python Programs

A number of programs were written in Python to manage and manipulate data collected in this study.

D.2.1 Processing Exported Crater Data

A large CSV file, containing all the craters counted in the study area, is processed by `separations_shapes.py`. This program produces three files:

- `craters.csv` – a list of the following fields for each crater: unique number, latitude, longitude, and diameter.
- `crater_pairs.csv` – pairings of craters that are within 20 km of each other. Includes crater numbers, latitudes, longitudes, and separation distance for each identified pair. The separation is computed by using a great circle arc, assuming Ceres to be a sphere.
- `crater_pairs_shapefile.csv` – An ArcGIS-compatible shape file containing shapes representing each pair of craters. The generated shape is a line between the center

points of the two craters in a pair, along with a label for display that names the two craters' numbers.

The program also tallies the crater separations of all identified pairs (the ones written to `crater_pairs.csv`) into 10 logarithmic bins between 1 and 20 for later use.

D.2.2 Computing Impactor Diameters

To estimate the diameters of the impactors that created the impact craters from the study, a simple program `impactor_diam.py` was created. It reads in the `craters.csv` file created by `separations_shapes.py` and, for each crater, uses an implementation of the following equation to compute an estimated impactor diameter (see sections 1.2.3.3 and 2.2 for details):

$$d = [D/14.44475]^{1.277}$$

where D is the crater diameter in km, and d is the impactor diameter in km. All the ingested crater columns, plus the impactor diameter in meters, are written to `impactor_diam.csv`.

D.2.3 Monte Carlo Simulation

`montecarlo_phase123.py` generates a number (equal to the number of craters in file `craters.csv`) of random crater locations within the study area. It identifies all unique pairings of these randomly generated craters whose separation is ≤ 20 km, and tallies these pairs into 10 logarithmic bins.

The simulation is executed 1000 times, and the tallies from all runs (and their averages) are written to file `montecarlo_phase123.csv`.

NOTE: Each run of the program will produce slightly different results.

D.2.4 Chi Squared Test

A simple program, `chi_squared.py`, performs a Chi Square Test on the binned counts of crater separation values from both the actual observed craters (computed by the program `separations_shapes.py`) and the simulated craters (tallied by the program `montecarlo_phase123.py`).

REFERENCES

Barlow, N. G., Boyce, J. M., Costard, F. M., Craddock, R. A., Garvin, J. B., Sakimoto, S. E., . . . Soderblom, L. A. (2000). Standardizing the nomenclature of martian impact crater ejecta morphologies. *Journal of Geophysical Research: Planets, 105*(E11), 26733-26738.

Barucci, M. A., Fulchignoni, M., Ji, J., Marchi, S., & Thomas, N. (2015). The flybys of asteroids (2867) šteins,(21) lutetia, and (4179) toutatis. *Et Al., Asteroids IV,* University of Arizona Press, Tucson, 433-450.

Belton, M. J., Veverka, J., Thomas, P., Helfenstein, P., Simonelli, D., Chapman, C., . . . Pilcher, C. (1992). Galileo encounter with 951 gaspra: First pictures of an asteroid. *Science 257*(5077), 1647-1652.

Benner, L. A., Busch, M. W., Giorgini, J. D., Taylor, P. A., & Margot, J. (2015). Radar observations of near-earth and main-belt asteroids. *Asteroids IV,* University of Arizona Press, Tucson, 165-182.

Binzel, R. P., & Van Flandern, T. C. (1979). Minor planets: The discovery of minor satellites. *Science 203*(4383), 903-905.

Biren, M., van Soest, M., Wartho, J., Hodges, K., & Spray, J. (2016). Diachroneity of the clearwater west and clearwater east impact structures indicated by the (U–Th)/He dating method. *Earth and Planetary Science Letters, 453*, 56-66.

Bottke Jr, W. F., & Melosh, H. J. (1996). Binary asteroids and the formation of doublet craters. *Icarus, 124*(2), 372-391.

Bottke Jr, W. F., Nolan, M. C., Greenberg, R., & Kolvoord, R. A. (1994). Velocity distributions among colliding asteroids. *Icarus, 107*(2), 255-268.

Bottke, W. F., Cellino, A., Paolicchi, P., & Binzel, R. (2002). *Asteroids III,* University of Arizona Press, Tucson.

Burchell, M. J., & Grey, I. D. (2001). Oblique hypervelocity impacts on thick glass targets. *Materials Science and Engineering: A, 303*(1-2), 134-141.

Carry, B. (2012). Density of asteroids. *Planetary and Space Science, 73*(1), 98-118.

Chapman, C. R. (1974). Cratering on mars I. cratering and obliteration history. *Icarus, 22*(3), 272-291.

Chapman, C., Veverka, J., Thomas, P., Klaasen, K., Belton, M., Harch, A., . . . Davies, M. (1995). Discovery and physical properties of dactyl, a satellite of asteroid 243 ida.

Chauvineua, B., Farinella, P., & Harris, A. (1995). The evolution of earth-approaching binary asteroids: A monte carlo dynamical model. *Icarus, 115*(1), 36-46.

Christensen, P., Engle, E., Anwar, S., Dickenshied, S., Noss, D., Gorelick, N., & Weiss-Malik, M. (2009). (2009). JMARS-a planetary GIS. *AGU Fall Meeting Abstracts, 2009.*

Ciarniello, M., De Sanctis, M., Ammannito, E., Raponi, A., Longobardo, A., Palomba, E., . . . Schröder, S. (2017). Spectrophotometric properties of dwarf planet ceres from the VIR spectrometer on board the dawn mission. *Astronomy & Astrophysics, 598*, A130.

Cook, A. (1971). 624 hektor: A binary asteroid? *NASA Special Publication, 267*, 155.

Cook, C. M., Melosh, H. J., & Bottke, W. F. (2003). Doublet craters on venus. *Icarus, 165*(1), 90-100.

Ćuk, M. (2007). Formation and destruction of small binary asteroids. *The Astrophysical Journal Letters, 659*(1), L57.

Davis, D., Chapman, C., Greenberg, R., Weidenschilling, S., & Harris, A. (1979). Collisional evolution of asteroids-populations, rotations, and velocities. *Asteroids, 1*, 528-557.

Davison, T. M., Collins, G. S., Elbeshausen, D., Wünnemann, K., & Kearsley, A. (2011). Numerical modeling of oblique hypervelocity impacts on strong ductile targets. *Meteoritics & Planetary Science, 46*(10), 1510-1524.

Dence, M. R., Innes, M., & Beals, C. (1965). On the probable meteorite origin of the clearwater lakes, quebec. *Journal of the Royal Astronomical Society of Canada, 59*, 13.

Doressoundiram, A., Paolicchi, P., Verlicchi, A., & Cellino, A. (1997). The formation of binary asteroids as outcomes of catastrophic collisions. *Planetary and Space Science, 45*(7), 757-770.

Drummond, J., Carry, B., Merline, W., Dumas, C., Hammel, H., Erard, S., . . . Chapman, C. (2014). Dwarf planet ceres: Ellipsoid dimensions and rotational pole from keck and VLT adaptive optics images. *Icarus, 236*, 28-37.

Dunham, D. W., & Maley, P. D. (1977). Possible observation of a satellite of a minor planet. *Minor Planet Bulletin, 5*, 16-17.

Durda, D. D., Bottke, W. F., Enke, B. L., Merline, W. J., Asphaug, E., Richardson, D. C., & Leinhardt, Z. M. (2004). The formation of asteroid satellites in large impacts: Results from numerical simulations. *Icarus, 167*(2), 382-396.

Duxbury, T. C., Newburn, R. L., Acton, C. H., Carranza, E., McElrath, T. P., Ryan, R. E., . . . Cheuvront, A. R. (2004). Asteroid 5535 annefrank size, shape, and orientation: Stardust first results. *Journal of Geophysical Research: Planets, 109*(E2).

Elbeshausen, D., Wünnemann, K., & Collins, G. S. (2009). Scaling of oblique impacts in frictional targets: Implications for crater size and formation mechanisms. *Icarus, 204*(2), 716-731.

Ermakov, A., Fu, R., Castillo-Rogez, J., Raymond, C., Park, R., Preusker, F., . . . Zuber, M. (2017). Constraints on ceres' internal structure and evolution from its shape and gravity measured by the dawn spacecraft. *Journal of Geophysical Research: Planets, 122*(11), 2267-2293.

Farinella, P. (1992). Evolution of earth-crossing binary asteroids due to gravitational encounters with the earth. *Icarus, 96*(2), 284-285.

Farinella, P., & Davis, D. R. (1992). Collision rates and impact velocities in the main asteroid belt. *Icarus, 97*(1), 111-123.

Farinella, P., Paolicchi, P., & Zappalà, V. (1982). The asteroids as outcomes of catastrophic collisions. *Icarus, 52*(3), 409-433.

Fuse, T., Yoshida, F., Tholen, D., Ishiguro, M., & Saito, J. (2008). Searching satellites of asteroid itokawa by imaging observation with hayabusa spacecraft. *Earth, Planets and Space, 60*(1), 33-37.

Gault, D. E. (1974). (1974). Impact cratering. Paper presented at the *A Primer in Lunar Geology,* NASA.

Gault, D. E., & Wedekind, J. A. (1978). (1978). Experimental studies of oblique impact. Paper presented at the *Lunar and Planetary Science Conference Proceedings, 9,* 3843-3875.

Gehrels, T., Drummond, J., & Levenson, N. (1987). The absence of satellites of asteroids. *Icarus, 70*(2), 257-263.

Hamilton, D. P., & Burns, J. A. (1991). Orbital stability zones about asteroids. *Icarus, 92*(1), 118-131.

Hamilton, D. P., & Burns, J. A. (1992). Orbital stability zones about asteroids: II. the destabilizing effects of eccentric orbits and of solar radiation. *Icarus, 96*(1), 43-64.

Hamilton, D. P., & Krivov, A. V. (1997). Dynamics of distant moons of asteroids. *Icarus, 128*(1), 241-249.

Hartmann, W. (1979). Diverse puzzling asteroids and a possible unified explanation. *Asteroids, 1*, University of Arizona Press, Tucson, 466-479.

Herrick, R. R., & Forsberg-Taylor, N. K. (2003). The shape and appearance of craters formed by oblique impact on the moon and venus. *Meteoritics & Planetary Science, 38*(11), 1551-1578.

Hiesinger, H., Marchi, S., Schmedemann, N., Schenk, P., Pasckert, J., Neesemann, A., . . . Fu, R. (2016). Cratering on ceres: Implications for its crust and evolution. *Science, 353*(6303).

Holsapple, K. (1993). The scaling of impact processes in planetary sciences. *Annual Review of Earth and Planetary Sciences, 21*(1), 333-373.

Holsapple, K., & Schmidt, R. (1982). On the scaling of crater dimensions: 2. impact processes. *Journal of Geophysical Research: Solid Earth, 87*(B3), 1849-1870.

Horedt, G., & Neukum, G. (1984). Comparison of six crater-scaling laws. *Earth, Moon, and Planets, 31*(3), 265-269.

Ivanov, B. A. (2001). Mars/Moon cratering rate ratio estimates. *Space Science Reviews, 96*(1-4), 87-104.

Jacobson, S. A., & Scheeres, D. J. (2011). Dynamics of rotationally fissioned asteroids: Source of observed small asteroid systems. *Icarus, 214*(1), 161-178.

Johnston W.R., M. K. (2014). Doublet crater. *Encyclopedia of planetary landforms*, Springer, NewYork.

Johnston, W. R. (2016). *Binary minor planets V9.0. EAR-A-COMPIL-5-BINMP-V9.0*

Marchi, S., Bottke, W., O'Brien, D., Schenk, P., Mottola, S., De Sanctis, M., . . . Russell, C. (2014). Small crater populations on vesta. *Planetary and Space Science, 103*, 96-103.

Margot, J., Pravec, P., Taylor, P., Carry, B., & Jacobson, S. (2015). Asteroid systems: Binaries, triples, and pairs. *Encyclopedia of planetary landforms*, Springer, NewYork.

McFadden, L. A., Skillman, D. R., Memarsadeghi, N., Li, J., Joy, S., Polanskey, C., . . . Palmer, E. (2015). Vesta's missing moons: Comprehensive search for natural satellites of vesta by the dawn spacecraft. *Icarus, 257*, 207-216.

McMahon, J. H. (1978). The discovery of a satellite of an asteroid. *Minor Planet Bulletin, 6*, 14-17.

Melosh, H. J. (1989). *Impact cratering: A geologic process.* Oxford University Press, New York.

Melosh, H. (1980). Cratering mechanics-observational, experimental, and theoretical. *Annual Review of Earth and Planetary Sciences, 8*(1), 65-93.

Melosh, H., Ingram, J., & Bottke, W. (1996). (1996). The abundance of doublet craters on mars. Paper presented at the *Lunar and Planetary Science Conference, 27*

Melosh, H., & Ivanov, B. (1999). Impact crater collapse. *Annual Review of Earth and Planetary Sciences, 27*(1), 385-415.

Melosh, H., & Stansberry, J. (1991). Doublet craters and the tidal disruption of binary asteroids. *Icarus, 94*(1), 171-179.

Merline, W. J., Weidenschilling, S. J., Durda, D. D., Margot, J., Pravec, P., & Storrs, A. D. (2002). Asteroids do have satellites. *Asteroids III,* University of Arizona Press, Tucson.

Merline, W., Close, L. M., Dumas, C., Chapman, C., Roddier, F., Menard, F., . . . Morgan, T. (1999). Discovery of a moon orbiting the asteroid 45 eugenia. *Nature, 401*(6753), 565-568.

Miljković, K., Collins, G. S., Mannick, S., & Bland, P. A. (2013). Morphology and population of binary asteroid impact craters. *Earth and Planetary Science Letters, 363*, 121-132.

Millis, R., & Dunham, D. (1989). (1989). Precise measurement of asteroid sizes and shapes from occultations. *Asteroids II,* University of Arizona Press, Tucson.

Nathues, A., Sierks, H., Gutierrez-Marques, P., Ripken, J., Hall, I., Buettner, I., . . . Chistensen, U. (2016). Dawn FC2 calibrated ceres images V1. 0. *NASA Planetary Data System, 265*

Oberbeck, V. R. (1973). Simultaneous impact and lunar craters. *The Moon, 6*(1-2), 83-92.

Oberbeck, V. R., & Aoyagi, M. (1972). Martian doublet craters. *Journal of Geophysical Research, 77*(14), 2419-2432.

Oberbeck, V., Quaide, W., Arvidson, R., & Aggarwal, H. (1977). Comparative studies of lunar, martian, and mercurian craters and plains. *Journal of Geophysical Research, 82*(11), 1681-1698.

O'Keefe, J. D., & Ahrens, T. J. (1993). Planetary cratering mechanics. *Journal of Geophysical Research: Planets, 98*(E9), 17011-17028.

Oliphant, T. E. (2007). Python for scientific computing. *Computing in Science & Engineering*, *9*(3).

Öpik, E. J. (1969). The moon's surface. *Annual Review of Astronomy and Astrophysics, 7*(1), 473-526.

Ostro, S., Chandler, J., Hine, A., Rosema, K., Shapiro, I., & Yeomans, D. (1990). Radar images of asteroid 1989 PB. *Science, 248*, 1523-1528.

Ostro, S. J., Hudson, R. S., Benner, L. A., Giorgini, J. D., Magri, C., Margot, J., & Nolan, M. C. (2002). Asteroid radar astronomy. *Asteroids III,* University of Arizona Press, Tucson*,* 151-168.

Pierazzo, E., & Melosh, H. (2000). Understanding oblique impacts from experiments, observations, and modeling. *Annual Review of Earth and Planetary Sciences, 28*(1), 141-167.

Pierazzo, E., & Collins, G. (2004). A brief introduction to hydrocode modeling of impact cratering. *Cratering in marine environments and on ice*, Springer, New York, 323-340.

Poelchau, M. H., & Kenkmann, T. (2008). Asymmetric signatures in simple craters as an indicator for an oblique impact direction. *Meteoritics & Planetary Science, 43*(12), 2059-2072.

Pravec, P., & Harris, A. W. (2007). Binary asteroid population: 1. angular momentum content. *Icarus, 190*(1), 250-259.

Pravec, P., Scheirich, P., Kušnirák, P., Šarounová, L., Mottola, S., Hahn, G., . . . Krzeminski, Z. (2006). Photometric survey of binary near-earth asteroids. *Icarus, 181*(1), 63-93.

Prettyman, T. H., Yamashita, N., Toplis, M. J., McSween, H. Y., Schorghofer, N., Marchi, S., . . . Russell, C. T. (2017). Extensive water ice within ceres' aqueously altered regolith: Evidence from nuclear spectroscopy. *Science, 355*(6320), 55-59.

Richardson, D. C., Bottke, W. F., & Love, S. G. (1998). Tidal distortion and disruption of earth-crossing asteroids. *Icarus, 134*(1), 47-76.

Roatsch, T., Kersten, E., Matz, K., Preusker, F., Scholten, F., Jaumann, R., . . . Russell, C. T. (2017). High-resolution ceres low altitude mapping orbit atlas derived from dawn framing camera images. *Planetary and Space Science, 140*, 74-79.

Roberts Jr, L. C., McAlister, H. A., Hartkopf, W. I., & Franz, O. G. (1995). A speckle interferometric survey for asteroid duplicity. *The Astronomical Journal, 110*, 2463.

Rubincam, D. P. (2000). Radiative spin-up and spin-down of small asteroids. *Icarus, 148*(1), 2-11.

Russell, C., & Raymond, C. (2011). The dawn mission to vesta and ceres. *Space Science Reviews, 163*(1-4), 3-23.

Scheeres, D. (2002). Stability of binary asteroids. *Icarus, 159*(2), 271-283.

Schmidt, R. M., & Housen, K. R. (1987). Some recent advances in the scaling of impact and explosion cratering. *International Journal of Impact Engineering, 5*(1-4), 543-560.

Sekiguchi, N. (1970). On the fissions of a solid body under influence of tidal force; with application to the problem of twin craters on the moon. *The Moon, 1*(4), 429-439.

Sierks, H., Keller, H., Jaumann, R., Michalik, H., Behnke, T., Bubenhagen, F., . . . Enge, R. (2011). The dawn framing camera. *Space Science Reviews, 163*(1-4), 263-327.

Spray, J. (2016). Earth impact database. Retrieved from http://www.passc.net/EarthImpactDatabase/index.html

Sweeney, J., Warner, N., Golombek, M., Kirk, R., Fergason, R., Pivarunas, A., . . . Hernandez, D. (2017). (2017). Constructing a semi-automated method in ArcMap to measure impact crater morphology. Paper presented at the *Lunar and Planetary Science Conference, 48*

Tanner, R. (1963). The orbital perturbations of a very large twin meteorite. *Journal of the Royal Astronomical Society of Canada, 57*, 109.

Timerson, B., Brooks, J., Conard, S., Dunham, D. W., Herald, D., Tolea, A., & Marchis, F. (2013). Occultation evidence for a satellite of the trojan asteroid (911) agamemnon. *Planetary and Space Science, 87*, 78-84.

Trask, N. J., & Guest, J. E. (1975). Preliminary geologic terrain map of mercury. *Journal of Geophysical Research, 80*(17), 2461-2477.

Trego, K. D. (1989). Multiple impacts in the earth's cratering history. *Earth, Moon, and Planets, 46*(3), 201-205.

Turtle, E., Pierazzo, E., Collins, G., Osinski, G., Melosh, H., Morgan, J., & Reimold, W. (2005). Impact structures: What does crater diameter mean. *Large Meteorite Impacts III: Geological Society of America Special Paper, 384*, 1-24.

Van Flandern, T., Tedesco, E., & Binzel, R. (1979). Satellites of asteroids. *Asteroids,* University of Arizona Press, Tucson, 443-465.

Vedder, J. D. (1998). Main belt asteroid collision probabilities and impact velocities. *Icarus, 131*(2), 283-290.

Veverka, J., Robinson, M., Thomas, P., Murchie, S., Bell, J. F.,3rd, Izenberg, N., . . . Miller, J. K. (2000). NEAR at eros: Imaging and spectral results. *Science, 289*(5487), 2088-2097.

Veverka, J., Thomas, P., Harch, A., Clark, B., Bell, J. F.,3rd, Carcich, B., . . . Cheng, A. (1997). NEAR's flyby of 253 mathilde: Images of a C asteroid. *Science, 278*(5346), 2109-2114.

Wagner, R., Neukum, G., & Schmedemann, N. (2012). (2012). Double and multiple craters on the satellites of saturn and their size distribution. Paper presented at the *Lunar and Planetary Science Conference, 43*

Wallis, D., Burchell, M., Cook, A., Solomon, C., & McBride, N. (2005). Azimuthal impact directions from oblique impact crater morphology. *Monthly Notices of the Royal Astronomical Society, 359*(3), 1137-1149.

Walsh, K. J., & Jacobson, S. A. (2015). Formation and evolution of binary asteroids. *Asteroids IV,* University of Arizona Press, Tucson, 375-393.

Walsh, K. J., & Richardson, D. C. (2006). Binary near-earth asteroid formation: Rubble pile model of tidal disruptions. *Icarus, 180*(1), 201-216.

Walsh, K. J., & Richardson, D. C. (2008). A steady-state model of NEA binaries formed by tidal disruption of gravitational aggregates. *Icarus, 193*(2), 553-566.

Walsh, K. J., Richardson, D. C., & Michel, P. (2008). Rotational breakup as the origin of small binary asteroids. *Nature, 454*(7201), 188-191.

Walsh, K. J., Richardson, D. C., & Michel, P. (2012). Spin-up of rubble-pile asteroids: Disruption, satellite formation, and equilibrium shapes. *Icarus, 220*(2), 514-529.

Weidenschilling, S. (1980). Hektor: Nature and origin of a binary asteroid. *Icarus, 44*(3), 807-809.

Weidenschilling, S. J., Paolicchi, P., & Zappala, V. (1989). Do asteroids have satellites?, *Asteroids II,* University of Arizona Press, Tucson.

Woronow, A. (1978). The expected frequency of doublet craters. *Icarus, 34*(2), 324-330.

Wren, P.F., & Fevig, R.A. (2017). Investigation of doublet craters on ceres as evidence of main belt binary asteroid systems. Paper presented at the *Lunar and Planetary Science Conference, 48.*

Wünnemann, K., Nowka, D., Collins, G., Elbeshausen, D., & Bierhaus, M. (2011). (2011). Scaling of impact crater formation on planetary surfaces—Insights from numerical modeling. Paper presented at the *Proceedings of the 11th Hypervelocity Impact Symposium,* Freiburg, Germany.

Young, L. A., Stern, S. A., Weaver, H. A., Bagenal, F., Binzel, R. P., Buratti, B., . . . Grundy, W. M. (2008). New horizons: Anticipated scientific investigations at the pluto system. *Space Science Reviews, 140*(1-4), 93-127.

Zahnle, K., Schenk, P., Levison, H., & Dones, L. (2003). Cratering rates in the outer solar system. *Icarus, 163*(2), 263-289.

Zappalà, V., Scaltriti, F., Farinella, P., & Paolicchi, P. (1980). Asteroidal binary systems: Detection and formation. *The Moon and the Planets, 22*(2), 153-162.